

University of Alberta

**Arsenic Effects on the Formation and Repair  
of Benzo(a)pyrene Diol Epoxide-DNA Adducts**

by

Shengwen Shen



A thesis submitted to the Faculty of Graduate Studies and Research in partial  
fulfilment of the requirements for the degree of **Doctor of Philosophy**

in

**Medical Sciences–Public Health Sciences**

Edmonton, Alberta

Spring 2006



Library and  
Archives Canada

Bibliothèque et  
Archives Canada

Published Heritage  
Branch

Direction du  
Patrimoine de l'édition

395 Wellington Street  
Ottawa ON K1A 0N4  
Canada

395, rue Wellington  
Ottawa ON K1A 0N4  
Canada

*Your file* *Votre référence*  
*ISBN: 0-494-14041-0*  
*Our file* *Notre référence*  
*ISBN: 0-494-14041-0*

#### NOTICE:

The author has granted a non-exclusive license allowing Library and Archives Canada to reproduce, publish, archive, preserve, conserve, communicate to the public by telecommunication or on the Internet, loan, distribute and sell theses worldwide, for commercial or non-commercial purposes, in microform, paper, electronic and/or any other formats.

The author retains copyright ownership and moral rights in this thesis. Neither the thesis nor substantial extracts from it may be printed or otherwise reproduced without the author's permission.

#### AVIS:

L'auteur a accordé une licence non exclusive permettant à la Bibliothèque et Archives Canada de reproduire, publier, archiver, sauvegarder, conserver, transmettre au public par télécommunication ou par l'Internet, prêter, distribuer et vendre des thèses partout dans le monde, à des fins commerciales ou autres, sur support microforme, papier, électronique et/ou autres formats.

L'auteur conserve la propriété du droit d'auteur et des droits moraux qui protègent cette thèse. Ni la thèse ni des extraits substantiels de celle-ci ne doivent être imprimés ou autrement reproduits sans son autorisation.

---

In compliance with the Canadian Privacy Act some supporting forms may have been removed from this thesis.

Conformément à la loi canadienne sur la protection de la vie privée, quelques formulaires secondaires ont été enlevés de cette thèse.

While these forms may be included in the document page count, their removal does not represent any loss of content from the thesis.

Bien que ces formulaires aient inclus dans la pagination, il n'y aura aucun contenu manquant.

  
**Canada**

## **Abstract**

Arsenic, with its demonstrated cancerous and noncancerous effects, poses a tremendous health risk to human populations worldwide. In Bangladesh alone, 35 million people are currently exposed to high concentrations (greater than 50  $\mu\text{g/L}$ ) of inorganic arsenic (iAs) in drinking water. Although arsenic is an established human carcinogen, its mechanistic mode of carcinogenicity is far from clear. Arsenic may act in a co-mutagenic/co-carcinogenic mechanism. Amongst the proposed hypotheses regarding arsenic carcinogenicity, inhibition of DNA repair processes has been suggested as one predominant mechanism. However, the underlying mechanism responsible for DNA repair inhibition remains elusive. The objective of this thesis was to determine how arsenic modulates the formation and repair of DNA adducts induced by benzo(a)pyrene diol epoxide (BPDE) in human cells.

A capillary electrophoresis-laser induced fluorescence (CE-LIF) based immunoassay was developed to measure BPDE-DNA adducts in human cells. The effects on the formation and repair of BPDE-DNA adducts by iAs and its metabolites were examined. In repair-deficient xeroderma pigmentosum group A (XPA) fibroblasts, arsenic pretreatment led to enhanced formation of BPDE-DNA adducts with trivalent arsenic compounds being more potent than pentavalent arsenic compounds. Most likely, arsenic exerted its enhancement by increasing cellular uptake of BPDE rather than by modulation of chromatin accessibility or by BPDE inactivation via the glutathione (GSH) conjugation system.

In confluent repair-proficient normal human fibroblasts, the presence of arsenic inhibited the repair of BPDE-DNA adducts with trivalent arsenic compounds being more

potent than pentavalent arsenic compounds. As the most potent inhibitor and a key metabolite of iAs, monomethylarsonous acid (MMA(III)) abrogated p53 accumulation induced by BPDE. More importantly, a striking temporal correlation between p53 expression and DNA repair capacity was observed. No similar correlations were found for repair proteins such as XPA, XPC and p62-TFIIH. p21 expression was modulated in a p53-dependent manner, implying that p53 was still functional and retained its wild-type conformation. Cell cycle analysis did not indicate that MMA(III) overrode the BPDE-induced G1/S arrest. Considering the well-demonstrated role of p53 in global genomic nucleotide excision repair (GG-NER), our results suggested that arsenic inhibited DNA repair by attenuating the expression of p53.

## Acknowledgements

I would like to express my sincere gratitude to my supervisor, Dr. X. Chris Le, for his intellectual and financial support throughout my program. His mentorship and scholarship really impress me and will benefit me for the rest of my life.

I wish to thank Dr. Michael Weinfeld, my co-supervisor, for allowing me to work in his lab and for his invaluable guidance and help. I appreciate the time and effort he has put in to make my thesis what it is. I also wish to thank Dr. Susan Andrew for her enthusiasm and dedication to this project as my supervisory committee member. I appreciate her constant encouragement and insightful suggestions. I want to thank Dr. Norman Dovichi and Dr. Xing-Fang Li for being my thesis examiners and for their thought-provoking questions and comments during my thesis defence.

I also wish to thank Dr. Altaf A. Wani for generously providing the BP1 antibody and Dr. Xuejun Sun and Dr. Razmik Mirzayans for their enthusiastic help.

The valuable support provided by Ms. Katerina Carastathis and Ms. Dianne Sergy is greatly appreciated.

My sincere thanks also go to Ms. Jane Lee, Ms. Louise Enns, Mr. Mesfin Fanta and other personnel in Dr. Weinfeld's lab for their technical assistance. Additionally, I express my heartfelt gratitude to Dr. Mike Lam, Dr. Hailin Wang, Dr. Zhilong Gong, Dr. Jeff Guthrie, Ms. Xiufen Lu, and my fellow graduate students in the EHS group for their tremendous help, cherished friendship and considerable support over the past few years. Thank you all for making my journey enjoyable.

The financial support provided by Alberta Health and Wellness, the Natural Sciences and Engineering Council of Canada (NSERC), the Canadian Water Network,

the National Cancer Institute of Canada, and the National Institutes of Health (U.S.) during the course of my project is gratefully acknowledged.

Finally, I would like to thank my parents, my brother, and my sister-in-law for their unwavering support and patience. I need to thank my wife, Feng, and my lovely son, Samuel, for their unconditional love and understanding.

# Table of Contents

	Page
<b>Chapter One: General Introduction.....</b>	<b>1</b>
1.1 HUMAN HEALTH EFFECTS OF ARSENIC.....	1
1.2 ARSENIC OCCURRENCE AND EXPOSURE.....	1
1.3 METABOLISM AND DISPOSITION OF ARSENIC.....	2
1.4 TOXICITY AND CARCINOGENICITY OF ARSENIC.....	4
1.5 SCOPE OF THESIS.....	7
1.6 REFERENCES.....	9
<b>Chapter Two: Method Development for the Detection of Benzo(a)pyrene Diol Epoxide-DNA Adducts.....</b>	<b>16</b>
2.1 INTRODUCTION.....	16
2.2 IMMUNOASSAY USING CAPILLARY ELECTROPHORESIS-LASER INDUCED FLUORESCENCE DETECTION.....	22
2.3 EXPERIMENTAL.....	24
2.3.1 Materials.....	25
2.3.2 Cells and cell cultures.....	25
2.3.3 DNA isolation.....	26
2.3.4 Instrumentation.....	26
2.3.5 Detection of BPDE-DNA adducts.....	28
2.4 RESULTS AND DISCUSSION.....	31
2.4.1 pH of the incubation buffer.....	31
2.4.2 Ionic strength of the incubation buffer.....	34
2.4.3 pH of the running buffer.....	39
2.4.4 Ionic strength of the running buffer.....	43
2.4.5 Injection time.....	48

<b>Table of Contents (<i>continued</i>)</b>	<b>Page</b>
2.4.6 Injection voltage .....	49
2.4.7 Separation voltage.....	50
2.4.8 Incubation time and temperature.....	51
2.4.9 Dose-response relationship.....	53
2.4.10 Choice of primary antibody .....	55
2.5 CONCLUSIONS .....	57
2.6 REFERENCES .....	58

## **Chapter Three: Effects of Arsenic on the Formation of Benzo(a)pyrene Diol Epoxide-DNA**

<b>Adducts .....</b>	<b>65</b>
3.1 INTRODUCTION.....	65
3.2 EXPERIMENTAL.....	69
3.2.1 Materials .....	69
3.2.2 Cells and cell cultures .....	70
3.2.3 Treatment of cells.....	70
3.2.4 DNA isolation.....	71
3.2.5 Detection of BPDE-DNA adducts .....	71
3.2.6 Cell number and colony formation assay .....	72
3.2.7 Cellular GSH content.....	72
3.2.8 GST activity assay .....	73
3.2.9 Chromatin accessibility .....	73
3.2.10 Effects of arsenic on the cellular uptake of BPDE .....	74
3.3 RESULTS AND DISCUSSION.....	75
3.3.1 Repair capability of the XPA cell line used .....	75
3.3.2 Effects of arsenic compounds on the formation of BPDE-DNA adducts .....	76
3.3.3 Cytotoxicity of arsenic compounds.....	83

<b>Table of Contents (<i>continued</i>)</b>	<b>Page</b>
3.3.4 Time-dependence of enhancement of BPDE-DNA adduct formation .....	87
3.3.5 Effects of arsenic on GSH-mediated inactivation of BPDE .....	89
3.3.6 Effects of arsenic on chromatin accessibility .....	95
3.3.7 Effects of arsenic on the cellular uptake of BPDE .....	101
3.4 CONCLUSIONS .....	106
3.5 REFERENCES .....	107

## **Chapter Four: Effects of Arsenic on the Repair of Benzo(a)pyrene Diol Epoxide-DNA Adducts.....118**

4.1 INTRODUCTION.....	118
4.2 EXPERIMENTAL.....	125
4.2.1 Materials .....	125
4.2.2 Cells and cell cultures .....	126
4.2.3 Treatment of cells.....	126
4.2.4 DNA isolation.....	126
4.2.5 Detection of BPDE-DNA adducts .....	127
4.2.6 Cell cycle analysis.....	128
4.2.7 Western blotting assay.....	128
4.3 RESULTS AND DISCUSSION.....	129
4.3.1 Effects of arsenic compounds on the repair of BPDE-DNA adducts .....	129
4.3.2 Time-dependence of inhibition of BPDE-DNA adduct repair .....	136
4.3.3 Kinetics of BPDE-DNA adduct repair .....	137
4.3.4 Repair inhibition in exponentially growing cells.....	141
4.3.5 Altered expression of repair-related proteins .....	144
4.4 CONCLUSIONS .....	153
4.5 REFERENCES .....	154

<b>Table of Contents (<i>continued</i>)</b>	<b>Page</b>
<b>Chapter Five: Conclusions and Synthesis.....</b>	<b>170</b>
<b>5.1 INTRODUCTION.....</b>	<b>170</b>
<b>5.2 ADVANCEMENTS IN KNOWLEDGE .....</b>	<b>171</b>
<b>5.2.1 Chapter 2: Developing and refining a tool for the measurement of                 BPDE-DNA adducts.....</b>	<b>171</b>
<b>5.2.2 Chapter 3: Examining and investigating the effects of arsenic on the                 formation of BPDE-DNA adducts .....</b>	<b>172</b>
<b>5.2.3 Chapter 4: Examining and investigating the effects of arsenic on the                 repair of BPDE-DNA adducts.....</b>	<b>173</b>
<b>5.3 FUTURE RESEARCH.....</b>	<b>175</b>
<b>5.4 CONCLUSIONS .....</b>	<b>176</b>
<b>5.5 REFERENCES .....</b>	<b>178</b>
 <b>Appendix: Introduction to Capillary Zone Electrophoresis (CZE).....</b>	 <b>180</b>
<b>REFERENCES .....</b>	<b>182</b>

## List of Tables

<b>Table</b>		<b>Page</b>
Table 2.1	Characteristics of different techniques for the analysis of DNA adducts .	21
Table 4.1	The Cell cycle analysis of confluent CRL2522 cells during repair in the presence or absence of 5 $\mu$ M MMA(III) following treatment with 1 $\mu$ M BPDE for 30 min. After the indicated times, cells were subjected to flow cytometry .....	140
Table 4.2	Summary of the cell cycle analysis data from Figure 4.11 .....	143

## List of Figures

<b>Figure</b>		<b>Page</b>
Figure 1.1	Biomethylation of arsenic involving alternate reduction of pentavalent arsenic to trivalent arsenic followed by oxidative addition of a methyl group .....	3
Figure 2.1	Immunoreaction between adducted DNA (Ag) and primary (Ab) and secondary (Ab*) antibodies .....	24
Figure 2.2	Schematic of the home-built capillary electrophoresis laser-induced fluorescence (CE-LIF) instrument .....	27
Figure 2.3	Electropherograms showing the effects of the pH of the incubation buffer on DNA analysis. ....	32
Figure 2.4	Relationship between the peak area ratio of treated DNA to control DNA and the pH of the incubation buffer. ....	33
Figure 2.5	Electropherograms showing the effects of the ionic strength of the incubation buffer on DNA analysis. ....	35
Figure 2.6	Relationship between the ionic strength of the incubation buffer and the migration time of the ternary complex.....	37
Figure 2.7a	Relationship between the ionic strength of the incubation buffer and the peak height of the ternary complex.....	38
Figure 2.7b	The peak height ratio of treated DNA to control DNA is dependent on the ionic strength of the incubation buffer.....	38
Figure 2.8	Electropherograms showing the effects of the pH of the running buffer on DNA analysis .....	40
Figure 2.9	Relationship between the pH of the running buffer and the migration time of the ternary complex .....	41
Figure 2.10a	Relationship between the pH of the incubation buffer and the peak height of the ternary complex .....	42
Figure 2.10b	The peak height ratio of treated DNA to control DNA is dependent on the pH of the incubation buffer.....	42

<b>List of Figures (continued)</b>	<b>Page</b>
Figure 2.11 Electropherograms showing the effects of the ionic strength of the running buffer on DNA analysis. ....	45
Figure 2.12 Relationship between the ionic strength of the running buffer and the migration time of the ternary complex.....	46
Figure 2.13a Relationship between the ionic strength of the running buffer and the peak height of the ternary complex .....	47
Figure 2.13b The peak height ratio of treated DNA to control DNA is dependent on the ionic strength of the incubation buffer.....	47
Figure 2.14 Electropherograms showing the effects of injection time on DNA analysis .....	48
Figure 2.15 Electropherograms showing the effects of injection voltage on DNA analysis.....	49
Figure 2.16 Electropherograms showing the effects of separation voltage on DNA analysis.....	50
Figure 2.17 Effects of incubation time and temperature .....	52
Figure 2.18 Electropherograms showing analyses of DNA extracted from GM04312C cells treated with various concentrations of BPDE for 30 min.....	53
Figure 2.19 Relationship between relative fluorescence intensity and BPDE concentration.....	54
Figure 2.20 Log-log plot of fluorescence intensity versus BPDE concentration .....	55
Figure 2.21 Histograms showing dose-response relationships with different primary antibodies .....	56
Figure 3.1 Major established pathway of metabolic activation of BaP, leading to the formation of BPDE-N <sup>2</sup> -dG.....	66
Figure 3.2 Repair of BPDE-DNA adducts in human fibroblasts (GM04312C). .....	75
Figure 3.3a Electropherograms obtained from DNA extracted from XPA cells pretreated for 24 h with different concentrations of iAs(III), and then incubated with 0.5 $\mu$ M BPDE for 30 min .....	77

<b>List of Figures (continued)</b>	<b>Page</b>
Figure 3.3b	Histograms representing the relative adduct levels after pretreatment with different iAs(III) concentrations ..... 77
Figure 3.4a	Electropherograms obtained from DNA extracted from XPA cells pretreated for 24 h with different concentrations of MMA(III), and then incubated with 0.5 $\mu$ M BPDE for 30 min ..... 78
Figure 3.4b	Histograms representing the relative adduct levels after pretreatment with different MMA(III) concentrations..... 78
Figure 3.5a	Electropherograms obtained from DNA extracted from XPA cells pretreated for 24 h with different concentrations of DMA(III), and then incubated with 0.5 $\mu$ M BPDE for 30 min ..... 79
Figure 3.5b	Histograms representing the relative adduct levels after pretreatment with different DMA(III) concentrations..... 79
Figure 3.6a	Electropherograms obtained from DNA extracted from XPA cells pretreated for 24 h with different concentrations of iAs(V), and then incubated with 0.5 $\mu$ M BPDE for 30 min ..... 80
Figure 3.6b	Histograms representing the relative adduct levels after pretreatment with different iAs(V) concentrations ..... 80
Figure 3.7a	Electropherograms obtained from DNA extracted from XPA cells pretreated for 24 h with different concentrations of MMA(V), and then incubated with 0.5 $\mu$ M BPDE for 30 min ..... 81
Figure 3.7b	Histograms representing the relative adduct levels after pretreatment with different MMA(V) concentrations ..... 81
Figure 3.8a	Electropherograms obtained from DNA extracted from XPA cells pretreated for 24 h with different concentrations of DMA(V), and then incubated with 0.5 $\mu$ M BPDE for 30 min ..... 82
Figure 3.8b	Histograms representing the relative adduct levels after pretreatment with different DMA(V) concentrations..... 82
Figure 3.9	Effects of iAs(III), MMA(III), DMA(III), iAs(V), MMA(V) and DMA(V) on the colony formation ability of GM04312C cells ..... 85

<b>List of Figures (continued)</b>	<b>Page</b>
Figure 3.10 Effects of iAs(III), MMA(III), DMA(III), iAs(V), MMA(V) and DMA(V) on the cell numbers of GM04312C cells. ....	86
Figure 3.11 The effect of iAs(III) on the enhancement of BPDE-DNA adduct formation is time-dependent .....	88
Figure 3.12 The effect of MMA(III) on the enhancement of BPDE-DNA adduct formation is time-dependent. ....	88
Figure 3.13 Effects of arsenic on cellular reduced GSH levels.....	91
Figure 3.14 Effects of arsenic on the activity of GST.....	94
Figure 3.15 DNA denaturation sensitivity of GM00038B and GM04312C cells with or without UVC irradiation .....	98
Figure 3.16 DNA denaturation sensitivity measured by the HCl/AO assay on 80-90% confluent GM04312C cells after treatment with various arsenic compounds for 24 h .....	99
Figure 3.17 Effects of the pretreatment with various arsenic species on the cellular uptake of BPDE .....	102
Figure 3.18 iAs(III) increased the cellular uptake of BPDE in a concentration-dependent manner .....	105
Figure 3.19 MMA(III) increased the cellular uptake of BPDE in a concentration-dependent manner .....	105
Figure 4.1 Proposed model for mammalian nucleotide excision repair (NER) .....	121
Figure 4.2 Proposed model for mammalian base excision repair (BER).....	122
Figure 4.3a Electropherograms obtained from DNA extracted from HNF cells incubated with 1 $\mu$ M BPDE for 30 min followed by repair for 24 h in the presence of different concentrations of iAs(III).....	130
Figure 4.3b Histograms representing the relative adduct levels after repair for 24 h in the presence of different iAs(III) concentrations. ....	130
Figure 4.4a Electropherograms obtained from DNA extracted from HNF cells incubated with 1 $\mu$ M BPDE for 30 min followed by repair for 24 h in the presence of different concentrations of MMA(III). ....	131

<b>List of Figures (continued)</b>	<b>Page</b>
Figure 4.4b	Histograms representing the relative adduct levels after repair for 24 h in the presence of different MMA(III) concentrations..... 131
Figure 4.5a	Electropherograms obtained from DNA extracted from HNF cells incubated with 1 $\mu$ M BPDE for 30 min followed by repair for 24 h in the presence of different concentrations of DMA(III)..... 132
Figure 4.5b	Histograms representing the relative adduct levels after repair for 24 h in the presence of different DMA(III) concentrations. .... 132
Figure 4.6a	Electropherograms obtained from DNA extracted from HNF cells incubated with 1 $\mu$ M BPDE for 30 min followed by repair for 24 h in the presence of different concentrations of iAs(V)..... 133
Figure 4.6b	Histograms representing the relative adduct levels after repair for 24 h in the presence of different iAs(V) concentrations. .... 133
Figure 4.7a	Electropherograms obtained from DNA extracted from HNF cells incubated with 1 $\mu$ M BPDE for 30 min followed by repair for 24 h in the presence of different concentrations of MMA(V) ..... 134
Figure 4.7b	Histograms representing the relative adduct levels after repair for 24 h in the presence of different MMA(V) concentrations..... 134
Figure 4.8a	Electropherograms obtained from DNA extracted from HNF cells incubated with 1 $\mu$ M BPDE for 30 min followed by repair for 24 h in the presence of different concentrations of DMA(V) ..... 135
Figure 4.8b	Histograms representing the relative adduct levels after repair for 24 h in the presence of different DMA(V) concentrations ..... 135
Figure 4.9	Inhibition of BPDE-DNA adduct repair by MMA(III) is time-dependent ..... 136
Figure 4.10	Repair kinetics of BPDE-DNA adducts in CRL2522 cells in the absence and presence of 5 $\mu$ M MMA(III). .... 137
Figure 4.11	Cell cycle profiles of BPDE-treated exponentially growing CRL2522 cells ..... 142

<b>List of Figures (continued)</b>	<b>Page</b>
Figure 4.12 Model of the assembly of the repair proteins involved upstream of GG- NER incision.....	146
Figure 4.13 Effects of 5 $\mu$ M MMA(III) on the expression of repair-related proteins XPA, p62, XPC, p53, and p21 during the repair of BPDE-DNA adducts over time .....	147
Figure 4.14 Temporal correlation between p53 levels and DNA repair efficiency after MMA(III) treatment.....	152

## List of Abbreviations

3-AB	3-aminobenzamide
Ab*	secondary antibody
Ab	primary antibody
Ag	antigen
AMS	accelerator mass spectrometry
AO	acridine orange
IAs	inorganic arsenic
iAs(III)	arsenite
iAs(V)	arsenate
AP	apurinic/apyrimidinic
APE1	5'-AP endonuclease
ATP	adenosine-5'-triphosphate
BaP	benzo(a)pyrene
BER	base excision repair
BPDE	benzo(a)pyrene diol epoxide
BPDE-N <sup>2</sup> -dG	the major adduct at the N <sup>2</sup> position of deoxyguanosine formed with BPDE
BPD-SG	the glutathione conjugate of BPDE
BSO	L-buthionine-S,R-sulfoximine
CDNB	1-chloro-2,4-dinitrobenzene
CE	capillary electrophoresis
CE-LIF	capillary electrophoresis laser induced fluorescence
CHO	Chinese hamster ovary
COX-2	cyclooxygenase-2
CPD	cyclobutane pyrimidine dimers
CYP1A1	cytochrome P-450 1A1
CZE	capillary zone electrophoresis
DABCO	1,4-diazobicyclo-[2,2,2]-octane
DDB2	damage-specific DNA-binding protein 2

DMA(III)	dimethylarsinous acid
DMA(V)	dimethylarsinic acid
DMSO	dimethylsulfoxide
ELISA	enzyme-linked immunosorbent assay
EOF	electroosmotic flow
Fpg	formamidopyrimidine glycosylase
GC	gas chromatography
$\gamma$ -GCS	$\gamma$ -glutamylcysteine synthetase
GG-NER	global genomic nucleotide excision repair
GGR	global genome repair
GPx	glutathione peroxidase
GR	glutathione reductase
GSH	reduced glutathione
GSSG	oxidized form of glutathione
GST	glutathione S-transferase
HPLC	high-performance liquid chromatography
HPRT	hypoxanthine phosphoribosyltransferase
IARC	International Agency for Research on Cancer
l	effective capillary length
L	total capillary length
LIF	laser induced fluorescence
LMPCR	ligation-mediated polymerase chain reaction
MCL	Maximum Contaminant Level
MMA(III)	monomethylarsonous acid
MMA(V)	monomethylarsonic acid
MMS	methylmethane sulfonate
MNU	N-methyl-N-nitrosourea
MRP2	multidrug resistance protein 2
MS	mass spectrometry
NA	numerical aperture
NER	nucleotide excision repair

NHF	normal human fibroblasts
PAH	polycyclic aromatic hydrocarbons
PARP	poly(ADP-ribose) polymerase
PBS	phosphate-buffered saline
PCNA	proliferating cell nuclear antigen
PMT	photomultiplier tube
PNK	polynucleotide kinase
pol	DNA polymerase
R	resolution
ROS	reactive oxygen species
SAM	S-adenosylmethionine
SSB	DNA single strand breaks
TCR	transcription-coupled repair
THF	tetrahydrofuran
TMA	trimethylarsine
TMAO	trimethylarsine oxide
$t_1$ and $t_2$	migration times of adjacent peaks
$t_m$	migration time of a solute
UDS	unscheduled DNA synthesis
UV	ultraviolet
V	applied voltage across the capillary
$w_1$ and $w_2$	peak widths of the same adjacent peaks
XPA	xeroderma pigmentosum complementation group A
XPC	xeroderma pigmentosum complementation group C
$\mu_{OBS}$	observed electrophoretic mobility
$\mu_{EP}$	electrophoretic mobility
$\mu_{EOF}$	electroosmotic mobility

# **Chapter One**

## **General Introduction**

### **1.1 Human Health Effects of Arsenic**

Arsenic, a metalloid, is a worldwide health concern due to both its cancerous and its noncancerous effects. Increased risk of skin, lung, bladder, and other internal cancers has been associated with chronic exposure to high arsenic concentrations (several hundred  $\mu\text{g/L}$ ) in drinking water (1-9). Occupational and medicinal exposure to arsenic has also been reported to increase the likelihood of developing various cancers (10-16). Aside from the carcinogenic effects, several studies have demonstrated that chronic ingestion of arsenic may have adverse effects on reproductive, neurological, cardiovascular, respiratory, hepatic, and hematological systems (1, 2, 17-26). In addition, manifestation of arsenic-related skin lesions and diabetes has also been reported.

### **1.2 Arsenic Occurrence and Exposure**

Arsenic is a natural occurring element in the earth's crust. When disturbed by mining activity, volcanic eruption or other natural processes, arsenic may be released into the environment. Burning of fossil fuels, ore smelting, and agricultural use of arsenic-containing compounds also introduce arsenic into the environment. High levels of arsenic in groundwater have been reported in areas rich in geological deposits of arsenic such as Taiwan, Argentina, Chile, Mexico, Thailand, China, Bangladesh, India, Finland, Romania, Hungary, and western sections of the United States (27). Drinking water industrially contaminated by arsenic is found in Japan, Australia, Greece, and Ghana.

In the general population, exposure to arsenic occurs primarily by ingestion of contaminated water and food. Inorganic arsenic (iAs) is the major form found in water. Concentrations are generally higher in groundwater than in surface water. Organic arsenic compounds, such as monomethylarsonic acid (MMA(V)) and dimethylarsinic acid (DMA(V)), which are usually biotransformation products, constitute a small percentage of the total arsenic in water (28). Food is a significant source of arsenic. In most food, iAs typically accounts for 65-75% of the total arsenic (28); however, organic arsenic compounds represent the majority of arsenic in food of marine origin. Arsenobetaine is the compound most commonly present in seafood. Its toxicity is low in humans and is rapidly excreted in urine. In seaweed and mussels, arsenic is predominantly present as arsenosugars, which are mainly metabolized to DMA(V) and can persist in the human body for a longer period of time than arsenobetaine (29).

### **1.3 Metabolism and Disposition of Arsenic**

iAs, including arsenite (iAs(III)) and arsenate (iAs(V)), is readily absorbed from the gastrointestinal tract. Once inside cells, iAs undergoes biomethylation, which is considered to be the major metabolic pathway for iAs (30). Glutathione (GSH) and other thiols (e.g., reduced lipoic acid) may act as reducing agents in the methylation process. After reduction by GSH or cysteine to its trivalent oxidation state, arsenic obtains methyl groups from S-adenosylmethionine (SAM) to become methylated (31). SAM is generally believed to be the main source of methyl groups for the methylation of arsenic and acts as a substrate for various methyltransferases involved in each methylation step. The generally accepted pathway for arsenic biomethylation is shown in **Figure 1.1**. Arsenic

methylating activity is localized mainly in the cytosol of hepatocytes. The capacity to methylate arsenic in other tissues is relatively low.

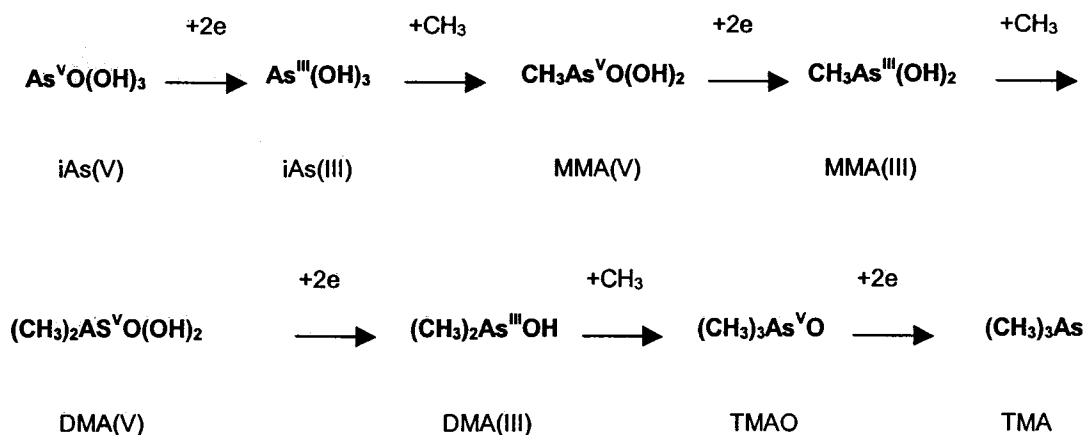


**Figure 1.1. Biomethylation of arsenic involving alternate reduction of pentavalent arsenic to trivalent arsenic followed by oxidative addition of a methyl group**

Humans methylate iAs to MMA(V), monomethylarsonous acid (MMA(III)), DMA(V), and dimethylarsinous acid (DMA(III)), and excrete these arsenic species in urine. In humans, the urinary content of metabolites of iAs generally consists of 10-30% iAs, 10-20% MMA(V), and 55-75% DMA(V). Further methylation of DMA(V) to trimethylarsine oxide (TMAO) and trimethylarsine (TMA) is not seen in humans but frequently occurs in microorganisms exposed to iAs(III). Differences in the methylation of iAs between animal species and among population groups have been observed. Most experimental animals methylate arsenic more efficiently and completely than humans and excrete less MMA(V) in urine (1). Some mammals (e.g., chimpanzee, marmoset monkey, and guinea pig) do not excrete MMA(V) but excrete mainly DMA(V) (1). Rats can methylate arsenic further to trimethylarsenicals (TMAO and TMA). TMAO has also been detected in trace percentages in urine from mice, hamsters, and humans following

exposure to DMA(V) (32). Pentavalent methylated metabolites such as MMA(V) and DMA(V) are readily excreted in urine. More efficient methylation means faster overall excretion of arsenic. However, trivalent arsenic species such as iAs(III), MMA(III), and DMA(III) are likely retained in tissues and result in increased toxicity.

#### 1.4 Toxicity and Carcinogenicity of Arsenic

The pentavalent methylated arsenic species have a higher rate of excretion and lower affinity for tissue sulfhydryl groups than iAs(III). This led to the conventional belief that methylation is a detoxification process. This belief was held for many years because MMA(V) and DMA(V), the primary excreted metabolites of iAs, are less acutely toxic than iAs(III) or iAs(V). However, it is now known that MMA(III) is more toxic than iAs(III) *in vitro* and *in vivo* (33), and DMA(III) is at least as cytotoxic as iAs(III) in most cell types (34). Taking into account the highly toxic metabolites MMA(III) and DMA(III), methylation is no longer considered a detoxification process. Pentavalent arsenic species are significantly less cytotoxic than their trivalent analogs (34). There is no apparent correlation between the susceptibility of cells to arsenic toxicity and their capacity to methylate iAs (34).

The exact mechanism of arsenic toxicity is not known, but several hypotheses have been proposed. At the biochemical level, iAs(V) may replace phosphate in many biochemical reactions because they have similar structures and properties. Depletion of adenosine-5'-triphosphate (ATP) by iAs(V) has been observed in cultured cells. In the trivalent state, inorganic and methylated arsenic may react with critical thiols in proteins and inhibit their activity. Inhibition of pyruvate dehydrogenase, NADPH-dependent

oxidoreductase, thioredoxin reductase, glutathione reductase (GR), and glutathione peroxidase (GPx) has been observed in different cell and cell-free systems.

Although there is sufficient epidemiological evidence to classify arsenic as a human carcinogen, its carcinogenic effects have not been conclusively demonstrated in laboratory animals (35). Arsenic compounds are therefore considered by the International Agency for Research on Cancer (IARC) as the only compounds for which there is sufficient evidence for human carcinogenicity but inadequate evidence for animal carcinogenicity (36). Lack of a good animal model has greatly hindered mechanistic studies of arsenic carcinogenesis and ultimately compromises the reliability of risk estimation in the current arsenic cancer risk assessment framework based on epidemiological studies of Taiwanese populations. An acceptable level of arsenic in drinking water remains under debate. The Maximum Contaminant Level (MCL) of arsenic in drinking water set by the U.S. Environmental Protection Agency is 10  $\mu\text{g/L}$  (37). The Canadian interim guideline level is 25  $\mu\text{g/L}$ , and this is under revision to a lower level.

So far, a variety of hypotheses regarding the carcinogenic modes of action of iAs have been proposed, involving both genetic and epigenetic mechanisms. They include genotoxicity, altered DNA methylation, altered DNA repair, oxidative stress, altered cell proliferation, co-carcinogenesis, and tumor promotion (38). However, no single hypothesis could explain all the adverse effects caused by arsenic. It may be naive to think of just one causative mode of action responsible for arsenic carcinogenicity (39).

Although no one single mechanism could be responsible for arsenic carcinogenicity, it is generally believed that direct DNA damage and the subsequent gene

mutation is not a major pathway of arsenic carcinogenesis. Arsenic causes chromosome abnormalities such as micronuclei and sister chromatid exchanges only at high (toxic) concentrations (40). Unlike classical carcinogens, arsenic fails to induce point mutations in bacterial or mammalian cells (41). By contrast, considerable evidence has pointed to arsenic promoting mutagenesis / carcinogenesis, both in *in vivo* bioassays and in *in vitro* cell culture systems. At non-toxic concentrations, co-mutagenic effects of arsenic with X-rays, ultraviolet (UV) radiation, or alkylating agents have repeatedly been observed (40). In line with this, most of the animal experiments provided negative results and some even reported a decrease in tumor induction by arsenic alone (42). Based on current evidence, it seems reasonable to consider that arsenic acts as a co-carcinogen.

Co-mutagenicity / co-carcinogenicity of arsenic might well explain the non-responsiveness in terms of tumor development in laboratory animals challenged with iAs(III) alone and the relative ease with which tumors were initiated when arsenic compounds were co-administered with a potent carcinogen (an initiator). This co-carcinogenic mechanism might also shed light on human studies. Multiple exposures to more than one carcinogen are a better representation of the environmental conditions for humans than controlled exposure to a single carcinogen under laboratory conditions. Co-exposure to cigarette smoking and arsenic has been shown to be linked to elevated rates of lung cancer. The interaction between smoking and arsenic ingestion has been revealed in several epidemiological studies. However, this interaction reportedly ranges from being synergistic (43-46) or positive (47), to having no effect (48-50). Poor study designs and complicated exposure scenarios in epidemiological studies are likely responsible for

these inconsistencies. Evidence from *in vitro* cell culture studies may resolve this uncertainty.

The effect of arsenic on the mutagenicity of other carcinogens remains largely unknown since iAs neither affects DNA directly nor forms adducts with DNA (51). DNA adduct formation (covalent DNA modifications by exogenous or endogenous reactive chemical agents) has been shown to be necessary for tumorigenesis (52, 53) and the steady state adduct levels are often linearly related to tumorigenic response (54). Therefore, the objective of this investigation was to determine how arsenic modulates the formation and repair of steady state DNA adducts in human cells.

## 1.5 Scope of Thesis

This thesis has been divided into five chapters. **Chapter 1** presents general background information on arsenic, including its health effects, occurrence, exposure, metabolism, disposition, toxicity, and carcinogenicity. The rationale for the study hypotheses is based on arsenic co-carcinogenesis and the overall objective is to explore the effects of arsenic exposure on the formation and repair of DNA adducts generated by classical carcinogens. **Chapter 2** briefly reviews current methodologies for the detection of DNA adducts. Strengths and limitations associated with each method are highlighted. Experimentally, a capillary electrophoresis laser induced fluorescence (CE-LIF) based immunoassay, a highly sensitive method developed in our group, was optimized and applied to detect the DNA adducts induced by benzo(a)pyrene diol epoxide (BPDE) and alterations in damage levels caused by additional exposure to arsenic. BPDE is the ultimate mutagen of benzo(a)pyrene (BaP), a common environmental carcinogen produced from incomplete combustion of organic materials, such as from cigarette smoke

(55,56). **Chapter 3** examines the effects of arsenic on the formation of BPDE-DNA adducts. By employing a repair-deficient cell line, the effects of arsenic on the formation of DNA adducts were differentiated from the effects on DNA repair. Changes in the BPDE-DNA adduct levels brought about by arsenic pretreatment could therefore be attributed to arsenic effects on the damage formation step only. Uptake of BPDE into cells and chromatin accessibility to BPDE were assessed after arsenic treatment. BPDE is readily bound to cellular GSH to form an inactive conjugate. This conjugation is catalyzed by glutathione S- transferase (GST) (57,58). Both cellular GSH levels and GST activity after arsenic treatment were measured. **Chapter 4** examines the effects of arsenic on the repair of BPDE-DNA adducts. Confluent repair-proficient cells were used for this purpose. Following BPDE treatment, changes in remaining BPDE-DNA adduct levels in the presence of arsenic species were detected, which were attributed to arsenic effects on DNA repair. The underlying reasons for repair inhibition by arsenic were further explored by studying the arsenic effects on the expressions of some repair-related proteins. **Chapter 5** summarizes the conclusions generated from this study, discusses the implications of this research, and suggests future research directions.

## 1.6 References

1. NRC (National Research Council). (1999) *Arsenic in Drinking Water*. National Academy Press, Washington, DC
2. NRC (National Research Council). (2001) *Arsenic in Drinking Water (update)*. National Academy Press, Washington, DC
3. Chiu HF, Ho SC, Wang LY, Wu TN, Yang CY. (2004) Does arsenic exposure increase the risk for liver cancer? *J Toxicol Environ Health A*, 67, 1491-1500
4. Lamm SH, Engel A, Kruse MB, Feinleib M, Byrd DM, Lai S, Wilson R. (2004) Arsenic in drinking water and bladder cancer mortality in the United States: an analysis based on 133 U.S. counties and 30 years of observation. *J Occup Environ Med*, 46, 298-306
5. Karagas MR, Tosteson TD, Morris JS, Demidenko E, Mott LA, Heaney J, Schned A. (2004) Incidence of transitional cell carcinoma of the bladder and arsenic exposure in New Hampshire. *Cancer Causes Control*, 15, 465-472
6. Chen Y, Ahsan H. (2004) Cancer burden from arsenic in drinking water in Bangladesh. *Am J Public Health*, 94, 741-744
7. Guo HR. (2004) Arsenic level in drinking water and mortality of lung cancer (Taiwan). *Cancer Causes Control*, 15, 171-177
8. Steinmaus C, Yuan Y, Bates MN, Smith AH. (2003) Case-control study of bladder cancer and drinking water arsenic in the western United States. *Am J Epidemiol*, 158, 1193-1201

9. Bates MN, Rey OA, Biggs ML, Hopenhayn C, Moore LE, Kalman D, Steinmaus C, Smith AH. (2004) Case-control study of bladder cancer and exposure to arsenic in Argentina. *Am J Epidemiol*, 159, 381-389
10. Welch K, Higgins I, Oh M, Burchfield C. (1982) Arsenic exposure, smoking and respiratory cancer in copper smelter workers. *Arch Environ Health*, 37, 325-335
11. Axelson O, Dahlgren E, Jansson C-D, Rehnlund SO. (1978) Arsenic exposure and mortality: a case-referent study from a Swedish copper smelter. *Br J Ind Med*, 35, 8-15
12. Jarup, L., Pershagen, G., Wall, S. (1989) Cumulative arsenic exposure and lung cancer in smelter workers: a dose-response study. *Am J Ind Med*, 15, 31-41
13. Enterline, P.E., Day, R., Marsh, G.M. (1995) Cancers related to exposure to arsenic at a copper smelter. *Occup Environ Med*, 52, 28-32
14. Taylor P.R., Qiao, Y.L., Schatzkin, A., Yao, S.X., Lubin, J., Mao, B.L., Rao, J.Y., McAdams, M., Xuan, X.Z., Li, J.Y. (1989) Relation of arsenic exposure to lung cancer among tin miners in Yunnan Province, China. *Br J Ind Med*, 46, 881-886
15. Robson AO, Jelliffe AM. (1963) Medicinal arsenic poisoning and lung cancer. *Br Med J*, 2, 204-209
16. Jolliffe DM. (1993) A history of the use of arsenicals in man. *J R Soc Med*, 86, 287-289
17. Calderon J, Navarro ME, Jimenez-Capdeville, ME, Santos-Diaz MA, Golden A, Rodriguez-Leyva I, Borja-Aburto V, and Diaz-Barriga F. (2001) Exposure to arsenic and lead and neuropsychological development in Mexican children. *Environ Res*, 85, 69-76

18. Ahsan H, Perrin M, Rahman A, Parvez F, Stute M, Zheng Y, Milton AH, Brandt-Rauf P, van Green A and Graziano J. (2000) Associations between drinking water and urinary arsenic levels and skin lesions in Bangladesh. *J Occup Environ Med*, 42, 1195-1201
19. Ahmad S, Sayed MH, Barua S, Khan MH, Faruquee MH, Jalil A, Hadi SA and Talukder HK. (2001) Arsenic in drinking water and pregnancy outcomes. *Environ Health Perspect*, 109, 629-631
20. Chen CJ, Hsueh YM, Lai MS, Shyu MP, Chen SY, Wu MM, Kuo TL and Tai TY. (1995) Increased prevalence of hypertension and long-term arsenic exposure. *Hypertension*, 25,53-60
21. Milton AH, Smith W, Rahman B, Hasan Z, Kulsum U, Dear K, Rakibuddin M, Ali A. (2005) Chronic arsenic exposure and adverse pregnancy outcomes in Bangladesh. *Epidemiology*, 16, 82-86
22. Lai MS, Hsueh YM, Chen CJ, Shyu MP, Chen SY, Kuo TL, Wu MM and Tai TY. (1994) Ingested inorganic arsenic and prevalence of diabetes mellitus. *Am J Epidemiol*, 139, 484-492
23. Mazumder DN, Haque R, Ghosh N, De BK, Santra A, Chakraborti D and Smith AH. (2000) Arsenic in drinking water and the prevalence of respiratory effects in West Bengal, India. *Int J Epidemiol*, 29, 1047-1052
24. Mukherjee SC, Rahman MM, Chowdhury UK, Sengupta MK, Lodh D, Chanda CR, Saha KC, Chakraborti D. (2003) Neuropathy in arsenic toxicity from groundwater arsenic contamination in West Bengal, India. *J Environ Sci Health Part A*, 38, 165-183

25. Rahman M, Tondel M, Ahmad SA and Axelson O. (1998) Diabetes mellitus associated with arsenic exposure in Bangladesh. *Am J Epidemiol*, 148, 198-203
26. Rodriguez VM, Jimenez-Capdeville ME, Giordano M. (2003) The effects of arsenic exposure on the nervous system. *Toxicol Lett*, 145, 1-18
27. Nordstrom DK. (2002) Public health. Worldwide occurrences of arsenic in drinking water. *Science*, 296, 2143-2145
28. Pontius FW, Brown KG, Chen C-J. (1994) Health implications of arsenic in drinking water. Special issue: Arsenic: the Quest for Answers. *Am Water Works Assoc J*, 86, 52-63
29. Le XC, Cullen WR and Reimer KJ. (1994) Human urinary arsenic excretion after one time ingestion of seaweed, crab and shrimp. *Clin Chem*, 40, 617-625
30. Aposhian HV. (1997) Enzymatic methylation of arsenic species and other new approaches to arsenic toxicity. *Annu Rev Pharmacol Toxicol*, 37, 397-419
31. Cullen WR, McBride BC and Reglinski J. (1984) The reaction of methylarsenicals with thiols: Some biological implications. *J Inorg Biochem*, 21, 179-194
32. Kenyon EM and Hughes MF. (2001) A concise review of the toxicity and carcinogenicity of dimethylarsinic acid. *Toxicology*, 160, 227-236
33. Petrick JS, Ayala-Fierro F, Cullen WR, Carter DE, Aposhian HV. (2000) Monomethylarsonous acid (MMA(III)) is more toxic than arsenite in Chang human hepatocytes. *Toxicol Appl Pharmacol*, 163, 203-207
34. Styblo M, Del Razo LM, Vega L, Germolec DR, LeCluyse EL, Hamilton GA, Reed W, Wang C, Cullen WR, Thomas DJ. (2000) Comparative toxicity of trivalent and

- pentavalent inorganic and methylated arsenicals in rat and human cells. *Arch Toxicol*, 74, 289-299
35. Huff J, Chan P and Nyska A. (2000) Is the human carcinogen arsenic carcinogenic to laboratory animals? *Toxicol Sci*, 55, 17-23
36. IARC (International Agency for Research on Cancer) (1980) IARC Monographs on the Evaluation of the Carcinogenic Risk of Chemicals to Humans: Some Metals and Metallic Compounds, Vol. 23. Lyon, France
37. U.S. Environmental Protection Agency (2001) Proposed Guidelines for Carcinogen Risk Assessment. (EPA/600/P-92/003C April 1996). *Fed Reg*, 61, 17960-18011 ([www.epa.gov/ncea/raf/cra\\_prop.html](http://www.epa.gov/ncea/raf/cra_prop.html))
38. Hughes MF. (2002) Arsenic toxicity and potential mechanisms of action. *Toxicol Lett*, 133, 1-16
39. Kitchin KT. (2001) Recent advances in arsenic carcinogenesis: modes of action, animal model systems, and methylated arsenic metabolites. *Toxicol Appl Pharmacol*, 172, 249-261
40. Gebel TW. (2001) Genotoxicity of arsenical compounds. *Int J Hyg Environ Health*, 203, 249-262
41. Simeonova PP and Luster MI. (2000) Mechanisms of arsenic carcinogenicity: genetic or epigenetic mechanisms? *J Environ Pathol Toxicol Oncol*, 19, 281-286
42. Wang Z, Rossman TG. (1996) The carcinogenicity of arsenic. In: Chang LW, Magos L, Suzuki T, eds. *Toxicology of Metals*. Lewis Publishers. pp 221-229

43. Hertz-Picciotto I, Smith AH, Holtzman D, Lipsett M and Alexeeff G. (1992) Synergism between occupation arsenic exposure and smoking in the induction of lung cancer. *Epidemiology*, 3, 23-31
44. Pershagen G, Wall S, Taube A and Linnman L. (1981) On the interaction between occupational arsenic exposure and smoking and its relationship to lung cancer. *Scand J Work Environ Health*, 7, 302-309
45. Ferreccio C, Gonzalez C, Milosavjevic V, Marshall G, Sancha AM and Smith AH. (2000) Lung cancer and arsenic concentrations in drinking water in Chile. *Epidemiology*, 11, 673-679
46. Tsuda T, Babazono A, Yamamoto E, Kurumatani N, Mino Y, Ogawa T, Kishi Y and Aoyama H. (1995) Ingested arsenic and internal cancer: a historical cohort study followed for 33 years. *Am J Epidemiol*, 141, 198-209
47. Jarup L and Pershagen G. (1991) Arsenic exposure, smoking and lung cancer in smelter workers — a case control study. *Am J Epidemiol*, 134, 545-551
48. Rencher AC, Carter MW and McKee DW. (1977) A retrospective epidemiological study of mortality at a large western copper smelter. *J Occup Med*, 19, 754-758
49. Taylor PR, Qiao YL, Schatzkin A, Yao SX, Lubin J, Mao BL, Rao JY, McAdams M, Xuan XZ and Li JY. (1989) Relation of arsenic exposure to lung cancer among tin miners in Yunan Province, China. *Br J Ind Med*, 46, 881-886
50. Welch K, Higgins I, Oh M and Burchfiel C. (1982) Arsenic exposure, smoking and respiratory cancer in copper smelter workers. *Arch Environ Health*, 37, 325-335

51. Gradecka D, Palus J and Wasowicz W. (2001) Selected mechanisms of genotoxic effects of inorganic arsenic compounds. *Int J Occup Med Environ Health*, 14, 317-328
52. Poirier MC. (1997) DNA adducts as exposure biomarkers and indicators of cancer risk. *Environ Health Perspect*, 105 (Suppl 4), 907-912
53. Poirier MC and Weston A. (1996) Human DNA adduct measurements: State of the art. *Environ Health Perspect*, 104 (Suppl 5), 883-893
54. Nestmann ER, Bryant DW and Carr CJ. (1996) Toxicological significance of DNA adducts: summary of discussions with an expert panel. *Regul Toxicol Pharmacol*, 24, 9-18
55. Hecht SS. (1999) Tobacco smoke carcinogens and lung cancer. *J Natl Cancer Inst*, 91, 1194-1210
56. Phillips DH. (2002) Smoking-related DNA and protein adducts in human tissue. *Carcinogenesis*, 23, 1979-2004
57. Srivastava SK, Watkins SC, Schuetz E and Singh SV. (2002) Role of glutathione conjugate efflux in cellular protection against benzo[a]pyrene-7,8-diol-9,10-epoxide-induced DNA damage. *Mol carcinog*, 33, 156-162
58. Hesse S, Jernstrom B, Martinez M, Guenther T, Orrënius S, Christodoulides L, Ketterer B. (1982) Inactivation of DNA-binding metabolites of benzo[a]pyrene benzo[a]pyrene-7,8-dihydrodiol by glutathione and glutathione S-transferases. *Carcinogenesis*, 3, 757-760

## Chapter Two

### **Method Development for the Detection of Benzo(a)pyrene Diol Epoxide-DNA Adducts**

#### **2.1 Introduction**

Until the early 1980s, use of radiolabelled carcinogens was the major method to determine DNA adduct formation (1-4). This technique provides the most straightforward evidence for the binding of chemical carcinogens to DNA. After exposure to either  $^3\text{H}$  or  $^{14}\text{C}$ -labelled test substances, DNA is isolated from the cells or tissues under investigation, and the amount of radioactivity associated with the DNA is determined by liquid scintillation counting. It is essential that the label be located in a position that is resistant to loss during metabolism or formation of adducts to avoid false negatives. Indirect DNA damage caused by oxygen radicals or lipid peroxidation induced by a treatment cannot be detected by this method. On the other hand, the presence of radioactivity in purified DNA does not necessarily mean that DNA adducts are formed because in some cases substantial metabolic incorporation of the radiolabel into normal nucleotides can occur (5-7). To distinguish between metabolic incorporation and adduct formation, DNA has to be hydrolyzed to nucleotides or purine/pyrimidine bases, which are chromatographically separated, provided that sufficient radioactivity is available. However,  $^3\text{H}$ -labelled polycyclic aromatic hydrocarbons (PAH) present an additional problem for hydrolysis and chromatography of DNA because substantial radioactivity of unknown identity is lost (4). Moreover, in experiments performed with a  $^3\text{H}$  label, the loss or incorporation of the label through the hydrogen exchange process is possible, resulting in misleading results (8). In order to be able to measure 1 adduct per  $10^6$  or  $10^7$  nucleotides, the scintillation

counting (radioisotope decay) assay requires sufficiently high specific activity, or, where possible, needs to be performed on large DNA samples that can provide significant numbers of decay events.

In the late 1970s, accelerator mass spectrometry (AMS) was used to detect radioactivity. AMS is a nuclear physics technique used to measure isotope ratios with high selectivity, sensitivity, and precision (9,10). It involves the selection of ions on the basis of charge-changing, momentum, charge, energy, and energy loss before each ion is uniquely identified and counted by the detector. Measurement of DNA adducts with  $^{14}\text{C}$ -labelled carcinogens involves the isolation of carbon from purified DNA by oxidizing the sample directly to  $\text{CO}_2$ ,  $\text{N}_2$ , and  $\text{H}_2\text{O}$ . The  $\text{CO}_2$  is separated cryogenically and reduced to filamentous graphite before introduction into the ion source.  $^{14}\text{C}$  is measured as the isotope ratio  $^{14}\text{C}/^{13}\text{C}$  and converted to quantities by analysis of the total carbon content of the sample analyzed. AMS is used primarily to detect  $^{14}\text{C}$ , but can be used for other isotopes with a half-life of 10 years or longer (11, 12), which is not possible with conventional decay counting methods. AMS measurements are independent of the decay rate since AMS measures directly the number of isotope nuclei. Because there is between 1% and 10% of  $^{14}\text{C}$  in the sample relative to 0.01% for decay counting of radiocarbon, AMS offers a  $10^5$ -fold to  $10^6$ -fold improvement relative to decay counting for  $^{14}\text{C}$  measurement (11). For  $^3\text{H}$ , AMS offers approximately a  $10^3$ -fold improvement in sensitivity (11). DNA adduct analysis by AMS can be done with lower specific activities and smaller quantities of isotope than is practical with decay counting. Currently, AMS is the most sensitive quantitative method for DNA adduct measurement and can achieve the exceptional sensitivity of 1 adduct /  $10^{12}$  nucleotides (13). However, AMS provides no

information on the chemical form of the isotope and thus has the potential to provide false positives when genomic DNA isolates are measured. Confirmatory studies are often necessary to show that isotopes in the DNA are actually due to DNA adducts. Additionally, current AMS instrumentation is very expensive and only a few researchers have direct access to the equipment for DNA adduct analysis.

Due to the costs associated with the preparation of radiolabelled material and the hazards associated with its use, an array of techniques involving the use of non-radiolabelled carcinogens have been emerging for DNA adduct analysis. Among others,  $^{32}\text{P}$ -postlabelling stands out as the most commonly used assay for DNA adducts (14-17). In this method, adducted DNA is enzymatically digested to 3'-monophosphates of normal and adducted nucleotides, and the latter are then enriched and labelled at the 5'-end with  $^{32}\text{P}$  using polynucleotide kinase and [ $\gamma$ - $^{32}\text{P}$ ] adenosine-5'-triphosphate (ATP). The  $^{32}\text{P}$ -labelled adducted nucleotides are separated from  $^{32}\text{P}$ -labelled normal nucleotides by thin-layer chromatography, detected by exposure to X-ray film or scanning by electronic autoradiography, and quantified by measuring  $^{32}\text{P}$  incorporation. This method allows the detection of adducts from different chemicals with diverse structures. It requires only a small quantity of DNA (2-10  $\mu\text{g}$ ) and can detect 1 adduct /  $10^9$  nucleotides. Because it does not provide structural information for DNA adducts,  $^{32}\text{P}$ -postlabelling is prone to producing false positives and artifacts. Furthermore, the  $^{32}\text{P}$ -postlabelling assay may underestimate adduct levels because of incomplete DNA digestion, inefficiency of adduct labelling, and/or loss of adducts during enrichment and separation (8, 11). The labelling efficiency is often unknown and uncontrolled. Results from different laboratories are usually not comparable (18). Endogenous DNA adducts, called I-compounds (present at

levels as high as about 1 adduct per  $10^7$  DNA nucleotides), may co-migrate with adducts derived from aromatic carcinogens; intensification of I-compounds by the treatment may also occur. Both make adduct scoring subjective and interpretation of results difficult (8). Therefore, the quantitative data from  $^{32}\text{P}$ -postlabelling should be interpreted with caution.

Techniques that rely on knowledge of the structure and properties of particular DNA adducts to be detected include high performance liquid chromatography (HPLC), capillary electrophoresis (CE), capillary electrochromatography with electrochemical detection (19-21), fluorescence and phosphorescence spectroscopy (22-26), mass spectrometry (MS) (27-30), gas chromatography-mass spectrometry (GC-MS) (31-33), immunoassays and immunohistochemistry using adduct-specific anti-sera (34-39). Enzymatic digestion of adducted DNA is often needed before chromatographic separation. MS is probably the only universal technique for analysis of any particular DNA adduct, whereas electrochemical detection, fluorescence detection, and other spectroscopic detections either require fluorescence postlabelling or are restricted to certain classes of DNA adducts. In gas chromatographic techniques there is also a need to derivatize the carcinogen moiety from DNA adducts after hydrolysis prior to GC analysis. Suitable internal standards are needed to evaluate the efficiency of the hydrolysis or derivatization procedures for accurate quantification.

Since their inception in the mid-1970s, immunoassays have been in increasing use. With either monoclonal or polyclonal antibodies, immunoassays can be used for the analysis of a wide range of DNA adducts. Generally speaking, immunoassays are reliable and have good relative specificity because the antibodies employed to recognize adducts in the samples are elicited specifically against the adducts under investigation. In

addition, immunoassays are inexpensive and relatively easy to perform. However, this method requires immunization of animals with an immunogen and it is necessary to characterize the antibody and to minimize cross-reaction (11).

Methods for DNA adduct measurement that utilize repair enzymes have also been reported. One of the most sensitive is the alkyltransferase assay in which a bacterial alkyltransferase enzyme is used to measure O<sup>6</sup>-alkylguanine-type adducts in DNA in competition with an end-labelled oligonucleotide containing a single residue of O<sup>6</sup>-methylguanine (40). Unrepaired oligonucleotide probes are immunoprecipitated prior to radiocounting. Assays with similar competitive formats include the detection of 8-oxodeoxyguanosine using a bacterial repair enzyme, formamidopyrimidine glycosylase (Fpg)/exonuclease III, and the detection of bulky DNA lesions by use of the UvrABC excinuclease protein complex (41). However, use of these assays has been restricted by the availability of purified enzymes. Construction of substrates is critical for the purification of the enzymes (42). Alternatively, adducts can be enzymatically or chemically converted into DNA strand breaks and measured by the single cell gel electrophoresis (comet) assay.

An ingenious method that can detect adducts at specific nucleotides in particular genes such as p53 or hypoxanthine phosphoribosyltransferase (HPRT) was developed by Pfeifer et al. (43); it combines the use of the UvrABC excinuclease complex with ligation-mediated polymerase chain reaction (LMPCR). Gel electrophoresis, electroblotting, and hybridization follow after enzymatic digestion of adducted DNA and PCR amplification. The success of this technique depends in large part on the specificity

and efficiency of the cleavage reaction. Commonly used techniques for DNA adduct measurement are summarized in **Table 2.1**.

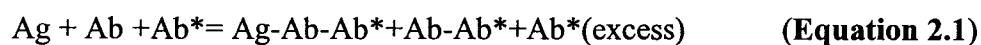
**Table 2.1. Characteristics of different techniques for the analysis of DNA adducts (adapted from [12], [18], [44])**

Method	Sensitivity adducts/ $10^8$ nts	DNA needed $\mu\text{g}$	Cost	Comments
Accelerated mass spectrometry	0.0026	500	High	use of radioactive substances
$^{32}\text{P}$ -postlabelling	0.1	2-10	Medium	- danger of underestimation - interference of "endogenous" spots - enzymatic digestion, enrichment - use of radioactive material - incomparable results
Fluorescence	0.5-7	>100	Low	- highly restrictive - requires fluorescence postlabelling - hydrolysis
Electrochemical detection	1-100	>100	Low	- highly restrictive - hydrolysis
Mass spectrometry	0.3-40	>100	High	- hydrolysis - derivatization needed in GC
Immunoassay	1-4	>100	Low	- reliable - interference of substances that compete with antibody recognition

## 2.2 Immunoassay Using Capillary Electrophoresis-Laser Induced Fluorescence Detection

After analyzing and weighing the strengths and limitations associated with the various techniques mentioned above, our group developed an immunoassay aimed at creating a “generic” method for DNA adduct measurement, as long as antibodies against the DNA adducts are available. This assay uses a monoclonal antibody against modified bases of interest in intact DNA. It requires minimal sample manipulation and no enzymatic digestion of DNA and is technically less involved. Unlike conventional immunoassays, especially the enzyme-linked immunosorbent assay (ELISA), this assay does not use microtiter wells, obviating the non-specific binding of antibodies to the solid phase substrate coated on the wells. Rather, the immunoreaction takes place in solution. A fluorescently-labelled secondary antibody fragment is used as a detection probe for highly sensitive laser induced fluorescence (LIF) detection.

In this immunoassay, an excess of both secondary (Ab\*) and primary (Ab) antibodies over the antigens (Ag) is required. Operationally, the primary antibody is titrated to give maximal response without creating an unnecessarily high background and wasting reagents while the secondary antibody should be sufficiently saturating to detect all the bound primary antibody, but not so excessive as to create high background. The immunoreaction is shown below (**Equation 2.1**) and is schematically represented in **Figure 2.1**.



Fluorescently-labelled secondary antibody-bound species are separated by CE and monitored using laser induced fluorescence (LIF) emitted by the fluorescently-tagged species. The general principle of capillary zone electrophoresis (CZE) is introduced in the **Appendix**. Capillary electrophoresis separation of the above mixture (**Figure 2.1** and **Equation 2.1**) results in two detectable peaks. The first eluting peak was attributed to the mixture of the binary complex Ab-Ab\* and excess Ab\*, and the second peak to the ternary complex Ag-Ab-Ab\*. The latter peak may split into multiple peaks under certain conditions. Coupling of CE with LIF detection with its renowned sensitivity is applicable to single molecule detection (45). An added bonus to the capillary electrophoresis-laser induced fluorescence (CE-LIF) based immunoassay is that any non-covalent association of a chemical carcinogen and its metabolites with DNA or contamination with proteins and RNA bound to chemicals can be removed during CE separation.

By means of this CE-LIF based immunoassay, thymine glycol was detected at the zeptomole ( $10^{-21}$  mol) level and used to study inducible DNA repair in response to a priming dose of 25 rad prior to a 2 Gy (1 Gy=100 rad) exposure (46), a clinically relevant dose for radiotherapy. This immunoassay was also employed to measure DNA adducts induced by benzo(a)pyrene diol epoxide (BPDE) in lung adenocarcinoma A549 cells (47-49). The CE-LIF based immunoassay requires only 0.5-2  $\mu\text{g}$  of DNA compared to 200-500  $\mu\text{g}$  of DNA in conventional immunoassays (44).

To validate this CE-LIF based immunoassay for the detection of BPDE-DNA adducts in other cell lines, and especially to optimize the experimental conditions to achieve our goal, a series of experiments was carried out, which included optimizing the immunoreaction conditions such as the pH and ionic strength of the incubation buffer,

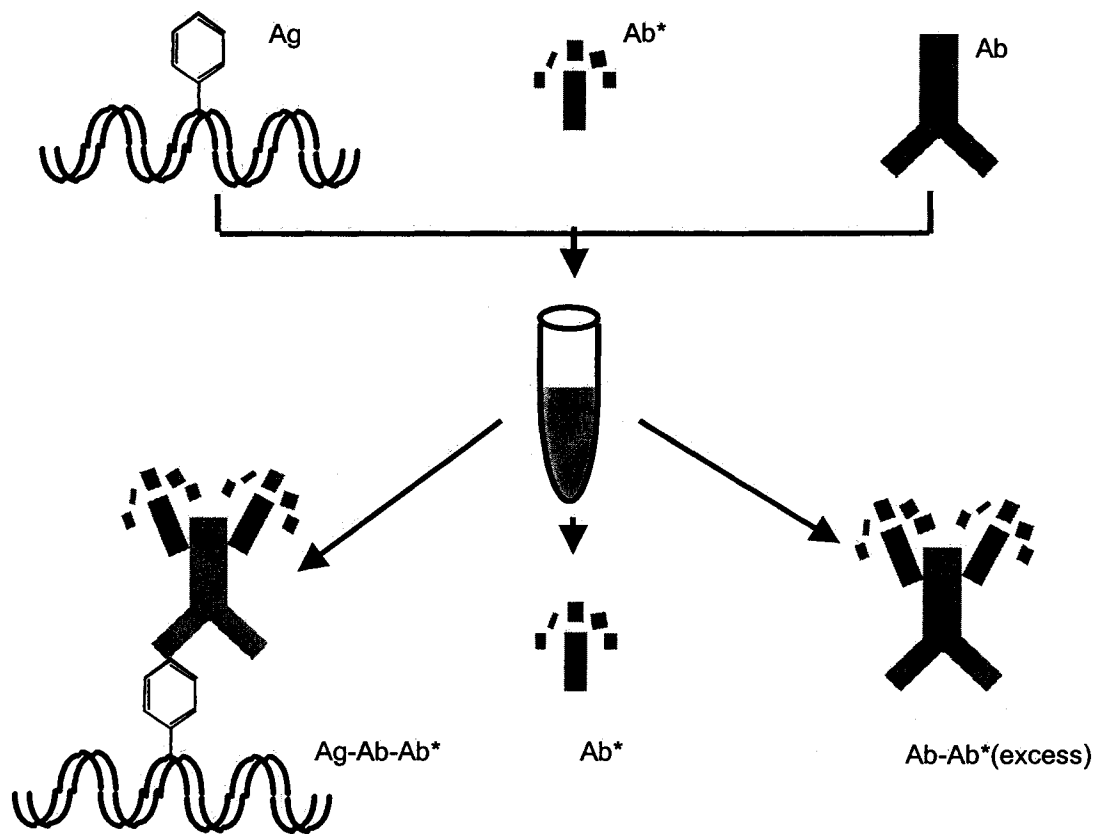


**Figure 2.1. Immunoreaction between adducted DNA (Ag) and primary (Ab) and secondary (Ab\*) antibodies**

incubation time, and temperature and optimizing the electrophoretic conditions such as the pH and ionic strength of the running buffer, injection time and voltage, and separation voltage.

## **2.3 Experimental**

### **2.3.1 Materials**

Racemic anti-BPDE was supplied by the NCI Chemical Carcinogen Repository (Midwest Research Institute, Kansas City, MO). To avoid hydrolysis of the epoxide, a stock of BPDE was always prepared fresh by dissolving BPDE in anhydrous tetrahydrofuran (THF) (>99.9% purity, Sigma-Aldrich, St. Louis, MO) immediately before use. Methylarsine oxide ( $\text{CH}_3\text{As}^{\text{III}}\text{O}$ ), kindly provided by Dr. WR Cullen (University of British Columbia, Vancouver, BC), was used as the precursor to monomethylarsonous acid (MMA(III)). A stock solution was prepared by dissolving the precursor in deionized water to a final concentration of 10 mM. To prevent oxidation of the trivalent methylated arsenic species, the stock solution was prepared shortly before the experiment.

### **2.3.2 Cells and cell cultures**

GM04312C cells (SV40 transformed XP complementation group A (XPA) GM02345 fibroblasts) were obtained from NIGMS Human Genetics Cell Repository (Camden, NJ). GM02345 harbors a G-to-C transversion at the 3-prime splice acceptor and results in missplicing of XPA. GM04312C cells were cultivated in Dulbecco's modified Eagle's medium/nutrient mixture F-12 (1:1 ratio) (Gibco BRL, Rockville, MD) supplemented with 10% fetal bovine serum. The cells were seeded in 100-mm dishes at a density of  $1 \times 10^6$  cells per dish and maintained at 37 °C in humidified air containing 5%

CO<sub>2</sub>. At 80%-90% confluence, the cells were incubated with BPDE for 30 min or pretreated with arsenic for 24 h before addition of BPDE, if required. The cells were washed with phosphate-buffered saline (PBS) after each drug treatment.

### **2.3.3 DNA isolation**

Cells were lysed in DNAzol® reagent (Invitrogen Life Technologies) and genomic DNA was precipitated with ice-cold 99.9% ethanol and washed twice with cold 70% ethanol. The DNA pellet was then air-dried and resuspended in deionized water and the solution was placed in an incubator at 37 °C overnight to facilitate the redissolution of DNA. DNA concentrations were measured at 260 nm using a SmartSpec™ 3000 spectrometer (Bio-Rad Laboratories, Cambridge, MA). The final concentration of DNA was brought to 250 µg/ml in water before analysis.

### **2.3.4 Instrumentation**

A laboratory-built CE-LIF system was used (50). A schematic is shown in **Figure 2.2**. Electrophoresis was driven by a high-voltage power supply (CZE 1000R, Spellman High Voltage Electronics, Plainview, NY). The parameters, including the sample injection time and voltage, separation voltage, and run time, were controlled by LabVIEW (National Instruments, Austin, TX) program on a Power Macintosh 7600/120 computer via a PCI-MIO-16XH-18 input/output board and an interface box (I-V converter). The capillaries used for these experiments were made of uncoated fused silica (Polymicro Technologies, Phoenix, AZ), with 20 µm i.d., 150 µm o.d., 25 cm total length, and 19 cm effective length. The injection end of the capillary was placed in a sample solution or running buffer, along with an electrode connected from the power

supply at a positive polarity. The other end of the capillary was inserted through a grounded holder and into a waste vial.

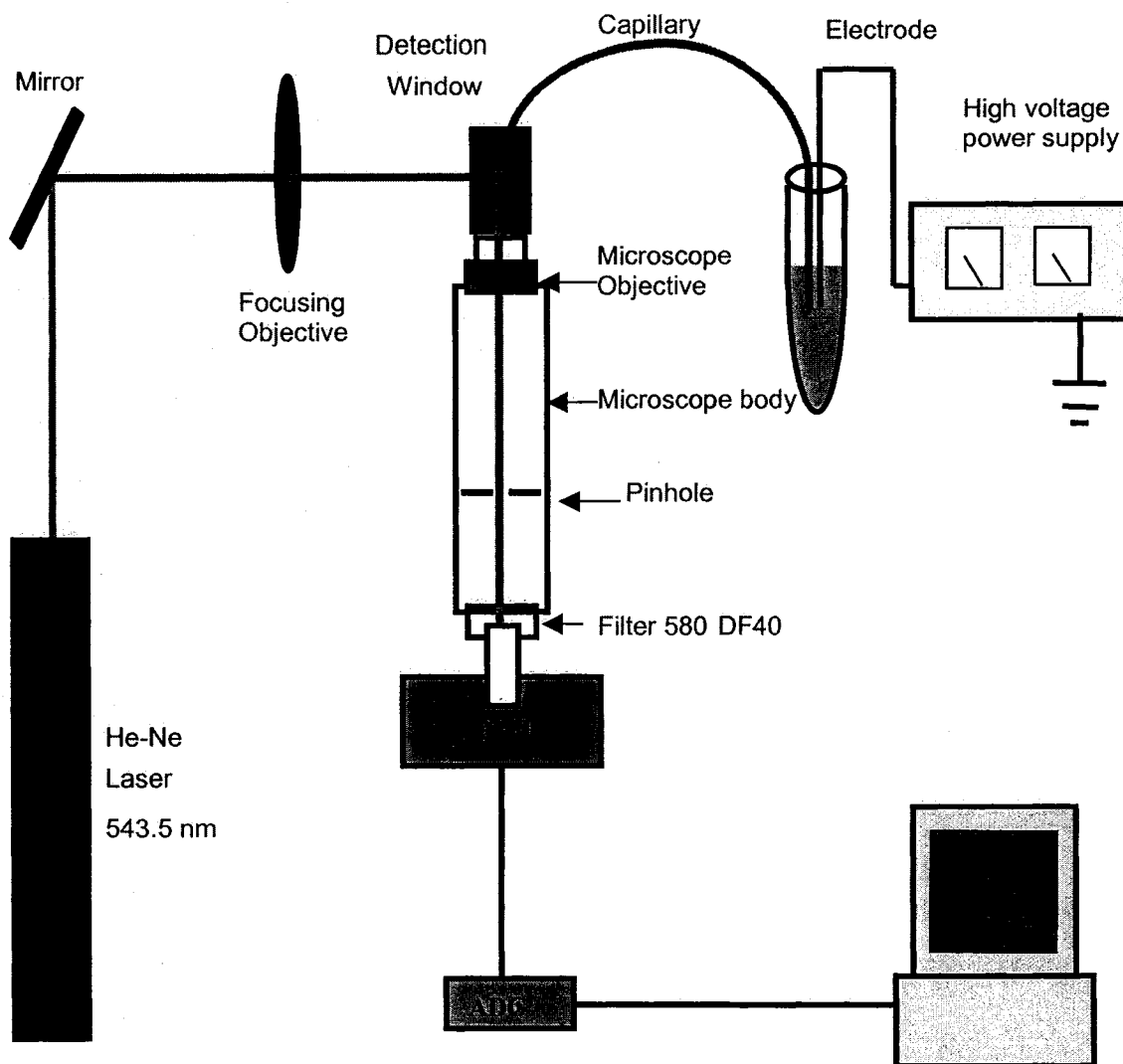


**Figure 2.2. Schematic of the home-built capillary electrophoresis laser-induced fluorescence (CE-LIF) instrument**

The LIF detector was built on an optical table using both commercial equipment and custom-made accessories. A green helium-neon laser (Melles Griot, Irvine, CA) with a 5 mW maximum output and an excitation wavelength of 543.5 nm was focused onto the capillary through a 6.3×, Numerical Aperture (NA) 0.2 microscope objective (Melles Griot), and fluorescence was collected at 90° from the excitation source via a 60×, NA 0.7 microscope objective (LWD-M Plan, Universe Kogaku, Oyster Bay, NY). The collected light was spectrally filtered with a 580DF40 band-pass filter and detected by an R1477 photomultiplier tube (PMT) (Hamamatsu Photonics, Japan). The PMT signal was transferred to the interface box and digitized by the input/output board. Data was collected at a sampling rate of 10 Hz through an RC filter.

An auxiliary microscope (10×, NA 0.25 ) was equipped for the alignment of the optics. This microscope was used to visualize the position of the laser beam with respect to both the sample flow through the capillary and the collection optics, and was illuminated by a light source positioned behind the pinhole. Alignment was achieved by initially fixing the position of the optical collection assembly, then adjusting the capillary and laser-focusing objectives using X-Y-Z translation stages. The angle of the fluorescence-collecting objective and the position of the collection assembly were also adjustable for optimization of alignment.

### **2.3.5 Detection of BPDE-DNA adducts**

Typically, 1 µg of DNA was heat-denatured at 100 °C for 5 min followed by cooling on ice for 3 min. DNA denaturation is required because the antibodies often do not recognize the lesion in duplex DNA. There are other DNA denaturing methods such as mild alkaline treatment (30 mM NaOH) and 90% (v/v) neutral formamide treatment

(approximately pH 8). However, they either dissociate the DNA-protein complex or are impractical for the denaturation of alkali-labile BPDE-DNA adducts (48, 51). Although heat treatment might generate DNA breaks, antibody binding is quasi-independent of molecular weight (52). Heat-denatured DNA was incubated with a mouse anti-BPDE antibody (clone 8E11, isotype IgG<sub>1</sub> (Trevigen Inc., Gaithersburg, MD), and a fluorescently-labelled goat anti-mouse antibody. The primary antibody 8E11 was raised against BPDE-modified guanosine coupled to bovine serum albumin. The goat anti-mouse antibody was received as a Zenon™ Alexa Fluor® 546 mouse IgG<sub>1</sub> labelling kit (Molecular Probes, Eugene, OR). This secondary antibody was a F<sub>ab</sub> fragment directed against the F<sub>c</sub> portion of an intact IgG primary antibody. It was labelled with a fluorophore Alexa Fluor® 546 whose optimum excitation wavelength was 553 nm, which was close to the He-Ne laser wavelength of 543.5 nm being used. Unlike other dyes of similar excitation wavelengths, the Alexa Fluor 546 dye has strong absorption with an extinction coefficient greater than 80,000 cm<sup>-1</sup>M<sup>-1</sup> and a long fluorescence lifetime (4 ns), both contributing to high sensitivity. A 3:1 molar ratio of the Zenon labelling kit component A to the anti-BPDE antibody was employed as recommended by the manufacturer. To the mixture of the DNA sample and the antibodies, an incubation buffer was added to bring the total sample volume to 20 µL. The incubation buffer contained 10 mM Tris and 80 mM glycine, and its pH was adjusted to pH 7.8 with acetic acid. After overnight incubation on ice in the dark, samples were electrokinetically injected into the capillary using an injection voltage of 10 kV for 10 s. The separation was carried out at room temperature with a separation voltage of 20 kV. The running buffer was a Tris-glycine mixture containing 30 mM Tris and 170 mM glycine at pH 8.3. Between runs, the

capillary was rinsed for 5 min with 0.02 M NaOH and 5 min electrophoretically with the running buffer.

To correct for changes in electro-osmotic flow (EOF), sampling variation, and possible adsorption to the capillary wall surface, a relative peak area (the peak area ratio of the second peak to the first peak) was used to measure BPDE-DNA adduct levels. Sampling variation is more of a problem in the electrokinetic injection mode than in the hydrodynamic injection mode. There is a practical justification for this correction: repeated injections of one sample produce consistent results after this correction although the absolute fluorescence intensity for each peak may change considerably in some cases. Therefore, when a peak area is mentioned below, it always refers to the relative peak area.

## 2.4 Results and Discussion

### 2.4.1 pH of the incubation buffer

A previous CE study showed that the binding between an antibody and DNA is pH-dependent (53). Although interactions between antibodies and DNA are favorably expedited in a buffer at pH close to neutrality and of low-to-moderate ionic strength, non-specific interactions, which mainly result from hydrophobic interactions between amino acid residues on the protein and the negatively charged DNA backbone, also increase. This increase is reflected in the background signal from control DNA in **Figure 2.3**. To reflect the true binding activity of the antibody to damaged sites, those apparent non-specific interactions need to be eliminated.

Incubation buffers of different pH values, as indicated in **Figure 2.3**, were prepared from 50 mM Tris and 400 mM glycine and adjusted with acetic acid or ammonium hydroxide to a desired pH value. After appropriate dilutions, all the incubation buffers possessed the same conductivity. The pH of the running buffer was kept constant at 8.5. In each panel, the lower trace shows the electropherogram for control DNA (undosed) and the upper trace for DNA extracted from cells treated with 1  $\mu$ M BPDE for 30 min. The DNA samples were incubated with antibodies at 4 °C overnight (approximately 16 h) and then injected at 10 kV for 10 s and electrophoresed at 20 kV. As shown in **Figure 2.4**, the peak area ratio is highest around pH 7.8. Therefore, pH 7.8 was chosen for subsequent DNA analyses.

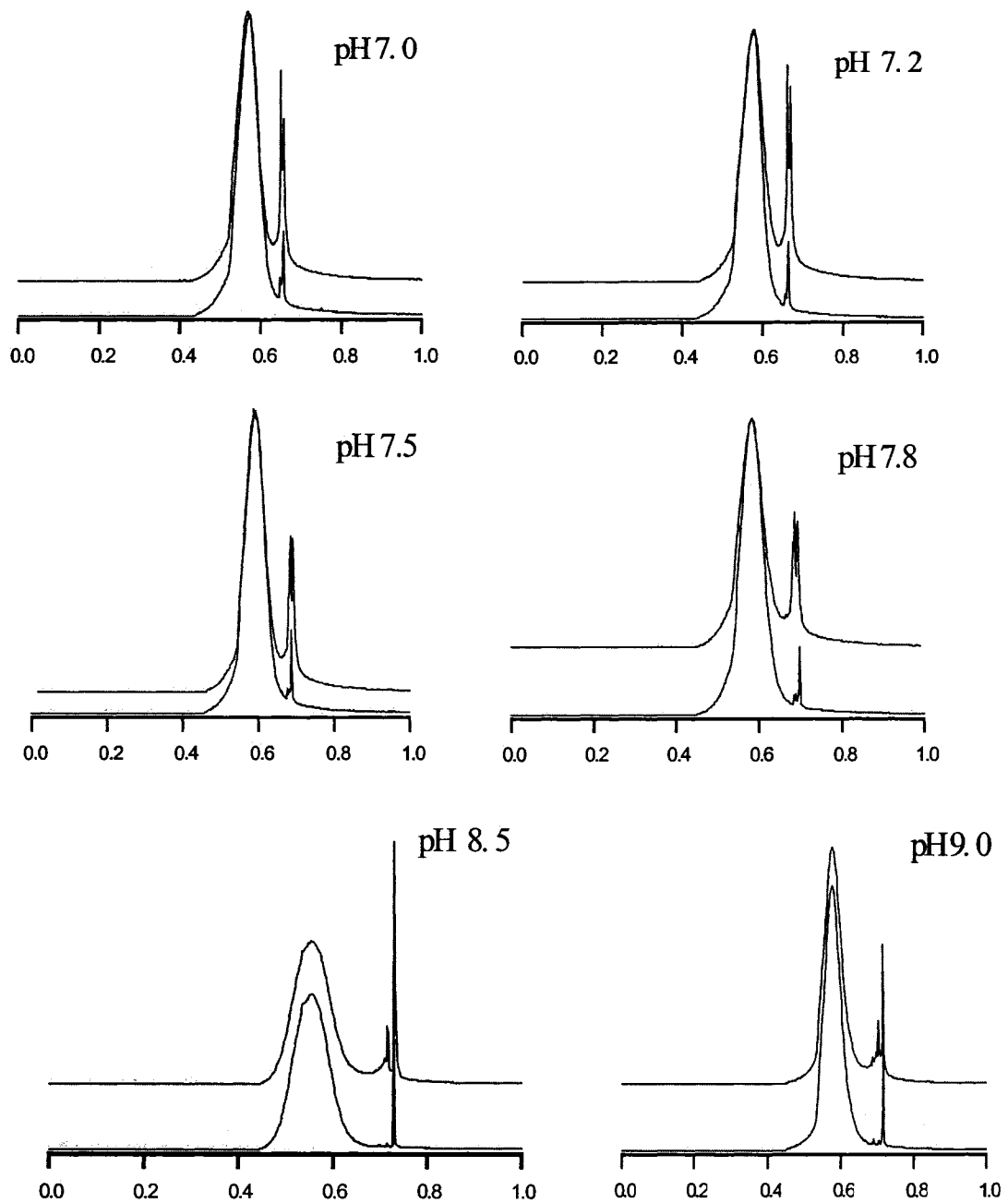


**Figure 2.3. Electropherograms showing the effects of the pH of the incubation buffer on DNA analysis. The vertical axis (not shown) is fluorescence intensity. The horizontal axis is the migration time in minutes. The upper traces were from the analysis of DNA extracted from cells treated with 1 μM BPDE for 30 min. The lower traces were from the analysis of DNA extracted from the control cells.**

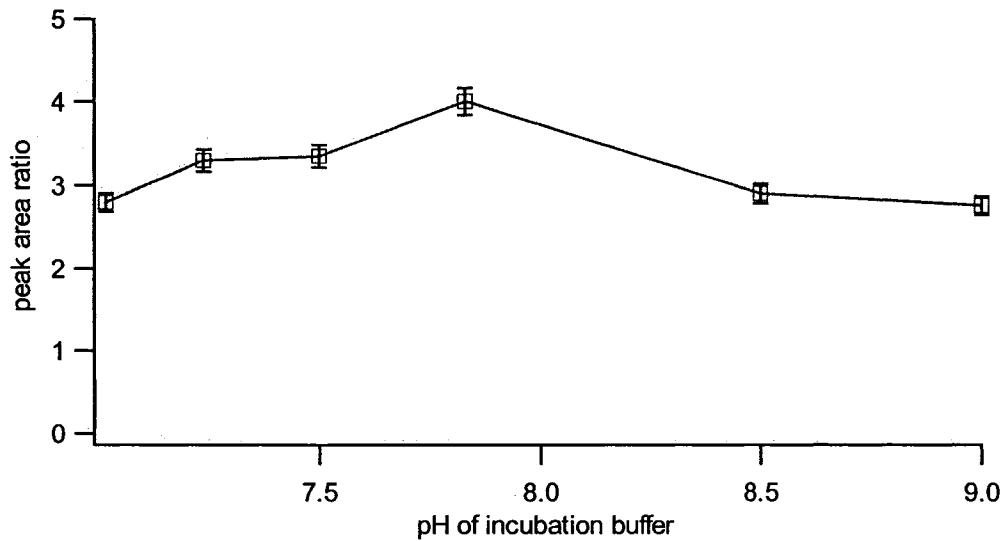


**Figure 2.4. Relationship between the peak area ratio of treated DNA to control DNA and the pH of the incubation buffer. Error bars indicate the standard deviation from three determinations.**

#### 2.4.2 Ionic strength of the incubation buffer

When the concentration of an incubation buffer increases, the electric field strength in the sample zone decreases. This decrease would result in a decrease in the electrophoretic force. However, the overall EOF remains almost the same, dictated by the composition and ionic strength of the running buffer. In this CZE format, the electrophoretic force and the EOF are in opposite directions while in magnitude the EOF is greater than the electrophoretic force. Therefore, the ternary complex moved faster when the concentration of the incubation buffer increased. The electropherograms are shown in **Figure 2.5** and the relationship between the migration time of the ternary complex and the ionic strength of the incubation buffer is depicted in **Figure 2.6**. When separation started to occur, the incubation equilibrium was broken because different components of the incubation mixture had different mobilities. Theoretically, the shorter the time a complex resides in a capillary, the less it dissociates into its respective components and the higher signal it registers in terms of peak height or peak area. We observed that the same logic applies to non-specific complexes. Therefore, the concentration of the incubation buffer was optimized at the condition at which the peak height ratio of treated DNA to control DNA was the largest. Incubation buffers of different ionic strength were prepared from the same concentrated pool with appropriate dilutions. A 1× incubation buffer was composed of 12.5 mM Tris and 100 mM glycine. The DNA samples were incubated with antibodies at 4 °C overnight (approximately 16 h) and then injected at 10 kV for 10 s and electrophoresed at 20 kV. At higher incubation buffer concentrations, poor resolution made it difficult to accurately measure peak areas. Thus, peak height was used as a parameter for optimization.

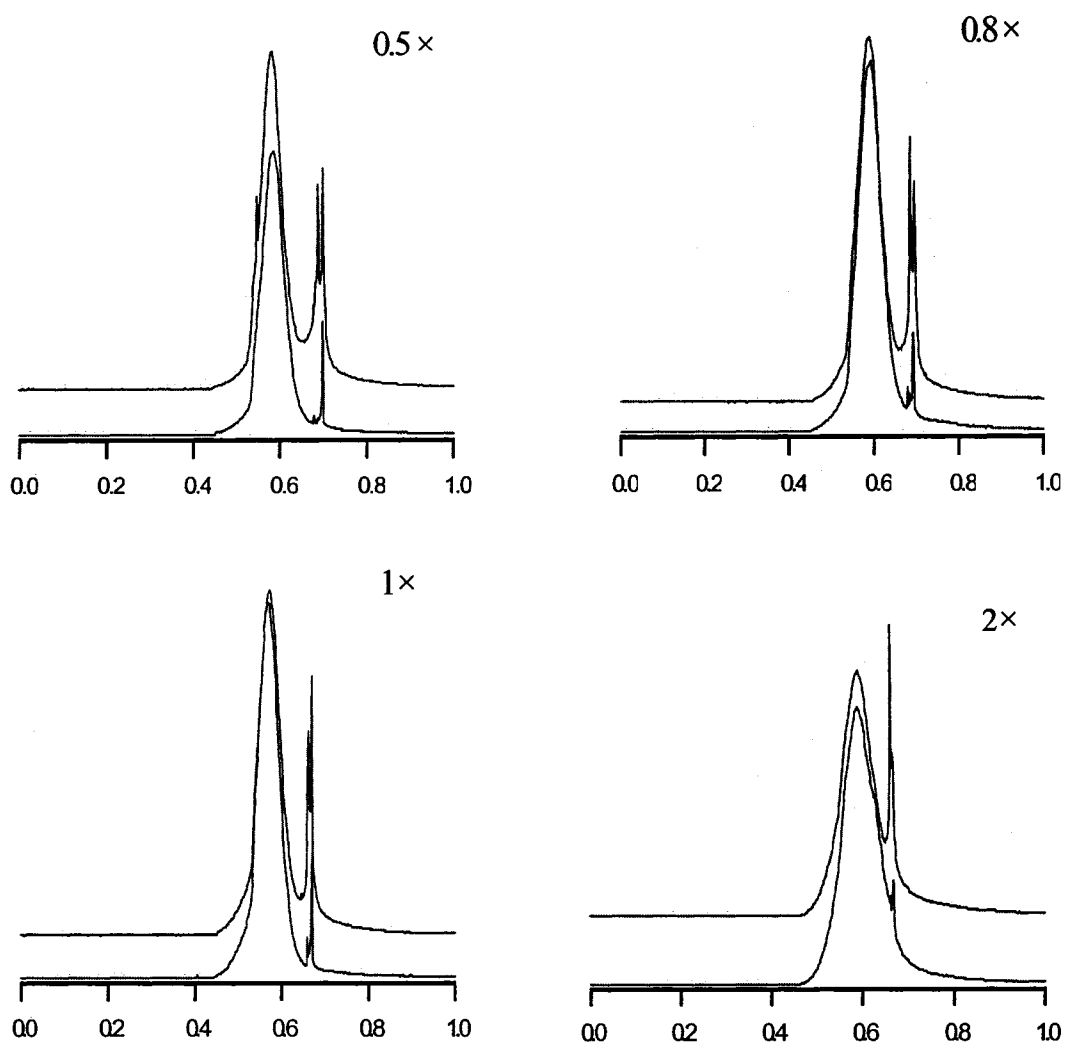


**Figure 2.5. Electropherograms showing the effects of the ionic strength of the incubation buffer on DNA analysis. 1×incubation buffer contained 12.5 mM Tris and 100 mM glycine. The vertical axis (not shown) is fluorescence intensity. The horizontal axis is the migration time in minutes. The upper traces were from the analysis of DNA extracted from cells treated with 1 μM BPDE for 30 min. The lower traces were from the analysis of DNA extracted from the control cells.**

The relationship between the peak height of the ternary complex and the ionic strength of the incubation buffer is shown in **Figure 2.7a** and **Figure 2.7b**. Interestingly, as we can see from **Figure 2.7a**, when the incubation buffer concentrations varied from 1× to 2×, the peak height for control DNA decreased while the peak height for treated DNA increased. Because in this high concentration range the peak resolution was lost, we cannot infer that this phenomenon was reflective of the actual binding activity for both specific complexation and non-specific complexation. Normally, when the incubation buffer has a much greater conductivity than the running buffer, destacking will occur. Destacking means the decompression of an analyte zone, which leads to peak broadening. As shown in **Figure 2.5**, the tailing from the first peak might have distorted the second peak, which surely affected peak height quantification.

It was observed that although the 0.8× incubation buffer gave the smallest peak height in the 0.5× and 1× concentration range for both treated DNA and control DNA, as shown in **Figure 2.7a**, it resulted in the largest peak height ratio of treated DNA to control DNA, as shown in **Figure 2.7b**. In other words, use of 0.8× incubation buffer could differentiate treated DNA and control DNA to the greatest extent. Thus, 0.8× concentrated incubation buffer was chosen for subsequent experiments. The acceptable resolution resulting from this condition also made possible an accurate peak area measurement with a view towards accurate quantification of adduct levels.

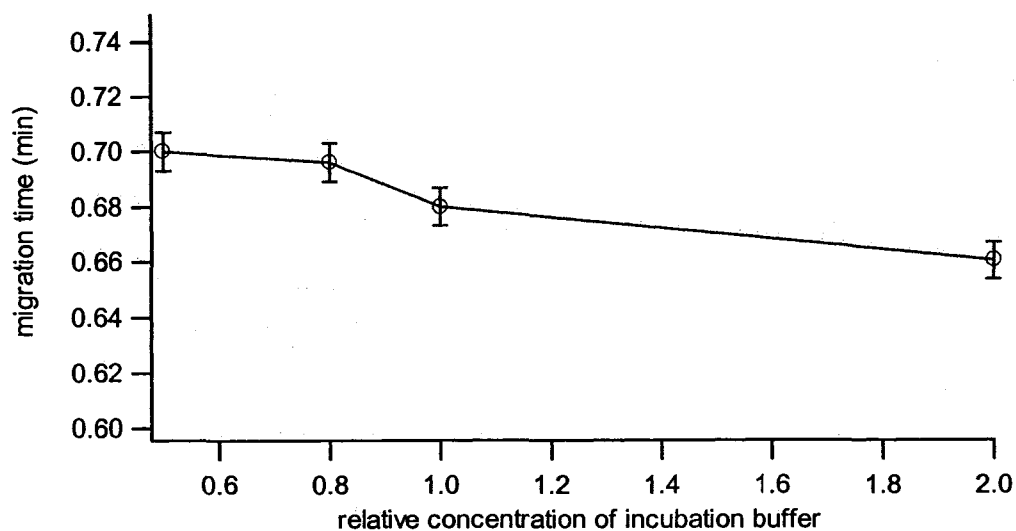


**Figure 2.6. Relationship between the ionic strength of the incubation buffer and the migration time of the ternary complex. When the second peak split, migration times of individual peaks averaged out. Error bars indicate the standard deviation from three determinations.**

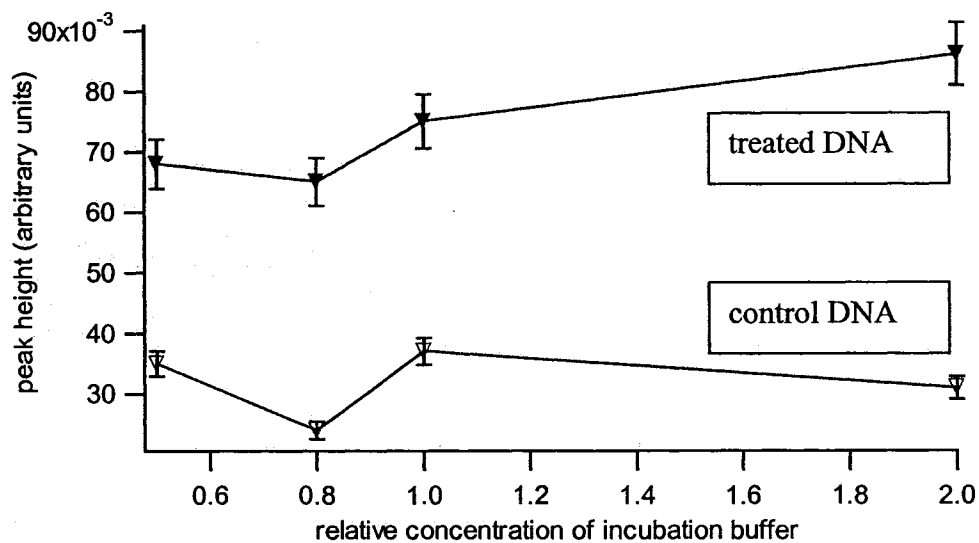


**Figure 2.7a.** Relationship between the ionic strength of the incubation buffer and the peak height of the ternary complex. When the second peak split, the highest peak (relative to baseline) was used to determine the peak height. Error bars indicate the standard deviation from three determinations.

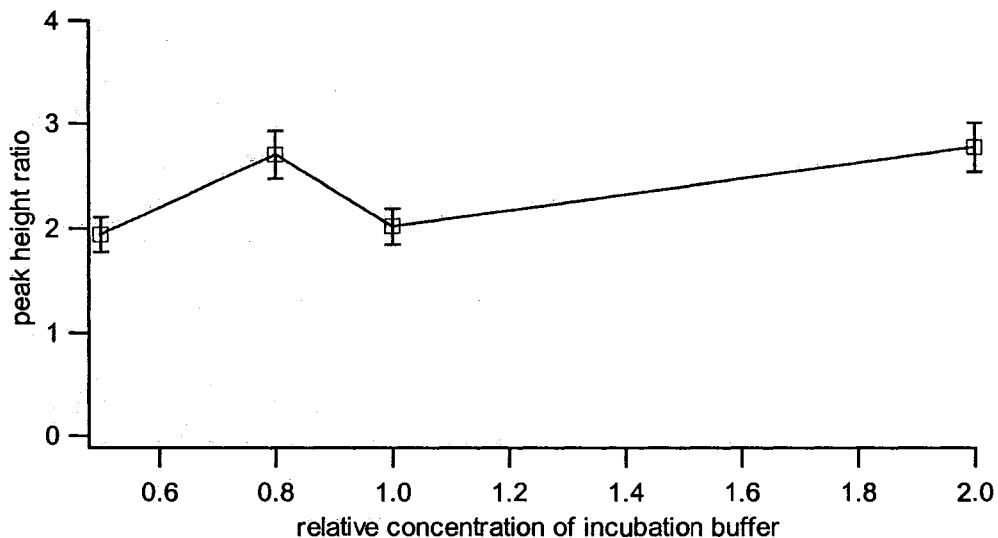


**Figure 2.7b.** The peak height ratio of treated DNA to control DNA is dependent on the ionic strength of the incubation buffer. Error bars indicate the standard deviation from three determinations.

### 2.4.3 pH of the running buffer

When the pH of a running buffer increases, the capillary surface charge becomes more negative, resulting in a greater EOF. Therefore, the ternary complex (second peak) moved faster when the pH of the running buffer increased, as shown in **Figure 2.8**. Running buffers of different pH values, as indicated, were prepared from 75 mM Tris and 425 mM glycine and adjusted with acetic acid or ammonium hydroxide to a desired pH value. After appropriate dilutions, all the running buffers possessed the same conductivity while the pH of the incubation buffer was kept constant at 7.8. In each panel, the lower trace shows the electropherogram for control DNA (undosed) and the upper trace for DNA from cells treated with 1  $\mu$ M BPDE for 30 min. The DNA samples were incubated with antibodies at 4 °C overnight (approximately 16 h) and then injected at 10 kV for 10 s and electrophoresed at 20 kV. The relationship between the pH of the running buffer and the migration time of the ternary complex is shown in **Figure 2.9**. At high pH values (9.0), the resolution deteriorated as expected. At a lower pH range (7.0-7.8), both peaks broadened or split, indicating that adsorption of proteins to the capillary wall surface took place.

**Figure 2.10a** shows the relationship between the peak height of the ternary complex and the pH of the running buffer. **Figure 2.10b** shows the relationship between the peak height ratio of treated DNA to control DNA and the pH of the running buffer. For the same reason mentioned above, the peak height was considered for optimization. The running buffer at pH 8.3 gave the highest ratios (**Figure 2.10b**). Therefore, pH 8.3 was chosen for subsequent experiments.

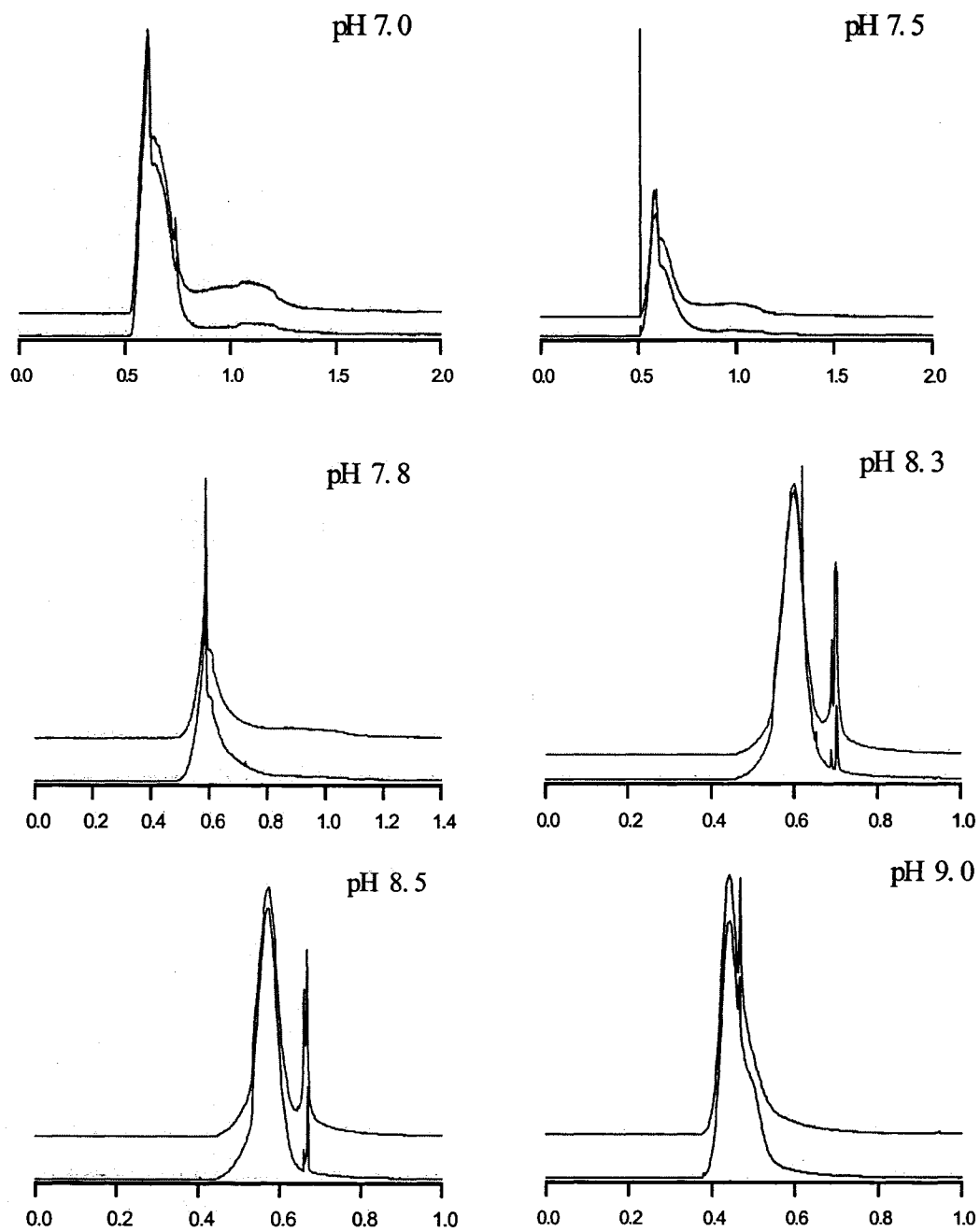


**Figure 2.8. Electropherograms showing the effects of the pH of the running buffer on DNA analysis. The vertical axis (not shown) is fluorescence intensity. The horizontal axis is the migration time in minutes. The upper traces were from the analysis of DNA extracted from cells treated with 1 μM BPDE for 30 min. The lower traces were from the analysis of DNA extracted from the control cells.**

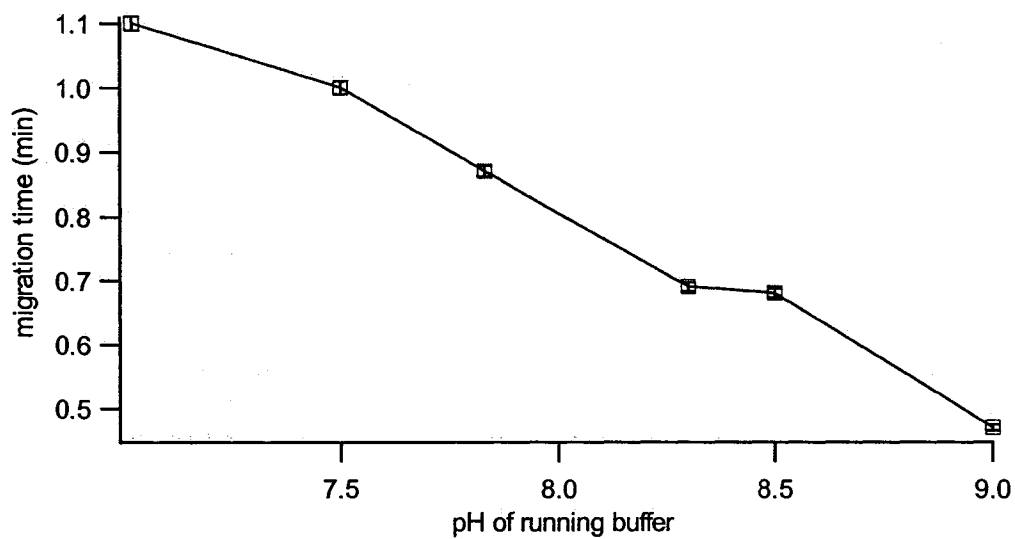


**Figure 2.9. Relationship between the pH of the running buffer and the migration time of the ternary complex. When the second peak split, the migration times of individual peaks averaged out. Error bars indicate the standard deviation from three determinations.**

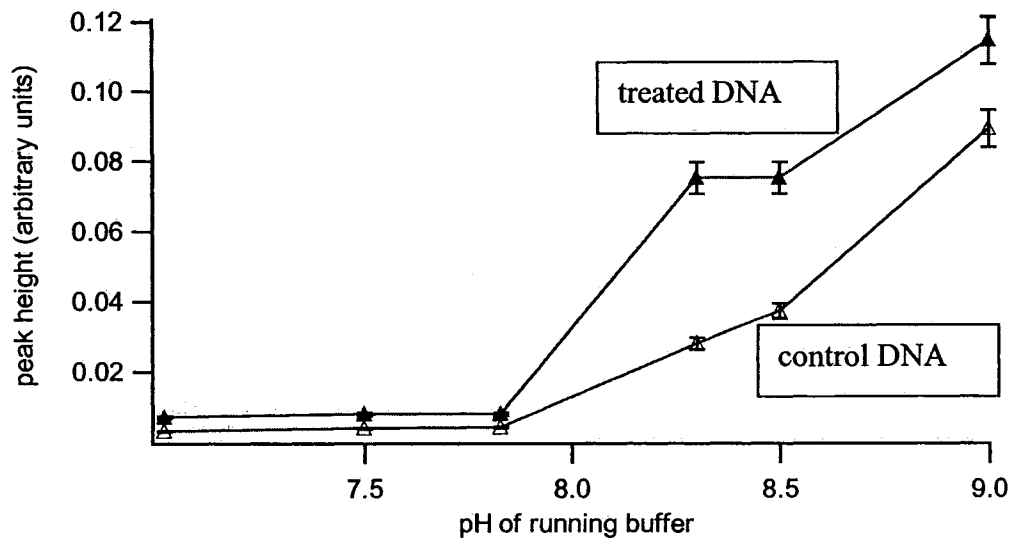


**Figure 2.10a. Relationship between the pH of the incubation buffer and the peak height of the ternary complex. When the second peak split, the highest peak was used to determine the peak height. Error bars indicate the standard deviation from three determinations.**

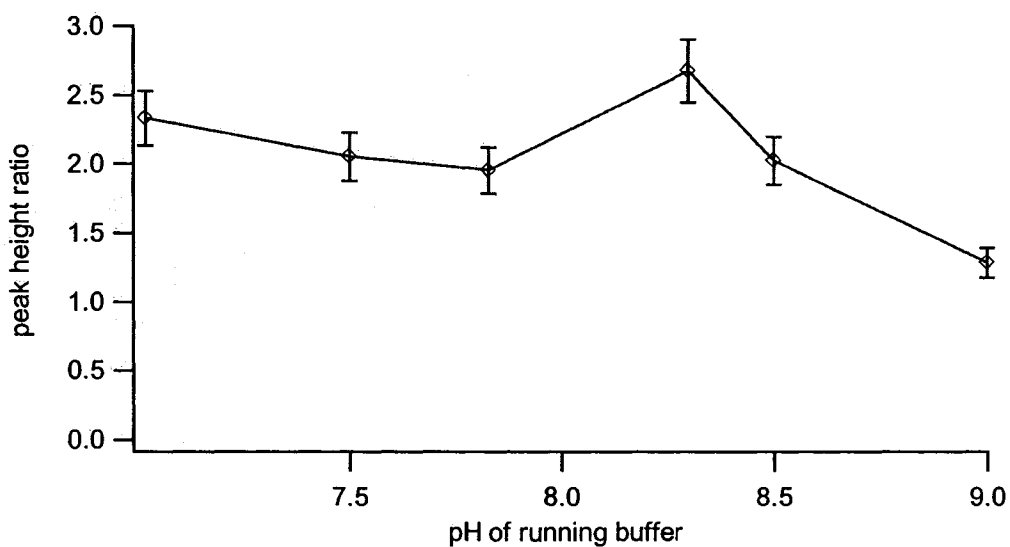


**Figure 2.10b. The peak height ratio of treated DNA to control DNA is dependent on the pH of the incubation buffer. Error bars indicate the standard deviation from three determinations.**

#### 2.4.4 Ionic strength of the running buffer

Running buffers of different ionic strength were prepared from the same concentrated pool with appropriate dilutions. The 0.8× concentrated running buffer gave a current of 1.5  $\mu\text{A}$ . In each panel (**Figure 2.11**), the lower trace shows the electropherogram for control DNA and the upper trace for DNA from cells treated with 1  $\mu\text{M}$  BPDE for 30 min. The DNA samples were incubated with antibodies at 4 °C overnight (approximately 16 h) and then injected at 10 kV for 10 s and electrophoresed at 20 kV. As shown in **Figure 2.11**, when the concentration of the running buffer increased, the migration time of the ternary complex increased as predicted, because the EOF decreases with increasing ionic strength of the running buffer. **Figure 2.12** shows the relationship between the ionic strength of the running buffer and the migration time of the ternary complex. The relationship seems to be linear in the concentration range under investigation, suggesting that the surface charge of the ternary complex did not change significantly. This implied that the ternary complex was stable in this concentration range (0.5×-2×).

**Figure 2.13a** shows the relationship between peak height and the ionic strength of the incubation buffer. When the concentration of the running buffer increased over 0.8×, the peak heights for both treated DNA and control DNA decreased. This decrease could be the combined effects of two factors: the first one is a greater dissociation of the complex during separation when the separation time was prolonged. In a previous study of the interaction of a fluorescently-labelled BPDE-90mer with an anti-BPDE antibody (47), there was a corresponding decrease in the amount of complex (the ratio of bound to unbound DNA adducts) detected as the ionic strength of the running buffer increased. The other factor is a possible separation of the complex mixtures themselves from each

other when they had different conformations or different compositions. This refers to the complexes resulting from the binding of DNA molecules with the antibody at different molar ratios or the binding of the antibody with DNA molecules of different lengths. In binding stoichiometric studies of a fluorescently-labelled BPDE-16mer with an anti-BPDE antibody (54), two bound complexes of different compositions were separated from each other. Which complex predominates is dependent on the relative concentration of the antibody to the antigen. When the concentration of the antibody increased, the predominance was shifted from  $AbAg_2$  (1:2 complex) to  $AbAg$  (1:1 complex). Even at a very high antibody concentration, the 1:2 complex was still observed. In addition, the molecular weights of genomic DNA molecules are unlikely to be uniform. After binding to antibodies, their difference in molecular weight may be observed in CZE, resulting in peak broadening and a reduced peak height.

When 0.5× concentrated running buffer was used, both peaks were distorted, probably because of destacking effects or strong adsorption of antibodies to the capillary wall. The 0.8× concentrated running buffer was the best choice because it gave the highest peak height ratio, as shown in **Figure 2.13b**. Without much dissociation or adsorption occurring, this concentration gave a nominally single peak for the complex. Repeated injections also showed great reproducibility both in migration time and in peak shape.

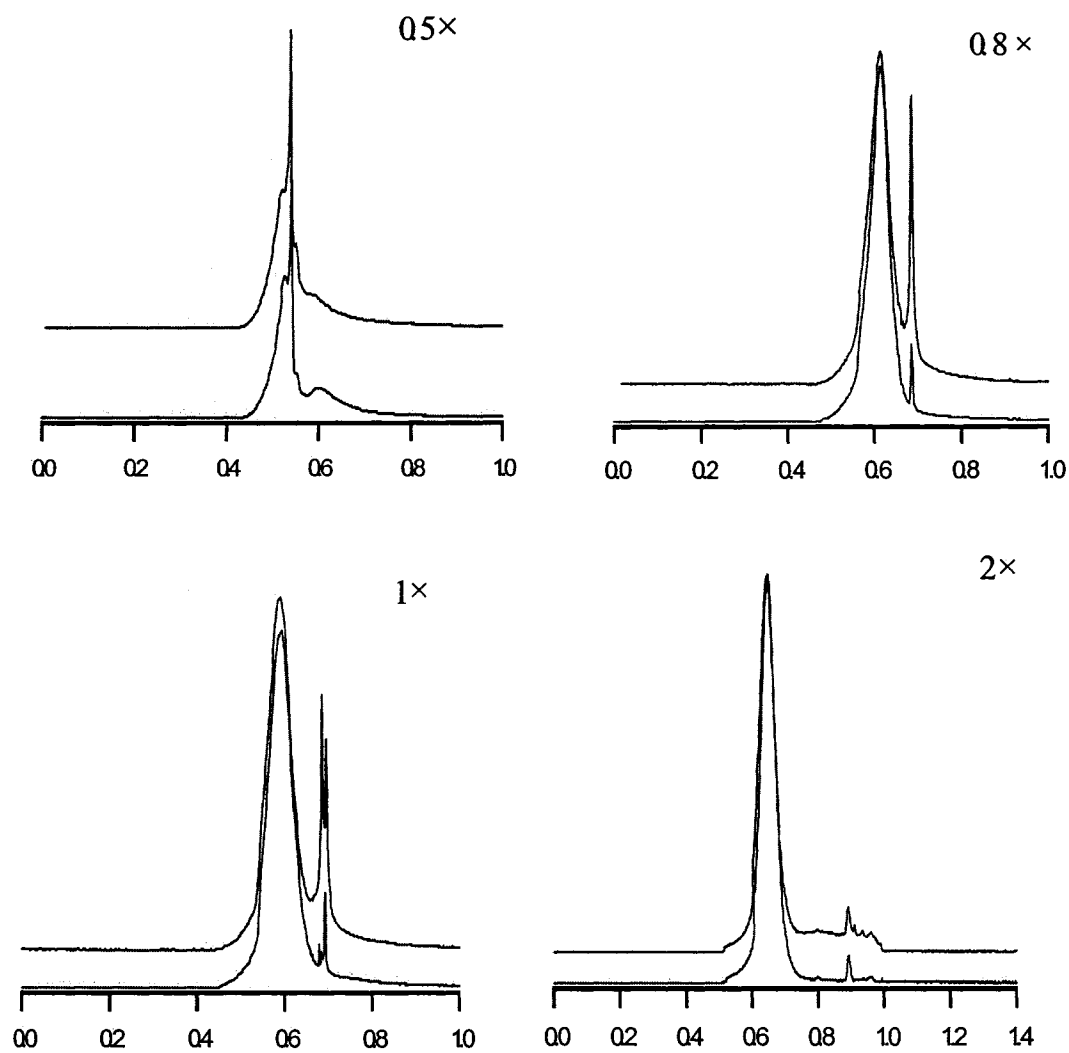


**Figure 2.11. Electropherograms showing the effects of the ionic strength of the running buffer on DNA analysis. The vertical axis (not shown) is fluorescence intensity. The horizontal axis is the migration time in minutes. The upper traces were from the analysis of DNA extracted from cells treated with 1  $\mu$ M BPDE for 30 min. The lower traces were from the analysis of DNA extracted from the control cells.**

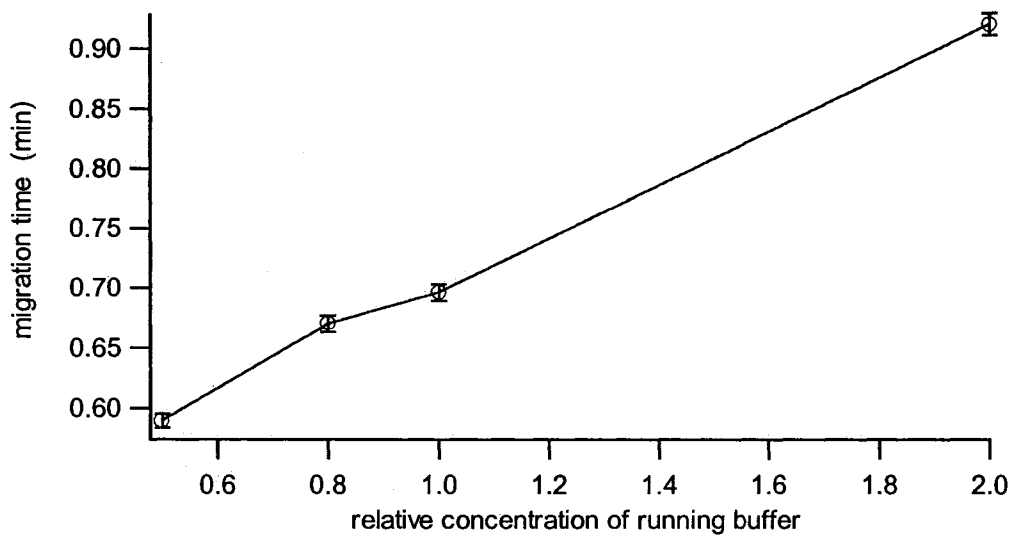


**Figure 2.12. Relationship between the ionic strength of the running buffer and the migration time of the ternary complex. When the second peak split, migration times of individual peaks averaged out. Error bars indicate the standard deviation from three determinations.**

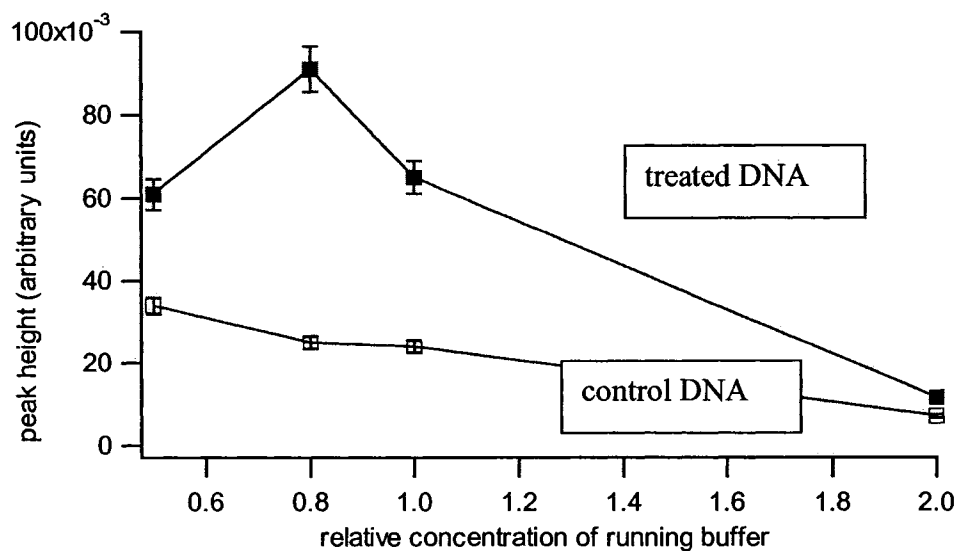


**Figure 2.13a. Relationship between the ionic strength of the running buffer and the peak height of the ternary complex. When the second peak split, the highest peak was used to determine the peak height. Error bars indicate the standard deviation from three determinations.**

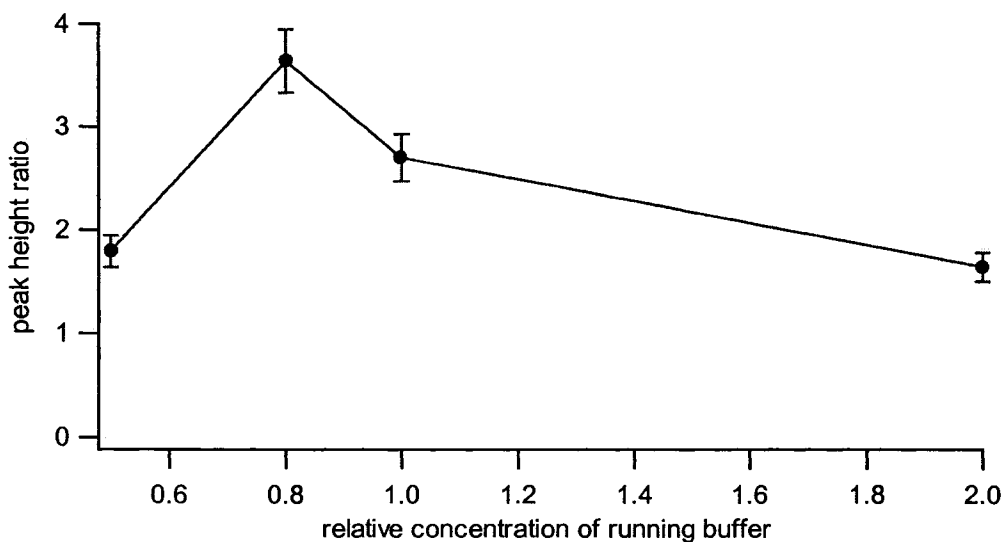


**Figure 2.13b. The peak height ratio of treated DNA to control DNA is dependent on the ionic strength of the incubation buffer. Error bars indicate the standard deviation from three determinations.**

### 2.4.5 Injection time

When the injection time was as short as 5 s, the complex peak was split as shown in **Figure 2.14**. This splitting probably occurred because a shorter injection time led to a narrower sample zone, which ended up with relatively more time and latitude for separation in a given length of capillary. The splitting indicated better resolution. The resolution deteriorated when the injection time was set at 15 s. Therefore, an intermediate injection time of 10 s was chosen as the standard injection time.

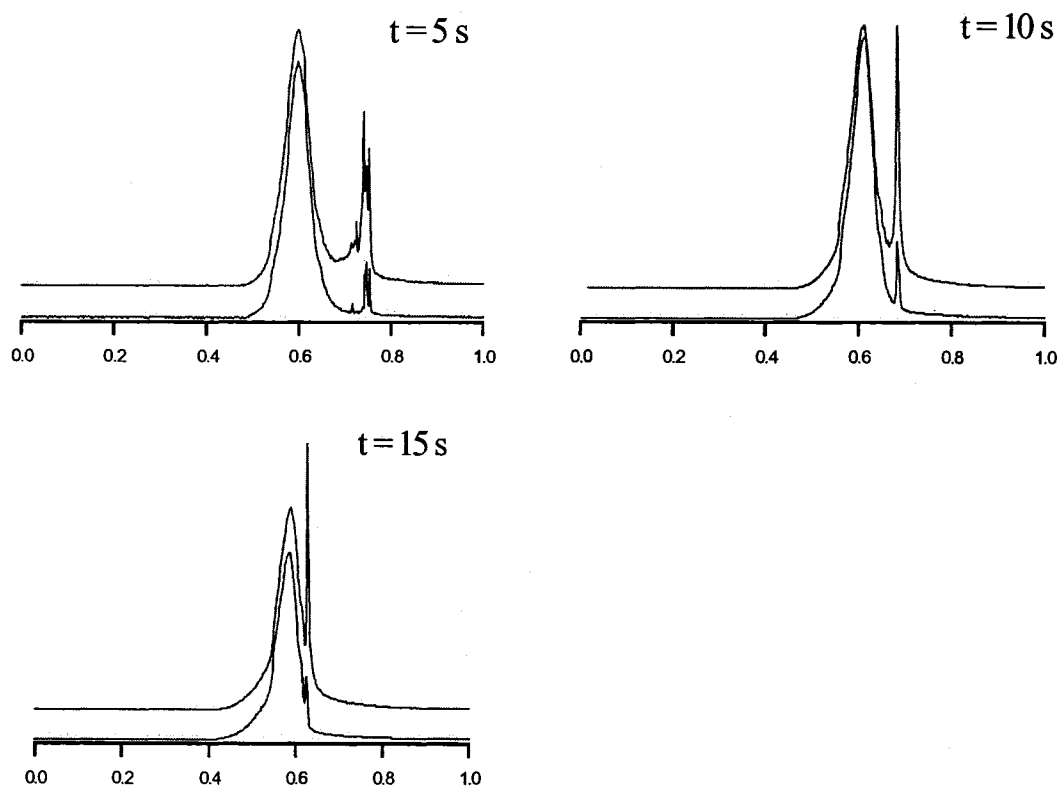


**Figure 2.14.** Electropherograms showing the effects of injection time on DNA analysis. The DNA samples were injected at 10 kV and electrophoresed at 20 kV. The vertical axis (not shown) is fluorescence intensity. The horizontal axis is the migration time in minutes. The upper traces were from the analysis of DNA extracted from treated cells. The lower traces were from the analysis of DNA extracted from control cells.

#### 2.4.6 Injection voltage

When the injection voltage was set lower, the complex peak was split as shown in **Figure 2.15**. The splitting indicated better separation, as a result of the effect similar to when shorter injection times were applied. However, an injection voltage as high as 15 kV degraded the resolution. Thus, an intermediate injection voltage of 10 kV was chosen as the standard injection voltage for subsequent experiments.

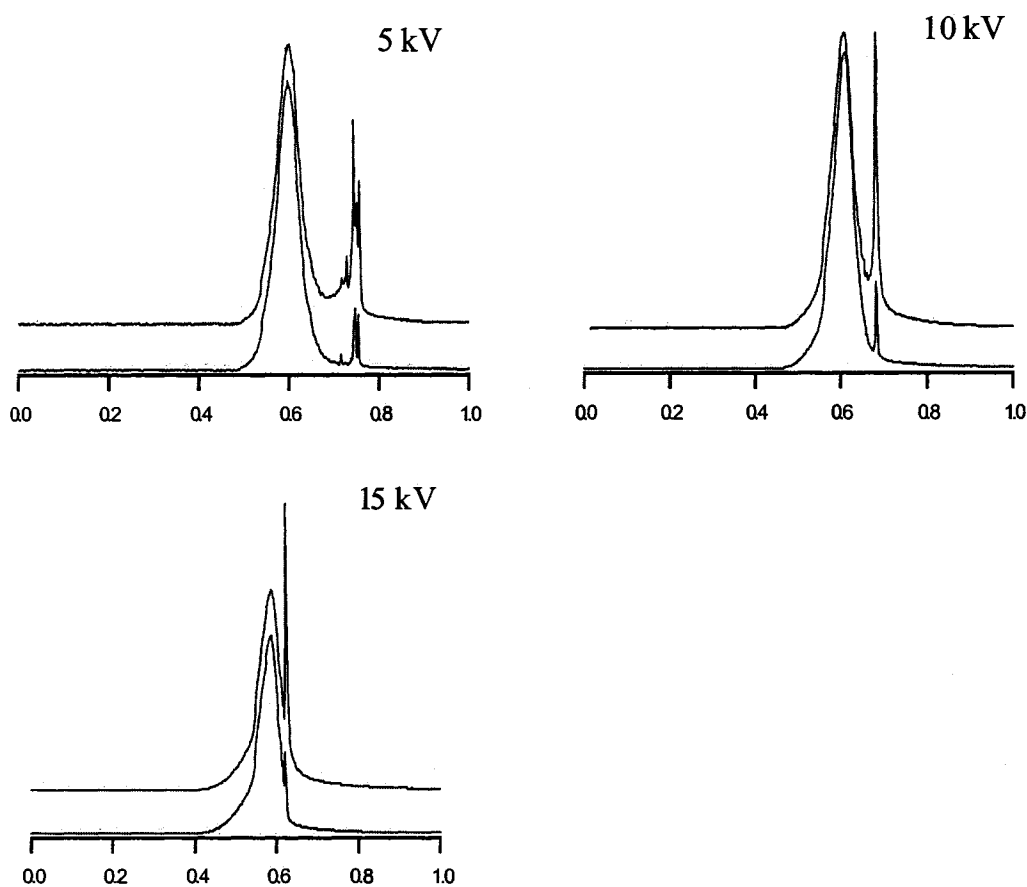


**Figure 2.15.** Electropherograms showing the effects of injection voltage on DNA analysis. The DNA samples were injected for 10 s and electrophoresed at 20 kV. The vertical axis (not shown) is fluorescence intensity. The horizontal axis is the migration time in minutes. The upper traces were from the analysis of DNA extracted from treated cells. The lower traces were from the analysis of DNA extracted from control cells.

### 2.4.7 Separation voltage

The separation voltage can change the separation time dramatically, as shown in **Figure 2.16**. The higher the separation voltage, the shorter the time needed for separation. However, when the separation voltage was set at as high as 25 kV, reproducibility was not as acceptable as when the separation voltage was set at 20 kV. Therefore, in subsequent experiments, the separation voltage was set at 20 kV. Under such conditions, the complex registered as a nominally single peak. The peak shape was less likely to change and high reproducibility was easily obtained.

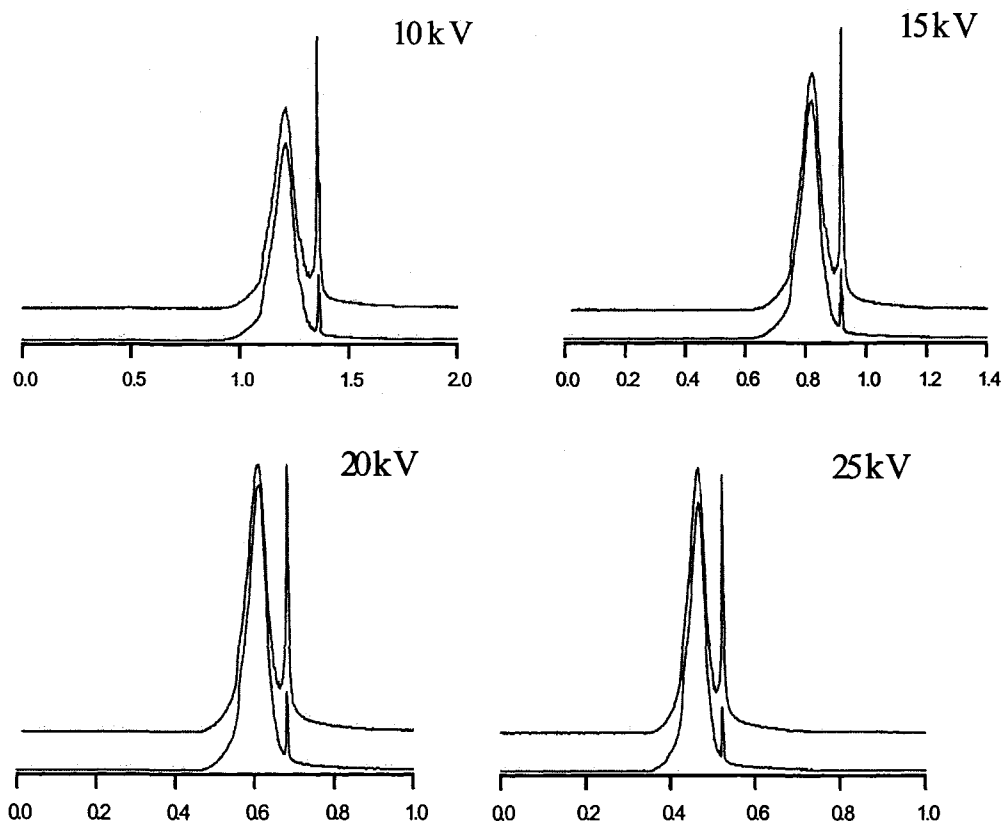


**Figure 2.16.** Electropherograms showing the effects of separation voltage on DNA analysis. The DNA samples were injected at 10 kV for 10 s. The vertical axis (not shown) is fluorescence intensity. The horizontal axis is the migration time in minutes. The upper traces were from the analysis of DNA extracted from treated cells. The lower traces were from the analysis of DNA extracted from control cells.

#### 2.4.8 Incubation time and temperature

To detect small changes in adduct levels, we had to first improve the sensitivity of the method for adduct detection. The purpose of all the optimizations described above was to increase the signals from the true positive samples over those of the controls. In most cases, cross-reactivity decreases over the time of incubation, and in theory is minimal at equilibrium (55). However, equilibrium is hard to define, especially when antibody activity is considered. The activity of antibodies could be lost over time, resulting in the dissociation of immunocomplexes or the generation of “new” non-specific interactions.

Because our goal is to see how arsenic treatment affects BPDE-DNA adduct levels, three types of DNA samples were used to perform the optimization: control DNA without any treatment, DNA extracted from cells treated with BPDE only, and DNA extracted from cells treated sequentially with arsenic and BPDE. The peak area ratios between these DNA samples are shown in **Figure 2.17**. The reasons underlying the observed changes over time and/or with different temperature could be complex formation, subsequent stability, and antibody activity. When incubation was carried out at 4 °C for 16 h, the peak area ratio of DNA from arsenic treated cells to DNA from dummy treated cells was the largest, after correcting for the control DNA. Therefore, in subsequent experiments DNA samples were incubated with antibodies at 4 °C for 16 h.

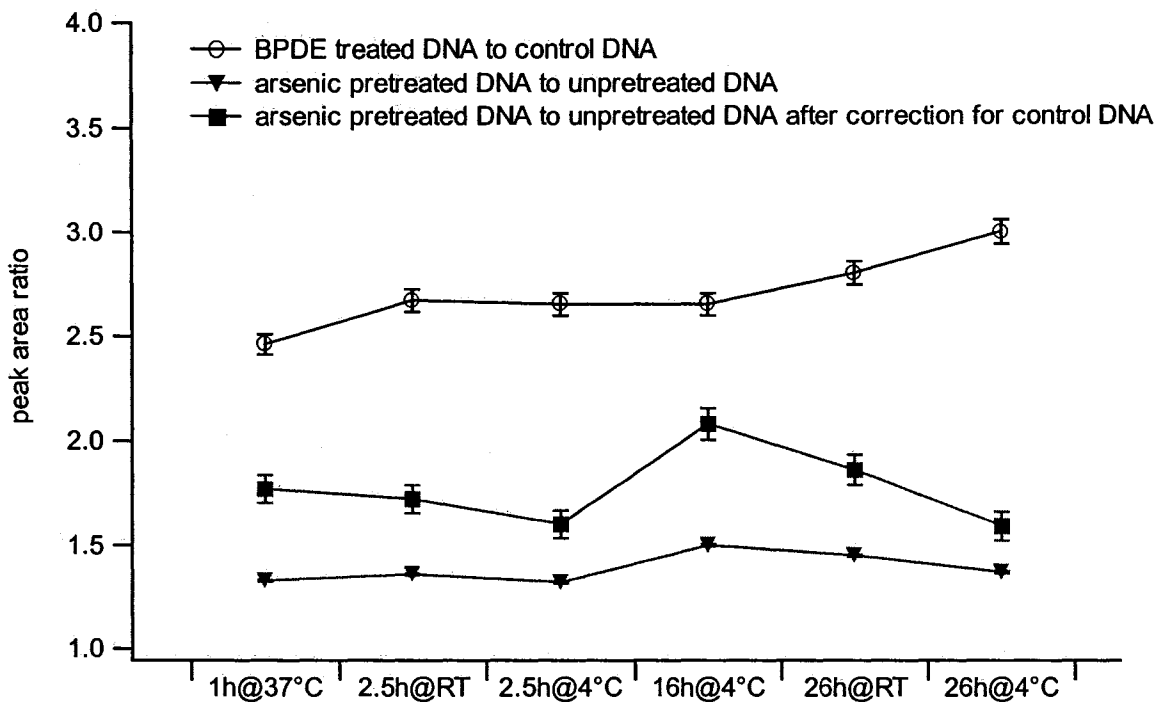


**Figure 2.17. Effects of incubation time and temperature: the peak area ratio of DNA samples extracted from cells treated with 0.5  $\mu$ M BPDE for 30 min to control DNA (open circle); the peak area ratio of DNA samples extracted from cells pretreated with 5  $\mu$ M MMA(III) to DNA samples extracted from cells without pretreatment (inverted filled triangle); the peak area ratio of DNA samples extracted from cells pretreated with 5  $\mu$ M MMA(III) to DNA samples extracted from cells without pretreatment, after correcting for control DNA by subtraction (filled square). Error bars indicate the standard deviation from three determinations.**

#### 2.4.9 Dose-response relationship

Before moving on to the targeted project, a dose-response relationship was established using one of the cell lines to be studied (**Figure 2.18**). The establishment of a dose-response relationship helps determine a convenient dose to be used in later experiments.

After correcting for the control, the relative fluorescence intensity representing the peak area ratio of the ternary antibody complex of BPDE-DNA to the unbound antibody was plotted against BPDE concentration. As shown in **Figure 2.19**, the fluorescence intensity increased as the BPDE concentration increased. The dose-response curve seemed to be linear, from 0  $\mu\text{M}$  up to 1-2  $\mu\text{M}$ . Beyond that concentration, the slope of the curve decreased substantially.

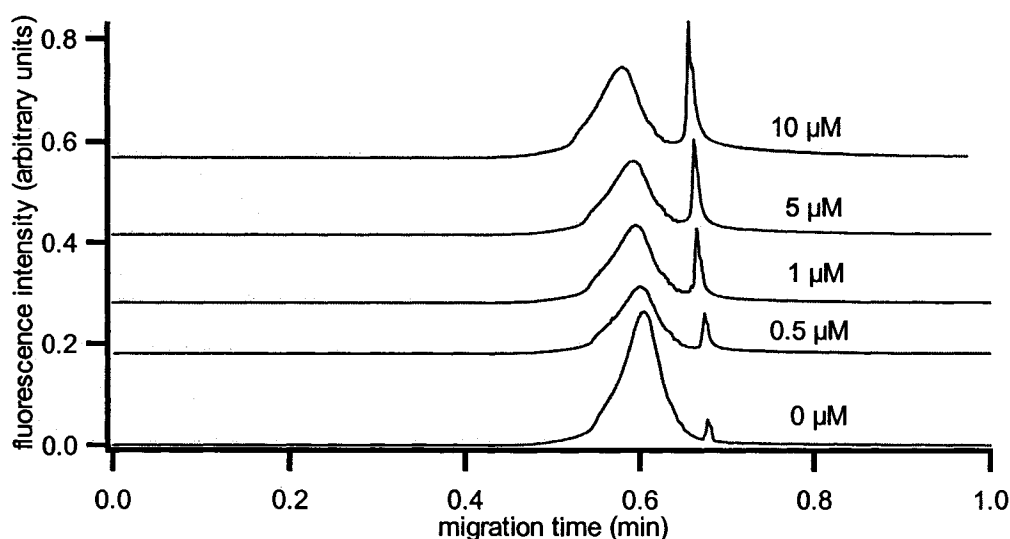


**Figure 2.18.** Electropherograms showing analyses of DNA extracted from GM04312C cells treated with various concentrations of BPDE for 30 min.

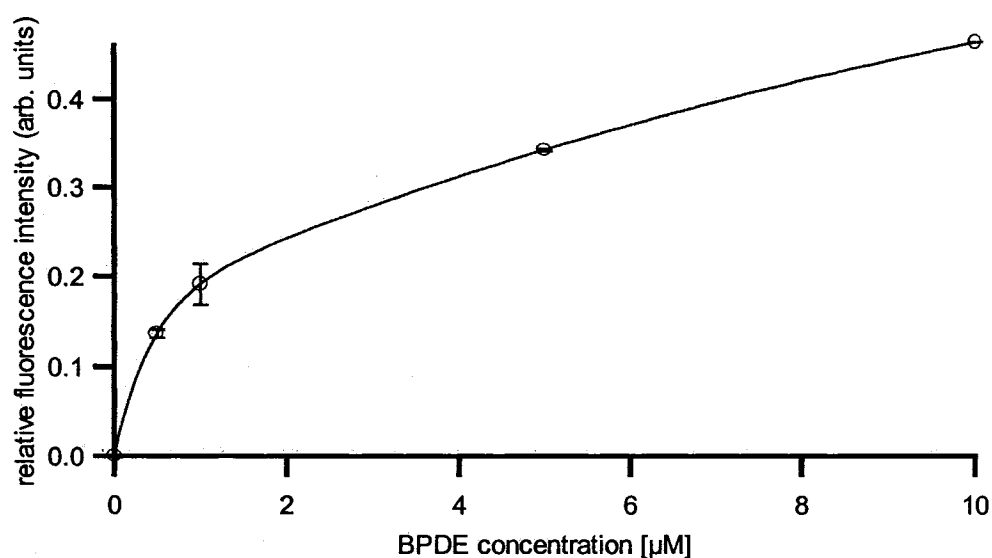


**Figure 2.19.** Relationship between relative fluorescence intensity (after being corrected for control) and BPDE concentration. Error bars indicate the standard deviation from three experiments.

When the logarithm of fluorescence intensity was plotted against the logarithm of BPDE concentration, the relationship was linear over the whole concentration range under investigation, as shown in **Figure 2.20**. The correlation coefficient was 0.9987. This suggested that fluorescence signals could be used as surrogates for adduct levels. With appropriate standards, this relative measurement can be converted into absolute quantitation. A similar log-log relationship between fluorescence intensity and BPDE concentrations was also observed with DNA samples isolated from human lymphoblasts incubated with BPDE at concentrations up to 1000  $\mu\text{M}$  by Vahakangas et al. (56).

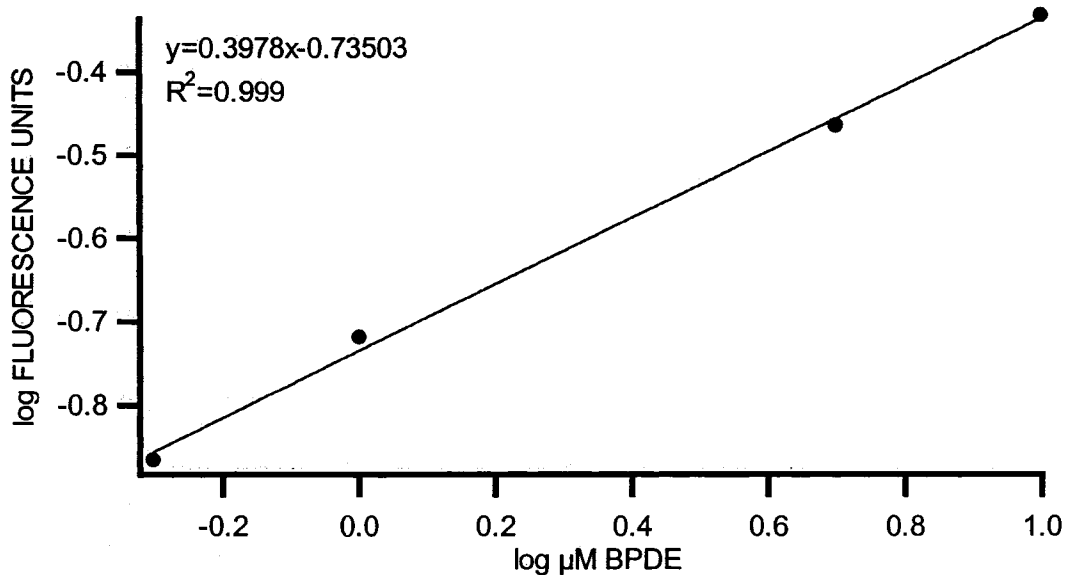


**Figure 2.20. Log-log plot of fluorescence intensity versus BPDE concentration**

#### 2.4.10 Choice of primary antibody

Two commercially available antibodies, 8E11 and 5D11 (Trevigen Inc.), and one antibody, BP1, which was generously provided by Dr. AA Wani of Ohio State University, were tested for appropriateness in this CE-based immunoassay in dose-response experiments. Secondary antibodies for labelling were selected according to the isotypes and clonal nature of the respective primary antibodies: Zenon™ Alexa Fluor® 546 Mouse IgG<sub>1</sub> for 8E11, Zenon™ Alexa Fluor® 546 Mouse IgG<sub>2a</sub> for 5D11, and Zenon™ Alexa Fluor® 546 Rabbit IgG for BP1. BP1 was reconstituted in 100  $\mu\text{l}$  of PBS as recommended by the provider and its concentration was determined by absorbance at 280 nm using 0.8 mg IgG protein/ml as the conversion factor. The final concentrations of the three antibodies were kept the same with a 1:3 molar ratio against their respective labelling components.

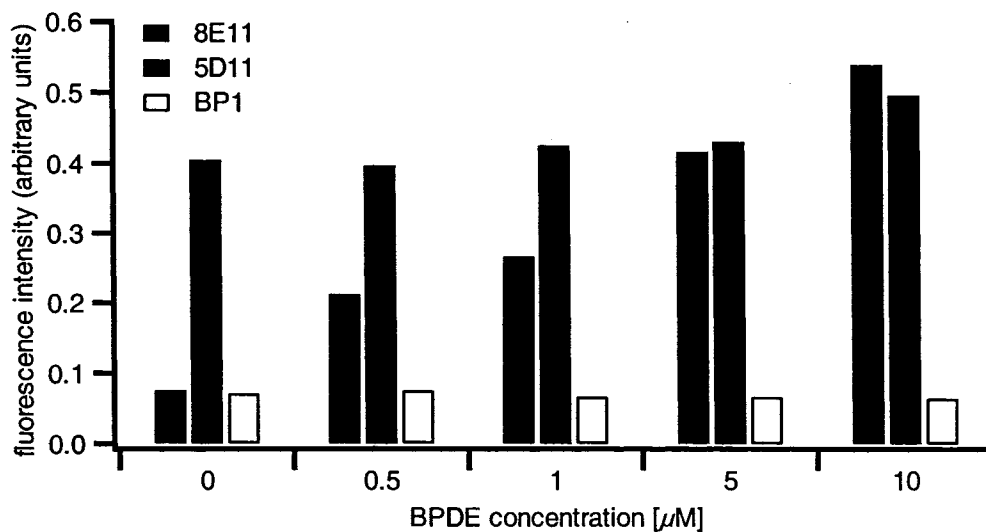


**Figure 2.21. Histograms showing dose-response relationships with different primary antibodies**

Because 5D11 and BP1 were produced using BPDE-modified DNA as antigens, the non-specific interaction between them and unmodified DNA was expected to be high. Surprisingly, among the three antibodies tested, the polyclonal antibody BP1 gave the weakest responses while the monoclonal antibody 5D11 constantly gave the strongest responses. Usually, when used in immunoassays, a polyclonal antibody is expected to be more sensitive than a monoclonal antibody at the expense of cross-reaction. However, this rule probably applies only to classical immunoassays like ELISA in which adsorption of analytes to solid phase substrates is needed, which may pose a steric hindrance for the antibody to access targeted sites.

A linear dose-response relationship was only observed with 8E11 as shown in **Figure 2.21**; therefore, 8E11 was chosen as the primary antibody and used for later experiments.

## **2.5 Conclusions**

The capillary electrophoresis based immunoassay developed in our group was readily applied to the detection of BPDE-DNA adducts. To study effects of arsenic on the formation and repair of BPDE-DNA adducts, the experimental conditions were further optimized and tailored to meet our goal. A dose-response relationship was established for one of the cell lines to be used in later experiments. The relative quantitation is easy to obtain and it is feasible to utilize this method to determine the changes in BPDE-DNA adduct levels in cells affected by arsenic, without resorting to expensive instrumentation and tedious procedures of sample manipulation.

## 2.6 References

1. Lutz WK. (1979) In vivo covalent binding of organic chemicals to DNA as a quantitative indicator in the process of chemical carcinogenesis. *Mutat Res*, 65, 289-356
2. Lutz WK. (1982) The covalent binding index-DNA binding in vivo as a quantitative indicator for genotoxicity. In: Banbury Report 13. Bridges BA, Butterworth BE, Weinstein IB, eds. *Indicator of Genotoxic Exposure*. Cold Spring Harbor: Cold Spring Harbor Laboratory. pp 89-204
3. Lutz WK. (1986) Quantitative evaluation of DNA binding data for risk estimation and for classification of direct and indirect carcinogens. *J Cancer Res Clin Oncol*, 112, 85-91
4. Matin CN, Lawley PD, Phillips DH, Venitt S, Waters R. (1993) Measurement of covalent binding to DNA in vivo. In: Kirkland DJ, Fox M, eds. *Supplementary Mutagenicity Tests: UKEMS Recommended Procedures*. Cambridge University Press. pp 78-104
5. Dahl GA, Miller JA, Miller EC. (1978) Vinyl carbamate as a promutagen and a more carcinogenic analog of ethyl carbamate. *Cancer Res*, 38, 3793-3804
6. Ribovich ML, Miller JA, Miller EC, Timmins LG. (1982) Labeled 1, N<sup>6</sup>-ethenoadenosine and 3, N<sup>4</sup>-ethenocytidine in hepatic RNA of mice given [ethyl-1,2-<sup>3</sup>H or ethyl-1-<sup>14</sup>C]ethyl carbamate (urethan). *Carcinogenesis*, 3, 539-546
7. Albro PW, Corbett JT and Schroeder JL. (1984) Metabolism of methyl-*n*-amyl ketone (MAK) and its binding to DNA of rat liver in vivo and in vitro. *Chem Biol Interact*, 51, 295-308

8. Reddy MV. (2000) Methods for testing compounds for DNA adduct formation. *Regul Toxicol Pharmacol*, 32, 256-263
9. Elmore DE. (1987) Ultrasensitive radioisotope, stable-isotope, and trace-element analysis in the biological sciences using tandem accelerator mass spectrometry. *Bio Trace Element Res*, 12, 231-245
10. Vogel JS, Turteltaub KW, Finkel R, Nelson DE. (1993) Accelerator mass spectrometry. *Anal Chem*, 67, 353A-359A
11. Phillips DH, Farmer PB, Belandf FA, Nath RG, Poirier MC, Reddy MV, and Turteltaub KW. (2000) Methods of DNA adducts determination and their application to testing compounds for genotoxicity. *Environ Mol Mutag*, 35, 222-233
12. Garner RC. (1998) The role of DNA adducts in chemical carcinogenesis. *Mutat Res*, 402, 67-75
13. Poirier MC, Santella RM and Weston A. (2000) Carcinogen macromolecular adducts and their measurement. *Carcinogenesis*, 21, 353-359
14. Randerath K, Reddy MV, Gupta RC. (1981)  $^{32}\text{P}$ -labeling test for DNA damage. *Proc Natl Acad Sci USA*, 78, 6126-6129
15. Gupta RC. (1985) Enhanced sensitivity of  $^{32}\text{P}$ -postlabeling analysis of aromatic carcinogen: DNA adducts. *Cancer Res*, 45, 5656-5662
16. Phillips DH. (1997) Detection of DNA modifications by the  $^{32}\text{P}$ -postlabelling assay. *Mutat Res*, 378, 1-12
17. Beach AC, Gupta RC. (1992) Human biomonitoring and the  $^{32}\text{P}$ -postlabeling assay. *Carcinogenesis*, 13, 1053-1074

18. Poirier MC and Weston A. (1996) Human DNA adduct measurements: state of the art. *Environ Health Perspect*, 104(suppl 5), 883-893
19. Park JW, Ames BN. (1988) 7-methylguanine adducts in DNA are normally present at high levels and increase on ageing: analysis by HPLC with electrochemical detection. *Proc Natl Acad Sci USA*, 85, 7467-7470
20. Halliwell B, Dizdaroglu M. (1992) The measurement of oxidative damage to DNA by HPLC and GC/MS techniques. *Free Radic Res Commun*, 16, 75-87
21. Inagaki S, Esaka Y, Sako M, Goto M. (2001) Analysis of DNA adducts bases by capillary electrophoresis with amperometric detection. *Electrophoresis*, 22, 3408-3412
22. Alexandrov K, Rojas M, Geneste O, Castegnaro M, Camus AM, Petruzzelli S, Giuntini C and Bartsch H. (1992) An improved fluorometric assay for dosimetry of benzo[a]pyrene diol-epoxide-DNA adducts in smokers' lung: comparison with total bulky adducts and aryl hydrocarbon hydroxylase activity. *Cancer Res*, 52, 6248-6253
23. Groopman JD, Donahue PR, Zhu J, Chen J and Wogan GN. (1985) Aflatoxin metabolism in humans: detection of metabolites and nucleic acid adducts in urine by affinity chromatography. *Proc Natl Acad Sci USA*, 82, 6492-6496
24. Weston A. (1993) Physical methods for the detection of carcinogen-DNA adducts in humans. *Mutat Res*, 288, 19-29
25. Schmitz OJ, Worth CC, Stach D and Wießler M. (2002) Capillary electrophoresis analysis of DNA adducts as biomarkers for carcinogenesis. *Angew Chem Int Ed*, 41, 445-448

26. Sharma M, Jain R, Ionescu E and Slocum HK. (1995) Capillary electrophoretic separation and laser-induced fluorescence detection of the major DNA adducts of cisplatin and carboplatin. *Anal Biochem*, 228, 307-311
27. Apruzzese WA, Vouros P. (1998) Analysis of DNA adducts by capillary methods coupled to mass spectrometry: a perspective. *J Chromatogr A*, 794, 97-108
28. Ding J, Vouros P. (1997) Capillary electrochromatography and capillary electrochromatography-mass spectrometry for the analysis of DNA adduct mixtures. *Anal Chem*, 69, 79-84.
29. Roberts DW, Churchwell MI, Beland FA, Fang JL, Doerge DR. (2001) Quantitative analysis of etheno-2'-deoxycytidine DNA adducts using on-line immunoaffinity chromatography coupled with LC/ES-MS/MS detection. *Anal Chem*, 73, 303-309.
30. Barry JP, Norwood C, Vouros P. (1996) Detection and identification of benzo[a]pyrene diol epoxide adducts to DNA utilizing capillary electrophoresis-electrospray mass spectrometry. *Anal Chem*, 68, 1432-1438.
31. Hecht SS, Carmella SG, Foiles PG, and Murphy SE. (1994) Biomarkers for human uptake and metabolic activation of tobacco-specific nitrosamines. *Cancer Res*, 54, 1912s-1917s
32. Marnett LJ, Burcham PC. (1993) Endogenous DNA adducts: potential and paradox. *Chem Res Toxicol*, 6, 771-785
33. Giese RW. (1991) Analysis of DNA adducts by mass spectrometry. In: Garner RC, Farmer PB, Steele GT, Wright AS, eds. *Human Carcinogen Exposure: Biomonitoring and Risk Assessment*. IRL Press, Oxford. pp 247-253

34. Poirier MC. (1981) Antibodies to carcinogen-DNA adducts. *J Natl Cancer Inst*, 67, 515-519
35. Poirier MC. (1993) Antisera specific for carcinogen-DNA adducts and carcinogen-modified DNA: applications for detection of xenobiotics in biological samples. *Mutat Res*, 288, 31-38
36. Muller R and Rajewsky MF. (1981) Antibodies specific for DNA components structurally modified by chemical carcinogens. *J Cancer Res Clin Oncol*, 102, 99-113
37. Shuker DE. (1999) DNA adducts in mammalian cells as indicators of exposure to carcinogens. In: McGregor DB, Rice JM and Venitt S, eds. *The Use of Short- and Medium-term Tests for Carcinogens and Data on Genetic Effects in Carcinogenic Hazard Evaluation*. IARC Scientific Publications No. 146. Lyon, France. pp 287-307
38. Den Engelse L, van Benthem J, Scherer E. (1990) Immunocytochemical analysis of in vivo DNA modification. *Mutat Res*, 233, 265-287
39. Santella RM. (1999) Immunologic methods for detection of carcinogen-DNA damage in humans. *Cancer Epidemiol Biomarkers Prev*, 8, 733-739
40. Souliotis VL, Kyrtopoulos SA. (1989) A novel, sensitive assay for O6-ethylguanine in DNA, based on repair by the enzyme O6-alkylguanine-DNA-alkyltransferase in competition with an oligonucleotide containing O6-methylguanine. *Cancer Res*, 49, 6997-7001.
41. Allan JM, Garner RC. (1994) The use of purified DNA repair proteins to detect DNA damage. *Mutat Res*, 313, 165-174

42. O'Connor TR. (1996) The use of DNA glycosylases to detect DNA damage. In: Pfeifer GP, ed. *Technologies for Detection of DNA Damage and Mutations*. Plenum Press, New York. pp 155-170
43. Pfeifer GP, Drouin R, Holmquist GP. (1993) Detection of DNA adducts at the DNA sequence level by ligation-mediated PCR. *Mutat Res*, 288, 39-46
44. de Kok TM, Moonen HJ, van Delft J, van Schooten FJ. (2002) Methodologies for bulky DNA adduct analysis and biomonitoring of environmental and occupational exposures. *J Chromatogr B*, 778, 345-355
45. Cheng YF and Dovichi NJ. (1988) Subattomole amino acid analysis by capillary zone electrophoresis and laser-induced fluorescence. *Science*, 242, 562-564.
46. Le XC, Xing JZ, Lee J, Leadon SA and Weinfeld M. (1998) Inducible repair of thymine glycol detected by an ultrasensitive assay for DNA damage. *Science*, 280,1066-1069
47. Xing JZ, Carnelley T, Lee J, Watson WP, Booth E, Weinfeld M, Le XC. (2000) Assay for DNA damage using immunochemical recognition and capillary electrophoresis. In Mitchelson KR, Cheng J, eds. *Capillary electrophoresis of Nucleic Acids, Vol.1: Introduction to the Capillary Electrophoresis of Nucleic Acids*. *Methods in Molecular Biology*, vol.162. Humana Press, New York. pp 419-428
48. Tan WG, Carnelley TJ, Murphy P, Wang H, Lee J, Barker S, Weinfeld M, Le XC. (2001) Detection of DNA adducts of benzo[a]pyrene using immunoelectrophoresis with laser-induced fluorescence analysis of A549 cells. *J Chromatogr A*, 924, 377-386

49. Wang HL, Lu ML, Lee J, Weinfeld M and Le XC. (2003) Immunoassay using capillary electrophoresis laser induced fluorescence detection for DNA adducts. *Anal Chim Acta*, 500, 13-20
50. Carnelley TJ, Barker S, Wang H, Tan WG, Weinfeld M and Le XC. (2001) Synthesis, characterization, and application of a fluorescent probe of DNA damage. *Chem Res Toxicol*, 14, 15113-1522
51. Tang MS. (1996) Mapping and quantification of bulky-chemical-induced DNA damage using UvrABC nucleases. In: Pfeifer GP, ed. *Technologies for Detection of DNA Damage and Mutations*. Plenum Press, New York. pp 139-153
52. Mitchell DL. (1996) Radioimmunoassay of DNA damaged by ultraviolet (UV) light. In: Pfeifer GP. ed. *Technologies for Detection of DNA Ddamage and Mutations*. Plenum Press, New York. pp 73-85
53. Heegaard NH, Olsen DT and Larsen KLP. (1996) Immuno-capillary electrophoresis for the characterization of a monoclonal antibody against DNA. *J Chromatogr A*, 744, 285-294
54. Wang H, Xing J, Tan W, Lam M, Carnelley T, Weinfeld M and Le XC. (2002) Binding stoichiometry of DNA adducts with antibody studied by capillary electrophoresis and laser-induced fluorescence. *Anal Chem*, 74, 3714-3719
55. Miller JJ, Levinson SS. (1996) Interferences in immunoassay. In: Diamandis EP and Christopoulos TK, ed. *Immunoassay*. Academic Press, San Diego. pp 172
56. Vahakangas K, Haugen A and Harris CC. (1985) An applied synchronous fluorescence spectrophotometric assay to study benzo[a]pyrene-diolepoxide-DNA adducts. *Carcinogenesis*, 6, 1109-1116

## Chapter Three

# Effects of Arsenic on the Formation of Benzo(a)pyrene Diol Epoxide-DNA Adducts

### 3.1 Introduction

There are several possibilities that could account for the enhancing effect of arsenic on mutagenicity induced by other carcinogens. Arsenic may modulate the efficiency of carcinogen-adduct formation, the repair efficiency of carcinogen adducts, or the fidelity of translesion synthesis. Considering that adduct formation is the preceding event to DNA repair and one of the earliest events in the initiation phase of cancer (1-3), the effects of arsenic on the formation of carcinogen-DNA adducts warrant investigation.

Benzo(a)pyrene (BaP) is a classical potent carcinogen implicated in the association between smoking and lung cancer development (4). Once inside cells, BaP is metabolized via a three-step process (5,6). Initially, BaP is metabolized largely by cytochrome P-450 1A1 (CYP1A1) to BaP-7,8-oxide, which in turn undergoes hydration to BaP-7,8-diol by epoxide hydrolase and can be further oxidized by either the P-450 monooxygenase system and/or a peroxidase, such as cyclooxygenase-2 (COX-2, also known as prostaglandin H synthase) (7) or myeloperoxidase (8) to benzo(a)pyrene diol epoxide (BPDE). BPDE may covalently bind to DNA, producing a major adduct at the N<sup>2</sup> position of deoxyguanosine (BPDE-N<sup>2</sup>-dG). The major pathway leading to the generation of BPDE-N<sup>2</sup>-dG is shown in **Figure 3.1**. Formation of BPDE-N<sup>2</sup>-dG is considered to be the critical event in carcinogenesis initiated by BaP (9). If this adduct is left unrepaired, a mutation can occur in DNA. On the other hand, detoxification of BPDE

can be effected by conjugation to reduced glutathione (GSH), a process that is catalysed by glutathione S-transferase (GST). Conjugated metabolites are more soluble in water than BaP so they are more readily excreted.

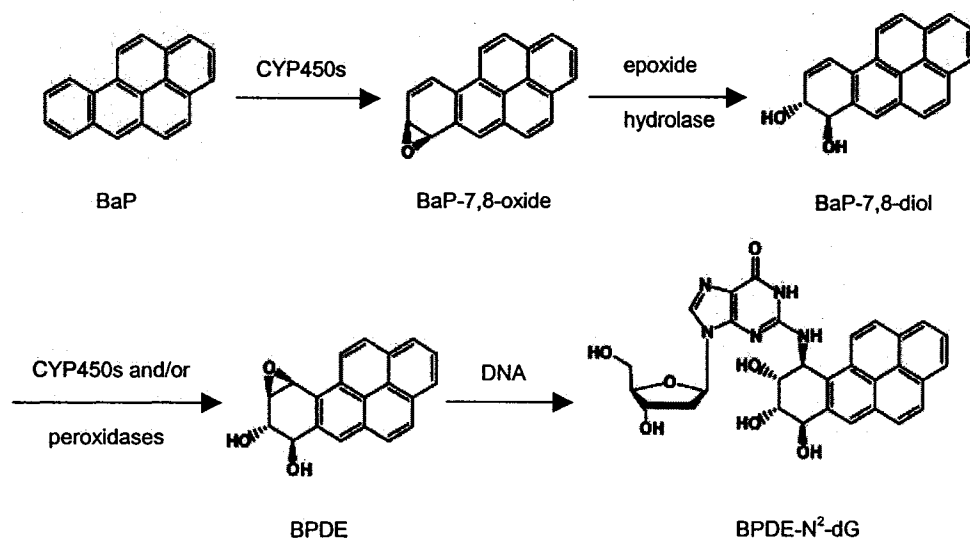


**Figure 3.1. Major established pathway of metabolic activation of BaP, leading to the formation of BPDE-N<sup>2</sup>-dG (adapted from [10]).**

Maier et al. (11) showed that exposure of mouse hepatoma Hepa-1 cells to low concentrations of arsenite (iAs(III)) increased BaP-induced BPDE-DNA adduct levels by as much as 18-fold while iAs(III) treatment did not alter the adduct removal kinetics. An *in vivo* study from the same research group reported that iAs(III) co-treatment increased the average BPDE-DNA adduct levels in both mouse lungs and skin, with the increase (~2-fold) in the lungs being statistically significant ( $P=0.038$ ) (12). In another *in vivo* study using mice, no more stable BPDE-DNA adducts were observed in the group exposed to iAs(III) plus BaP than in the group exposed to BaP alone (13). However, in a study with Sprague-Dawley rats, iAs(III) was shown to decrease BaP-induced BPDE-

DNA adduct formation (14). The  $^{32}\text{P}$ -postlabelling assay was the method of choice in these four studies. Recently, five arsenic species — iAs(III), monomethylarsonous acid (MMA(III)), dimethylarsinous acid (DMA(III)), monomethylarsonic acid (MMA(V)), and dimethylarsinic acid (DMA(V)) — have been examined by Schwerdtle et al. regarding their effect on the formation and repair of BPDE-DNA adducts in A549 human lung cancer cells (15). Using a high performance liquid chromatography (HPLC)/fluorescence assay, they observed that only iAs(III) and MMA(III) increased the BPDE-DNA adduct formation in the concentration range under investigation: 0-75  $\mu\text{M}$  for iAs(III), 0-7.5  $\mu\text{M}$  for MMA(III) and DMA(III), and 0-500  $\mu\text{M}$  for MMA(V) and DMA(V).

However, all these studies suffered from two main limitations. Firstly, these studies used either animal models (mouse and rat) or human tumor cells (Hepa-1, c37, and CX4 in one study and A549 in another). Extrapolation to normal human cells with a view to elucidating the carcinogenic mechanism of arsenic as a human carcinogen is largely uncertain. Secondly, repair-proficient cells were used. Therefore, the effect of arsenic on adduct repair could not be differentiated from its effect on adduct formation, especially with the treatment protocols used. In other words, the apparent formation enhancement might simply result from repair inhibition within the co-incubation period.

To confirm whether or not arsenic has an effect on the formation of BPDE-DNA adducts, a repair-deficient human cell line was chosen in our study so that changes in adduct levels could be unambiguously attributed to the effect of arsenic on adduct formation. Nucleotide excision repair (NER) is responsible for removing bulky lesions such as BPDE-DNA adducts from the genome. The xeroderma pigmentosum

complementation group A (XPA) protein is an early participant in the NER process. It is the only factor whose disruption completely eliminates NER (16). In addition, the XPA protein has no other known function in DNA metabolism. According to Lindahl and Wood, it seems to present the most suitable and specific target for disrupting NER by inhibition of its function (16). No heterogeneity in terms of repair capacity within the XPA complementation group has been shown (17). Therefore, SV40-transformed XPA fibroblasts (GM04312C) were used in our study. Abrogation of the p53 function by SV40 transformation could further diminish DNA repair (18).

Recent studies showed that although either BaP or iAs(III) alone increased the catalytic activity and expression of CYP1A1, iAs(III) inhibited the induction of CYP1A1 activity when co-administered with BaP (19-21). This inhibition was observed in some previous studies (22-24). Inhibition of CYP1A1 and the subsequent bioactivation of BaP was thought to be responsible for the observation that a combined administration of BaP and iAs(III) led to a reduction in adduct formation when compared with the BaP-treated group (14). However, one study showed that iAs(III) did not alter BaP-inducible CYP1A1 activity when it was added 30 min before BaP exposure (11); another study showed that a 6-h pretreatment with iAs(III) did not itself induce CYP1A1 or affect the BaP-mediated induction of CYP1A1, but resulted in a significant decrease in the expression level of COX-2 in CL3 human lung adenocarcinoma cells (25). Downregulation of COX-2 expression was also observed in human acute myeloid leukemia HL-60 cells treated with arsenic trioxide ( $As_2O_3$ ) (26). In addition, the metabolism of BaP is a multiple-pathway process and is far more complex than what is shown in **Figure 3.1**. To control for these uncertainties, the reactive metabolite BPDE

was used to generate BPDE-DNA adducts in this study. Thus, problems associated with the metabolic pathways, such as, for example, the Phase I bioactivation of BaP, were avoided. The time for incubation with BPDE was limited to only 30 min to further reduce any possibility of DNA repair.

## 3.2 Experimental

### 3.2.1 Materials

Racemic anti-BPDE and [<sup>3</sup>H]-anti-BPDE were supplied by the NCI Chemical Carcinogen Repository (Midwest Research Institute, Kansas City, MO). To avoid hydrolysis of the epoxide, a stock solution of BPDE was always prepared fresh by dissolving BPDE in anhydrous tetrahydrofuran (THF) (>99.9% purity, Sigma-Aldrich, St. Louis, MO) immediately before use. iAs(III) (99.4% purity) was obtained as an arsenic atomic absorption standard solution from Aldrich (Milwaukee, WI) and used as a stock solution with a concentration of 13.3 mM. Sodium arsenate (iAs(V), 99.4% purity) and DMA(V) (98% purity) were obtained from Sigma (St. Louis, MO). MMA(V) was purchased from Chem Service (West Chester, PA) and its purity was determined to be approximately 85% using an Elan 6100 DRC<sup>plus</sup> inductively coupled argon plasma mass spectrometer (PE Sciex, Concord, ON). Methylarsine oxide (CH<sub>3</sub>As<sup>III</sup>O) and dimethyliodoarsine ((CH<sub>3</sub>)<sub>2</sub>As<sup>III</sup>I) were kindly provided by Dr. WR Cullen (University of British Columbia, Vancouver, BC) and were used as the precursors to MMA(III) and DMA(III), respectively. Stock solutions of iAs(V), MMA(V), and DMA(V) were prepared in deionized water at concentrations of 1 M, and stock solutions of MMA(III) and DMA(III) were prepared by dissolving the precursors in deionized water to a final concentration of 10 mM. When preparing the stock solution of DMA(III), 3 volumes of

dimethylsulfoxide (DMSO) were used to dissolve  $(\text{CH}_3)_2\text{As}^{\text{III}}\text{I}$  before adding deionized water. To prevent oxidation of the trivalent methylated arsenic species, their stock solutions were prepared shortly before use.

### 3.2.2 Cells and cell cultures

GM04312C cells (SV40-transformed XPA fibroblasts GM02345) and GM00038B cells were obtained from the NIGMS Human Genetics Cell Repository (Camden, NJ). GM02345 harbors a G-to-C transversion at the 3-prime splice acceptor site of intron 3 of the XPA gene, which abolishes the canonical 3-prime splice site and results in missplicing of XPA. The GM04312C cells were cultivated in Dulbecco's modified Eagle's medium/nutrient mixture F-12 (DMEM/F12) (1:1 ratio) (Gibco BRL, Rockville, MD) supplemented with 10% fetal bovine serum. The cells were seeded in 100-mm dishes at a density of  $1 \times 10^6$  cells per dish and maintained at 37 °C in humidified incubators containing 5%  $\text{CO}_2$ . The cells were grown to about 80-90% confluence for treatments.

### 3.2.3 Treatment of cells

The cells were pretreated with various arsenic species at the indicated concentrations for the respective experiments in complete growth medium for 24 h. The cells were washed twice with phosphate-buffered saline (PBS) before the addition of BPDE in serum-free medium at a final concentration of 0.5  $\mu\text{M}$ . The concentrations of organic solvents used to dissolve BPDE and  $(\text{CH}_3)_2\text{As}^{\text{III}}\text{I}$  did not exceed 0.001%, to avoid the direct influence of DMSO or THF on the cells. After a 30-min incubation, BPDE was removed and the cells were washed with PBS three times before their DNA was extracted for measurement of the BPDE-DNA adducts.

### 3.2.4 DNA isolation

The cells were lysed in DNAzol® reagent (Invitrogen Life Technologies) and the genomic DNA was precipitated with ice-cold 99.9% ethanol and washed twice with cold 70% ethanol. The DNA pellet was air-dried and resuspended in deionized water and the solution was placed in an incubator at 37 °C overnight to facilitate the redissolution of DNA. DNA concentrations were measured at 260 nm using a SmartSpec™ 3000 spectrometer (Bio-Rad Laboratories, Cambridge, MA).

### 3.2.5 Detection of BPDE-DNA adducts

A capillary electrophoresis laser induced fluorescence (CE-LIF) based immunoassay, as described in **Chapter 2**, was used in this study to detect BPDE-DNA adducts. Typically, an aliquot of DNA was heat-denatured at 100 °C for 5 min followed by cooling on ice for 3 min. Denatured DNA was incubated with a mouse anti-BPDE antibody (Clone 8E11, isotype IgG<sub>1</sub>, Trevigen Inc., Gaithersburg, MD) and a fluorescently-labelled goat anti-mouse antibody. The goat anti-mouse antibody was received as a Zenon™ Alexa Fluor® 546 mouse IgG<sub>1</sub> labelling kit (Molecular Probes, Eugene, OR). To the mixture of the DNA sample and the antibodies, an incubation buffer was added to bring the total sample volume to 20 µL. The incubation buffer contained 10 mM Tris and 80 mM glycine, and its pH was adjusted to pH 7.8 with acetic acid. After overnight incubation on ice in the dark, samples were electrokinetically injected into the capillary using an injection voltage of 10 kV for 10 s. The separation was carried out at room temperature with a separation voltage of 20 kV. The running buffer was a Tris-glycine mixture containing 30 mM Tris and 170 mM glycine, at pH 8.3. Between runs,

the capillary was rinsed for 5 min electrophoretically with 0.02 M NaOH and 5 min with the running buffer.

### **3.2.6 Cell number and colony formation assay**

To determine the cytotoxic responses of GM04312C cells to different arsenic species, 80-90% confluent GM04312C cells were treated for 24 h with the test arsenic compounds. The cells were trypsinized and counted using a Z2 Coulter® Particle Count and Size Analyzer (Beckman Coulter™, Coulter Electronics Inc., Hialeah, FL).

For the colony formation assay, exponentially growing GM04312C cells were trypsinized and resuspended in DMEM/F12 medium. The cells were seeded into 60-mm dishes at densities from 100 to  $10^5$  cells per dish, and allowed to attach overnight so that no visible cell detachment was observed during treatment. The cells were treated with arsenic species at various concentrations for 24 h. After treatment, the cells were washed three times with ice-cold PBS and restored in fresh growth medium for colony formation. After 2-3 weeks, the colonies were stained with 0.25% methylene blue and counted, and the cloning capability was calculated based on the plating efficiency of untreated control cells.

### **3.2.7 Cellular GSH content**

The cellular GSH content was determined using a Bioxytech GSH-400 colourimetric assay kit (Oxis International, Portland, OR). Cells ( $10^6$ - $10^7$ ) were trypsinized, centrifuged, and washed with PBS. They were then resuspended in 100  $\mu$ l of ice-cold metaphosphoric acid. After 4 cycles of freeze-thaw, the solution was centrifuged at  $10,000\times g$  at 4 °C for 10 min. The clear supernatant was collected at 4 °C for the subsequent assay. Reagent R1 and NaOH from the assay kit were added to the

supernatant. After incubation at 25 °C for 10 min in the dark, the absorbance of the solution was measured at 400 nm. GSH concentrations in the solution were calculated from the absorbance and a pre-stored calibration curve of a GSH standard. The cellular GSH content is expressed as nmol of GSH per million cells.

### **3.2.8 GST activity assay**

Cellular GST activity was measured by a GST Colorimetric Activity Assay Kit (Biovision, Cedarlane Laboratory Ltd, ON) using 1-chloro-2,4-dinitrobenzene (CDNB) as the substrate. Briefly, the cells were trypsinized, centrifuged, and homogenized in 100 µl of GST Sample Buffer. After centrifugation at 10,000× g at 4 °C for 10 min, the supernatant was collected for the subsequent assay. GSH and CDNB in GST Assay Buffer were added to the supernatant and mixed. The absorbance was read at 340 nm using a SPECTRA MAX<sup>®</sup> 190 microplate spectrophotometer controlled by SOFTmax<sup>®</sup> PRO 4.0 (Molecular Devices Corporation, Sunnyvale, CA). Absorbance readings were repeatedly taken for a minimum of 5 time intervals, to obtain enzyme kinetic information. GST activity was expressed as nmoles of CDNB reduced per min per million cells.

### **3.2.9 Chromatin accessibility**

A denaturation sensitivity assay was used to examine chromatin accessibility, as described by Rubbi et al. (27), with some modifications. Cells were cultured in DMEM/F12 (1:1 ratio) (Gibco BRL, Rockville, MD) supplemented with 10% fetal bovine serum on coverslips placed in 35 mm dishes. After reaching 80-90% confluence, the cells were incubated with arsenic compounds at various concentrations. After a 24-h incubation, the cells were washed and fixed with 2% paraformaldehyde for 30 min, and then incubated with 50 µg/ml RNase A (Sigma) in PBS at room temperature for 1 h. The

cells were then denatured for 30 s with 0.1 M HCl. The denaturation was stopped with 20  $\mu\text{g/ml}$  acridine orange (AO) (Molecular Probes, Eugene, OR) in 0.1 M phosphate/citrate buffer (pH 2.6), and the coverslips were mounted with the addition of 1,4-diazobicyclo-[2,2,2]-octane (DABCO, Sigma D2522) and Mowiol 488 (Calbiochem 475904). A Zeiss LSM510 laser scanning confocal microscope (Carl Zeiss, Jena, Germany) with an F-Fluar 40 $\times$ , NA 1.3 objective lens was used to obtain fluorescence images. The cell samples were scanned using a 488 nm argon ion laser for excitation (0.75% transmission); both green (dsDNA) and red (ssDNA) fluorescence signals were detected through the 505/50BP and 650LP filters, respectively. The fraction of dsDNA was calculated as  $F_{\text{dsDNA}} = G/(G+R)$  and displayed numerically.

### **3.2.10 Effects of arsenic on the cellular uptake of BPDE**

GM04312C cells grown in 6-well plates were treated at 80-90% confluence with arsenic compounds for 24 h. After being washed twice with PBS, the cells were incubated with 0.5  $\mu\text{M}$  [ $^3\text{H}$ ]-anti-BPDE (2030 mCi/mmol) (Chemsyn Science Laboratories, Lenexa, KS) for 30 min. After washing with PBS three times, the cells were lysed in 0.2 M NaOH prior to radioactivity measurement. Cells in parallel wells were trypsinized and counted. The radioactivity of each sample was determined with an LS5801 Liquid Scintillation Counter (Beckman Coulter) and expressed as cpm/ $1 \times 10^6$  cells.

### 3.3 Results and Discussion

#### 3.3.1 Repair capability of the XPA cell line used

To justify the use of GM04312C cells as NER-deficient cells for studying the effect of arsenic on the formation of BPDE-DNA adducts, a repair experiment with GM04312C cells was carried out. The repair kinetics in this cell line are shown in **Figure 3.2**. Cells that were 80-90% confluent were used to avoid post-treatment replication. The differences in BPDE-DNA adduct levels between different repair times up to 24 h were not statistically significant ( $P>0.05$ ). These results confirmed that GM04312C cells lack the ability to repair BPDE-DNA adducts.

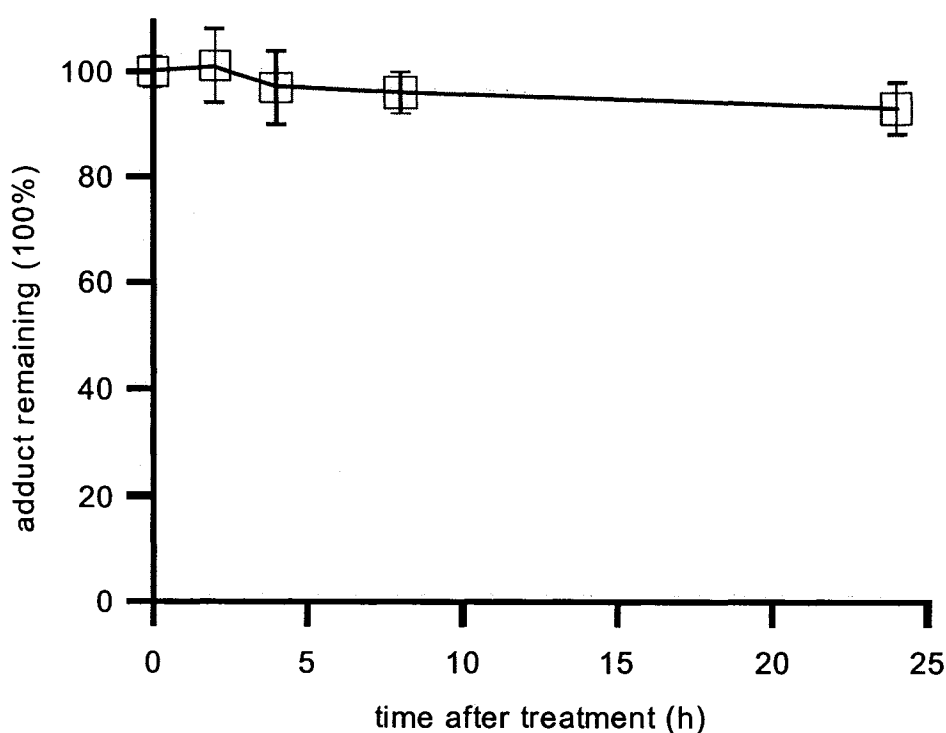


**Figure 3.2. Repair of BPDE-DNA adducts in human fibroblasts (GM04312C).** 80-90% confluent cells were treated with 1  $\mu$ M BPDE for 30 min, and then allowed to repair in complete medium for 0 h, 2 h, 4 h, 8 h, or 24 h. Error bars indicate the standard deviation of four determinations from two experiments.

### 3.3.2 Effects of arsenic compounds on the formation of BPDE-DNA adducts

Each of the six arsenic compounds under investigation was shown to be capable of enhancing the formation of BPDE-DNA adducts (Figures 3.3-3.8). Much lower concentrations of the trivalent arsenic species (iAs(III), MMA(III), and DMA(III)) than of the pentavalent arsenic species (iAs(V), MMA(V), and DMA(V)) were needed to enhance the formation of BPDE-DNA adducts. iAs(III) increased adduct formation by 39% at 10  $\mu\text{M}$  and by 87% at 100  $\mu\text{M}$  (Figure 3.3) while MMA(III) increased adduct formation by 100% at 5  $\mu\text{M}$  (Figure 3.4). Similarly, Schwerdtle et al. (15) observed that iAs(III) started to enhance adduct formation at 25  $\mu\text{M}$  and achieved 40% more adducts at 75  $\mu\text{M}$  while MMA(III) started the enhancement at 2.5  $\mu\text{M}$  and yield 60% more adducts at 5  $\mu\text{M}$ . Notably, in their study, DMA(III) did not show any enhancement over a concentration range up to 7.5  $\mu\text{M}$ . By contrast, in our study, DMA(III) increased adduct formation by 21% at 5  $\mu\text{M}$  (Figure 3.5). The difference in the magnitude of enhancement might be due to different treatment protocols or different cell lines used. In their study, exponentially growing A549 cells were pre-incubated with arsenic for 16 h, and then co-incubated with 50 nM BPDE and arsenic for 2 h. It is noteworthy that DMA(III) is easily oxidized (28); therefore, DMA(III) freshly synthesized by the provider was used in our study.

The pentavalent iAs(V) enhanced adduct formation only when its concentration reached 250  $\mu\text{M}$  (Figure 3.6). At high concentrations (2000  $\mu\text{M}$ ), MMA(V) and DMA(V) increased the formation of BPDE-DNA adducts (Figures 3.7-3.8), but over a concentration range of up to 500  $\mu\text{M}$ , MMA(V) and DMA(V) had no effect on adduct formation. These results were consistent with those of Schwerdtle et al. (15), although that group did not test MMA(V) or DMA(V) at higher concentrations.

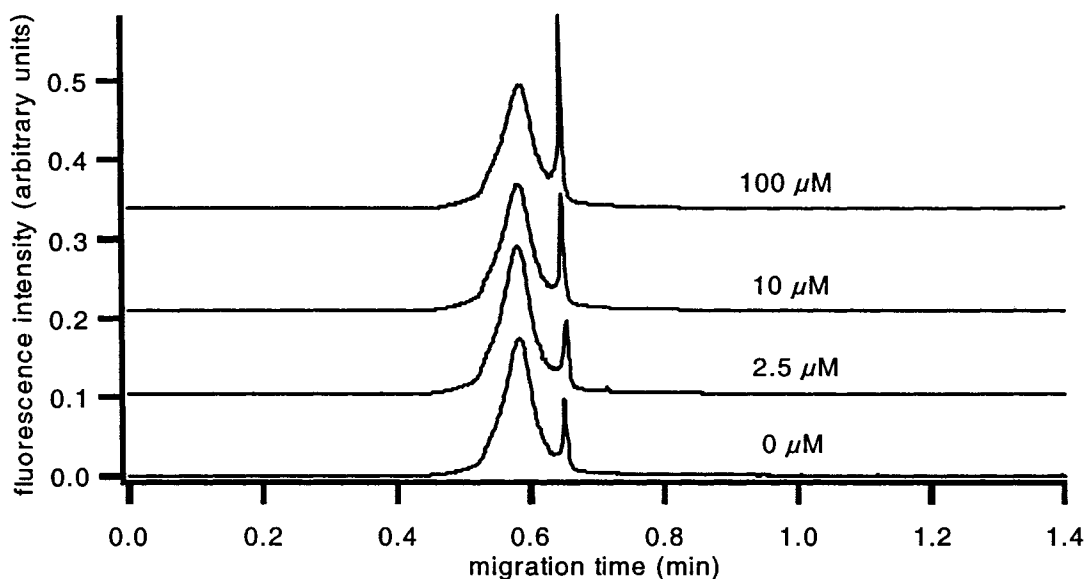


**Figure 3.3a.** Electropherograms obtained from DNA extracted from XPA cells pretreated for 24 h with different concentrations of iAs(III) as indicated, and then incubated with 0.5 μM BPDE for 30 min. The ratio of peak areas between the two peaks indicates the level of DNA adducts.

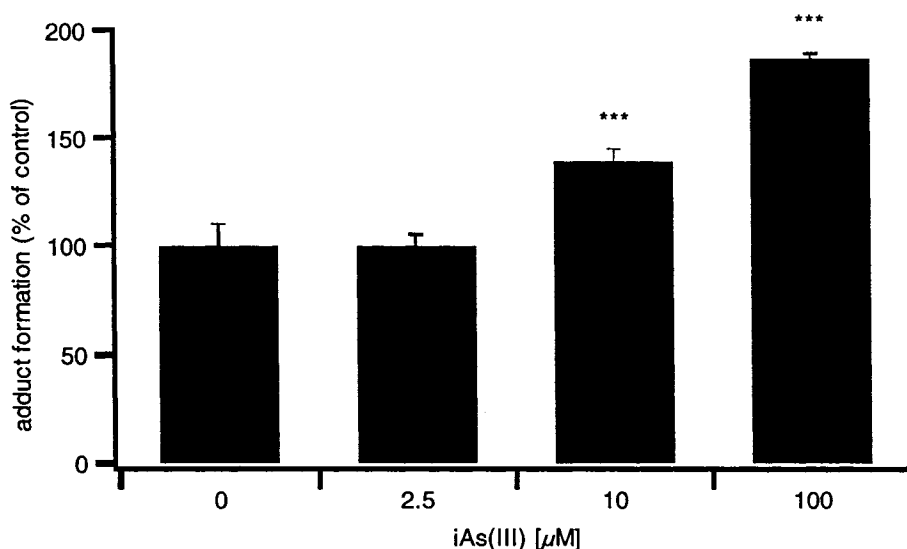


**Figure 3.3b.** Histograms representing the relative adduct levels after pretreatment with different iAs(III) concentrations. Adduct levels obtained from BPDE incubation alone were used as controls. \*\*\*P<0.01 using one-way Student's test. Error bars indicate the standard deviation from three experiments.

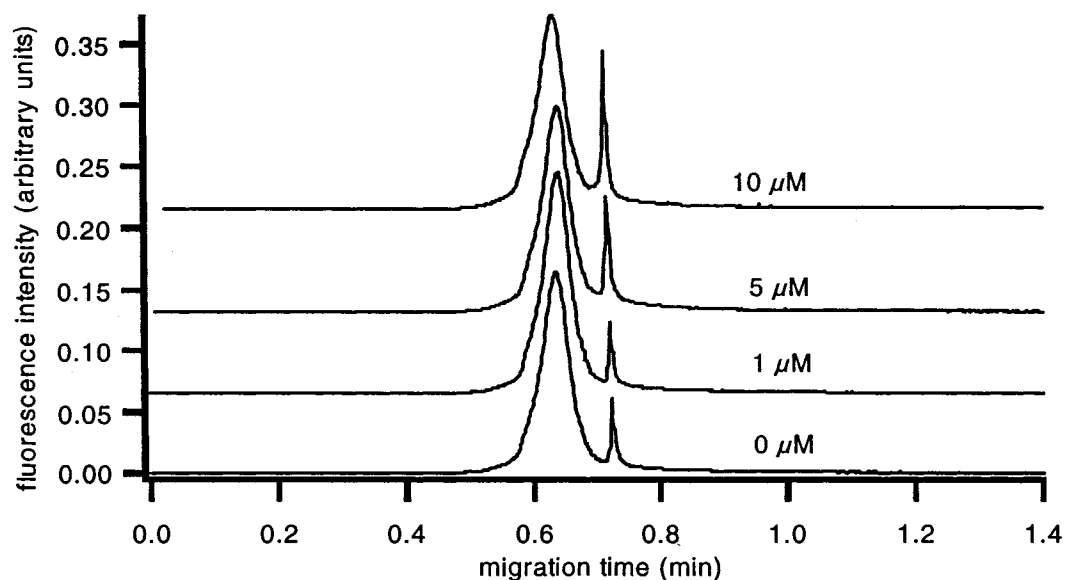


**Figure 3.4a.** Electropherograms obtained from DNA extracted from XPA cells pretreated for 24 h with different concentrations of MMA(III) as indicated, and then incubated with 0.5 μM BPDE for 30 min. The ratio of peak areas between the two peaks indicates the level of DNA adducts.

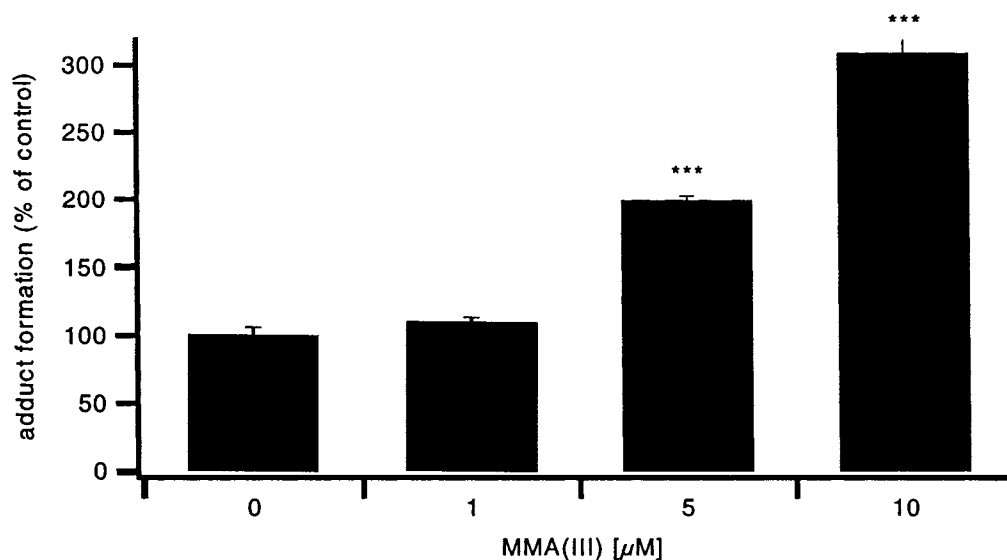


**Figure 3.4b.** Histograms representing the relative adduct levels after pretreatment with different MMA(III) concentrations. Adduct levels obtained from BPDE incubation alone were used as controls. \*\*\* $P < 0.01$  using one-way Student's test. Error bars indicate the standard deviation from three experiments.

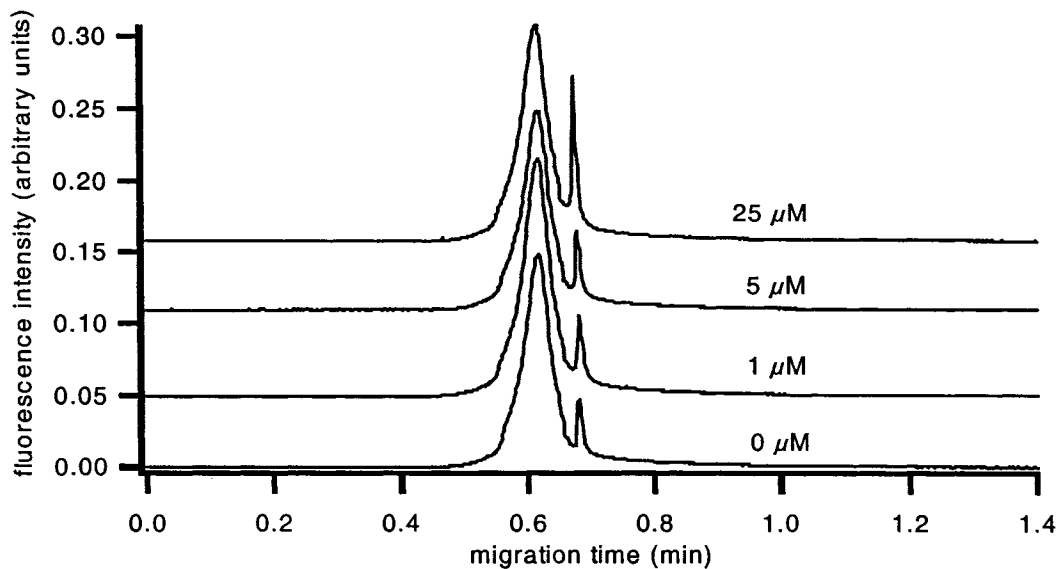


**Figure 3.5a.** Electropherograms obtained from DNA extracted from XPA cells pretreated for 24 h with different concentrations of DMA(III) as indicated, and then incubated with 0.5  $\mu\text{M}$  BPDE for 30 min. The ratio of peak areas between the two peaks indicates the level of DNA adducts.

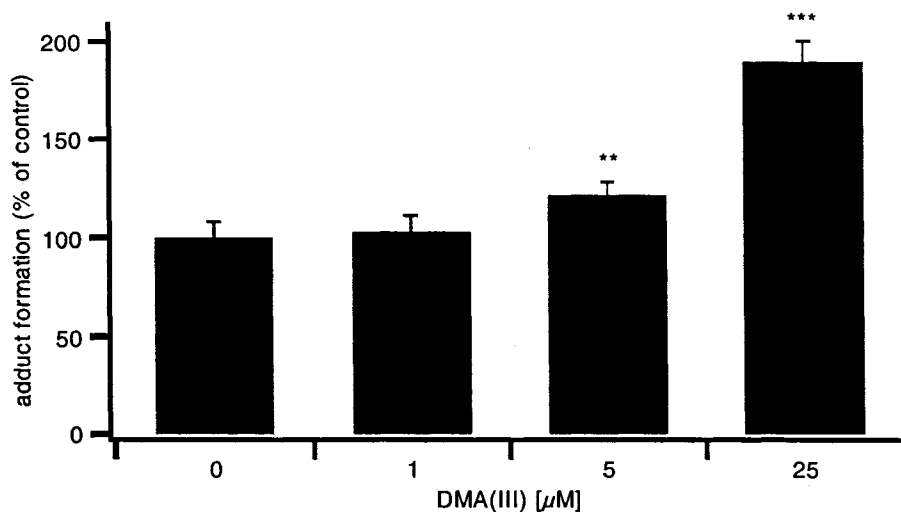


**Figure 3.5b.** Histograms representing the relative adduct levels after pretreatment with different DMA(III) concentrations. Adduct levels obtained from BPDE incubation alone were used as controls. \*\* $P < 0.05$ , \*\*\* $P < 0.01$  using one-way Student's test. Error bars indicate the standard deviation from three experiments.

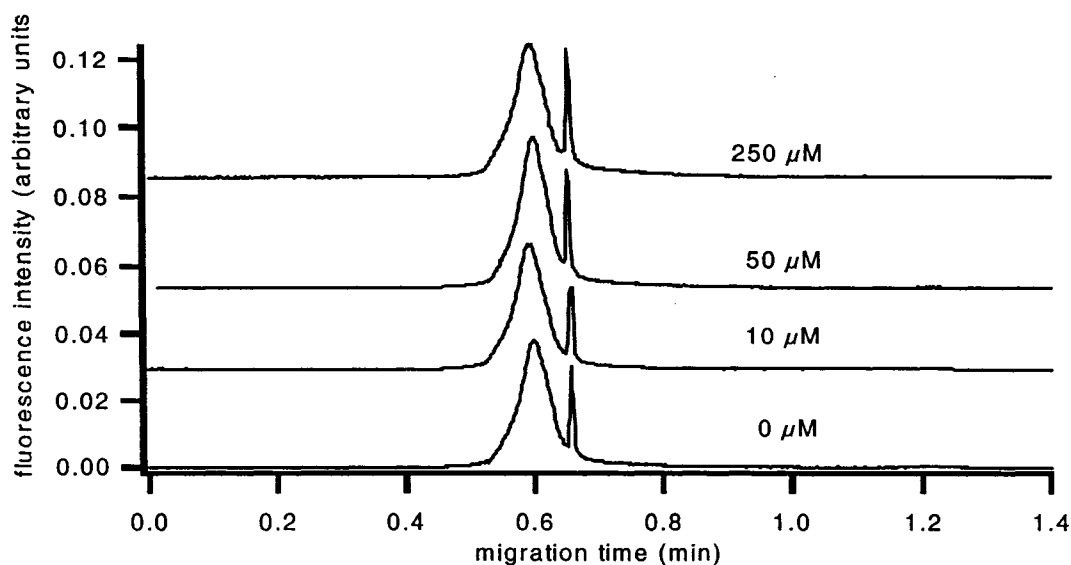


**Figure 3.6a.** Electropherograms obtained from DNA extracted from XPA cells pretreated for 24 h with different concentrations of iAs(V) as indicated, and then incubated with 0.5  $\mu\text{M}$  BPDE for 30 min. The ratio of peak areas between the two peaks indicates the level of DNA adducts.

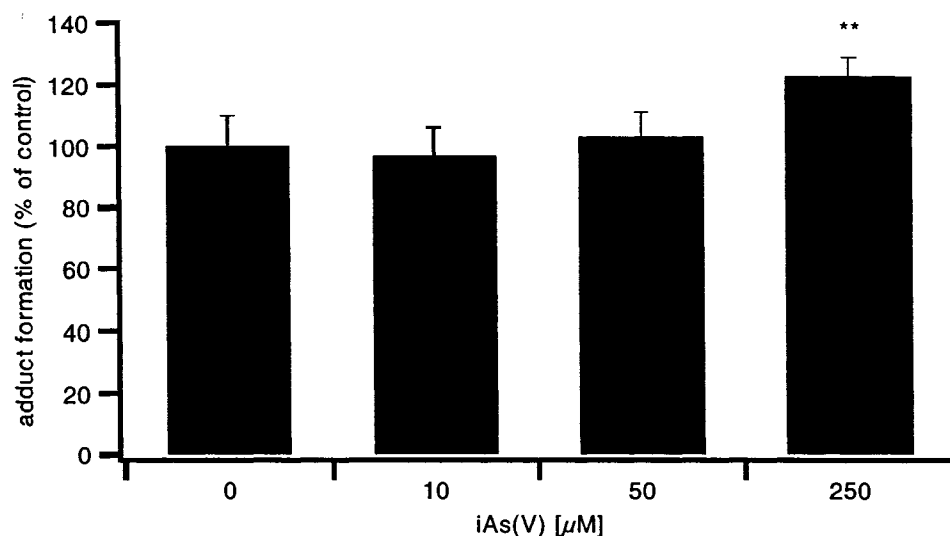


**Figure 3.6b.** Histograms representing the relative adduct levels after pretreatment with different iAs(V) concentrations. Adduct levels obtained from BPDE incubation alone were used as controls. **\*\*P<0.05** using one-way Student's test. Error bars indicate the standard deviation from three experiments.

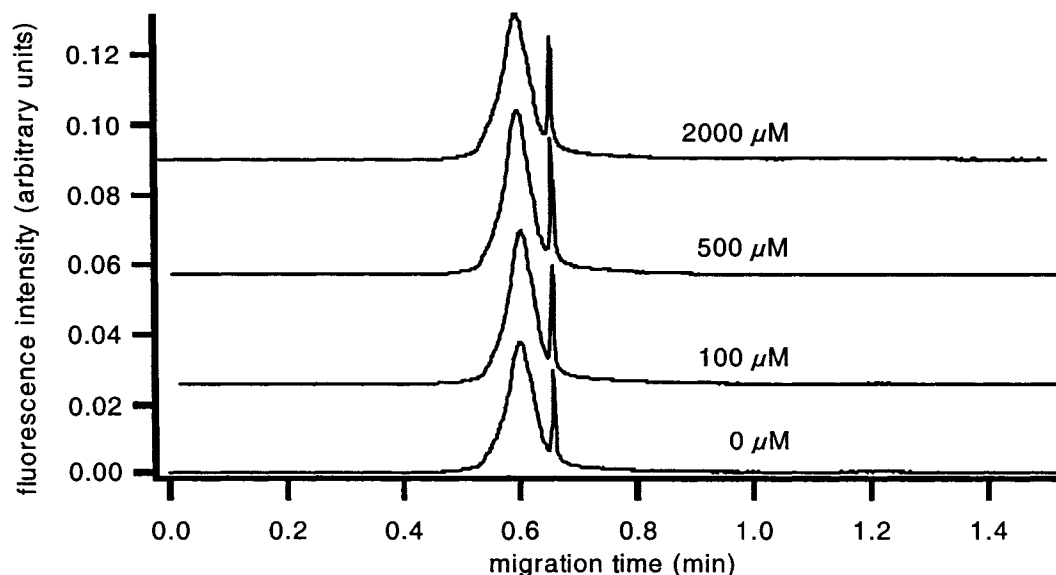


**Figure 3.7a.** Electropherograms obtained from DNA extracted from XPA cells pretreated for 24 h with different concentrations of MMA(V) as indicated, and then incubated with 0.5  $\mu\text{M}$  BPDE for 30 min. The ratio of peak areas between the two peaks indicates the level of DNA adducts.

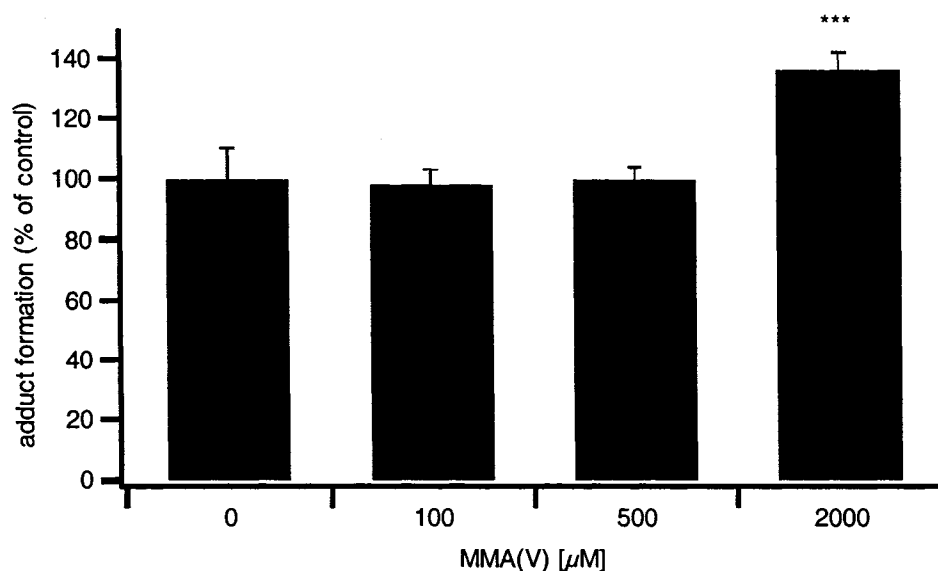


**Figure 3.7b.** Histograms representing the relative adduct levels after pretreatment with different MMA(V) concentrations. Adduct levels obtained from BPDE incubation alone were used as controls. \*\*\* $P < 0.01$  using one-way Student's test. Error bars indicate the standard deviation from three experiments.

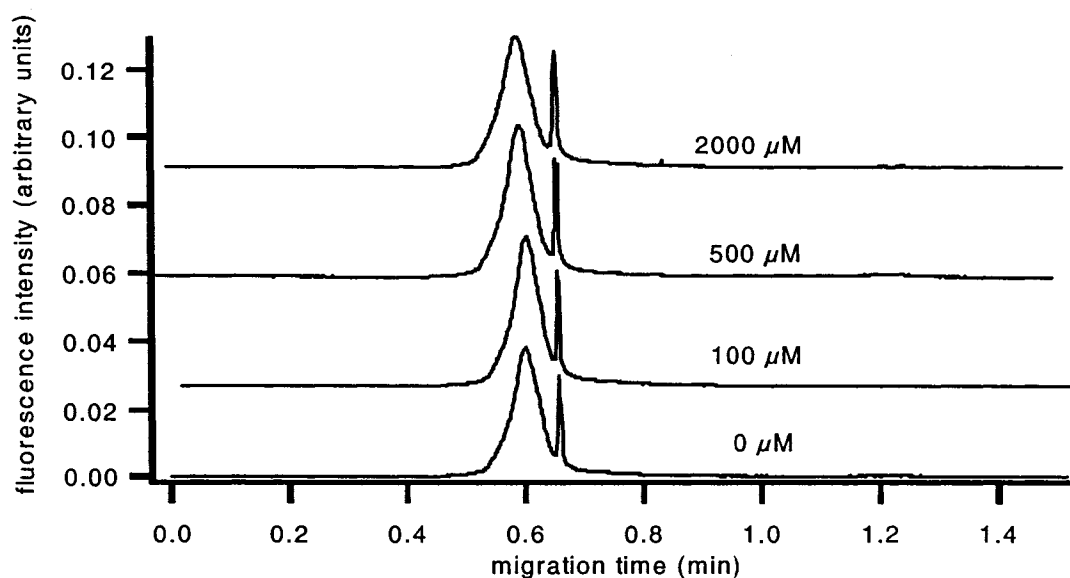


**Figure 3.8a.** Electropherograms obtained from DNA extracted from XPA cells pretreated for 24 h with different concentrations of DMA(V) as indicated, and then incubated with 0.5  $\mu\text{M}$  BPDE for 30 min. The ratio of peak areas between the two peaks indicates the level of DNA adducts.

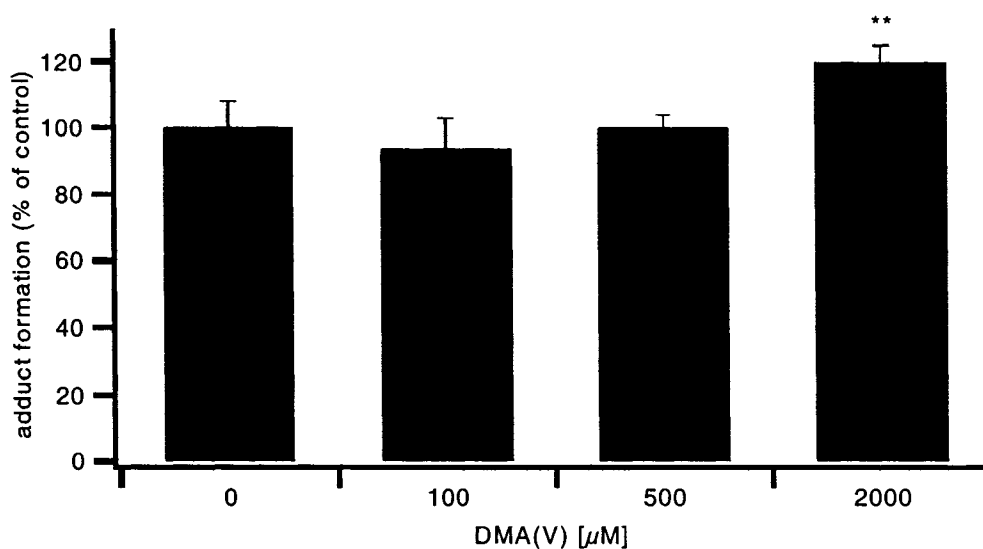


**Figure 3.8b.** Histograms representing the relative adduct levels after pretreatment with different DMA(V) concentrations. Adduct levels obtained from BPDE incubation alone were used as controls.  $**P < 0.05$  using one-way Student's test. Error bars indicate the standard deviation from three experiments.

### 3.3.3 Cytotoxicity of arsenic compounds

The colony formation assay is a conventional method used to assess the cytotoxicity of drugs on target cells. As seen in **Figure 3.9**, the trivalent methylated metabolites, MMA(III) and DMA(III), exerted higher cytotoxicity than iAs(III) on GM04312C cells, and much more so than did the pentavalent arsenic compounds. After treatment with 1  $\mu$ M MMA(III) or 5  $\mu$ M DMA(III) for 24 h, colony formation was reduced to 2-4% of the control. At higher concentrations of MMA(III) or DMA(III) or at 100  $\mu$ M iAs(III), no colonies were observed. These results suggested that the trivalent arsenic species were very toxic to these cells. However, the results from the colony formation assay should be used with caution in relation to our adduct formation experiments. Firstly, differences between colony formation and survival have been acknowledged (29). The colony formation assay measures the ability of cells to clone after treatment, not the survival of cells after treatment. There may be many cells that do survive but that lose the ability to clone. Secondly, the cells in our colony formation assay were treated at a relatively low density while the cells in our adduct formation experiments were treated at a higher density. Differences in cell density can have a significant effect on cell behaviors. Thirdly, in the colony formation assay, cells were only allowed to attach overnight after seeding while the cells in the adduct formation experiments were allowed to grow and reach 80-90% confluence. Cells may attach with different tenacity onto the dishes and therefore have different resistance to physical disturbance during PBS washes after remaining attached for different time periods. In addition, we had enough cells to conveniently extract cellular DNA after arsenic treatment and BPDE incubation, which indicated that a considerable number of cells had survived.

To obtain more relevant cell survival data, cell counts for cells with the same handling and at the same confluence as the cells in the adduct formation experiments were performed and are shown in **Figure 3.10**. The difference between colony formation and survival was clear from the cell counting. After treatment with 100  $\mu\text{M}$  iAs(III), 10  $\mu\text{M}$  MMA(III), or 25  $\mu\text{M}$  DMA(III) for 24 h, we did not observe any colonies formed (**Figure 3.9**). However, the same treatment spared 40%, 10%, or 15% of the control cells from cell killing, respectively (**Figure 3.10**). At 250  $\mu\text{M}$ , iAs(V) reduced colony formation to 5% of the control while approximately 55% of the control cells survived (**Figures 3.9 and 3.10**). Results from the colony formation assay and cell counting were similar for both MMA(V) and DMA(V), implying that the pentavalent methylated arsenic species exerted their cytotoxicity in an immediate and acute manner without considerable impact on colony formation ability. Schwerdtle et al. (15) also observed the same phenomenon. In their study, except for MMA(V) and DMA(V), cells were shown to be more sensitive when assessed by means of a colony formation assay than when direct cell counting was employed. At 7.5  $\mu\text{M}$ , MMA(III) and DMA(III) reduced the colony formation ability of A549 cells to 2% and 6% of the control, respectively. By contrast, at the same concentration, MMA(III) and DMA(III) retained the cell numbers at 45-55% of the control.

As expected, the GM04312C cells used in our study are more sensitive than the A549 cells in the colony formation assay, because the latter have a constitutive repair function. After recovery in complete growth medium for weeks, repair-proficient cells may divide and form clones. However, Hu et al. (30) have recently shown that there were no statistically significant differences ( $P>0.05$ ) in the colony formation ability after  $\text{NiCl}_2$

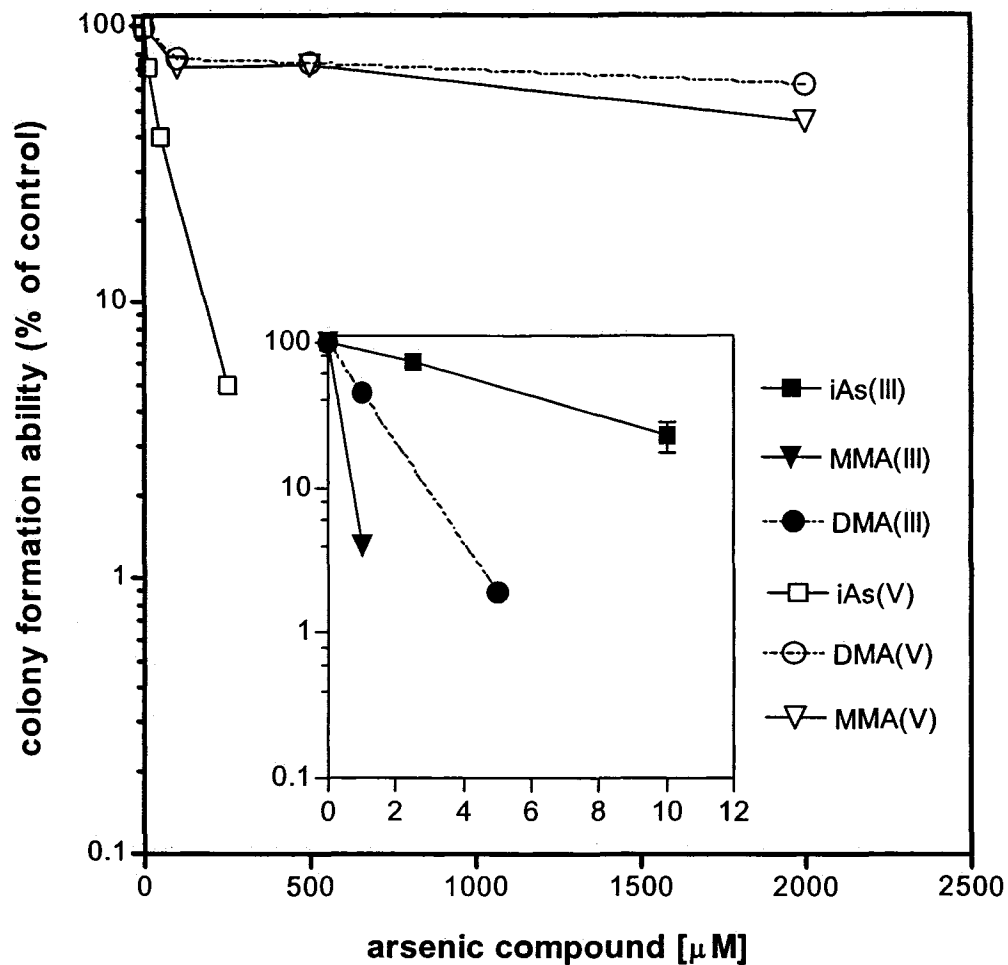


**Figure 3.9. Effects of iAs(III), MMA(III), DMA(III), iAs(V), MMA(V) and DMA(V) on the colony formation ability of GM04312C cells. An appropriate number of cells were seeded in each designated dish and allowed to attach overnight. After a 24-h treatment with various arsenic compounds at the indicated concentrations, cells were restored in fresh growth medium for colony formation. Error bars indicate the standard error of four determinations from two experiments.**

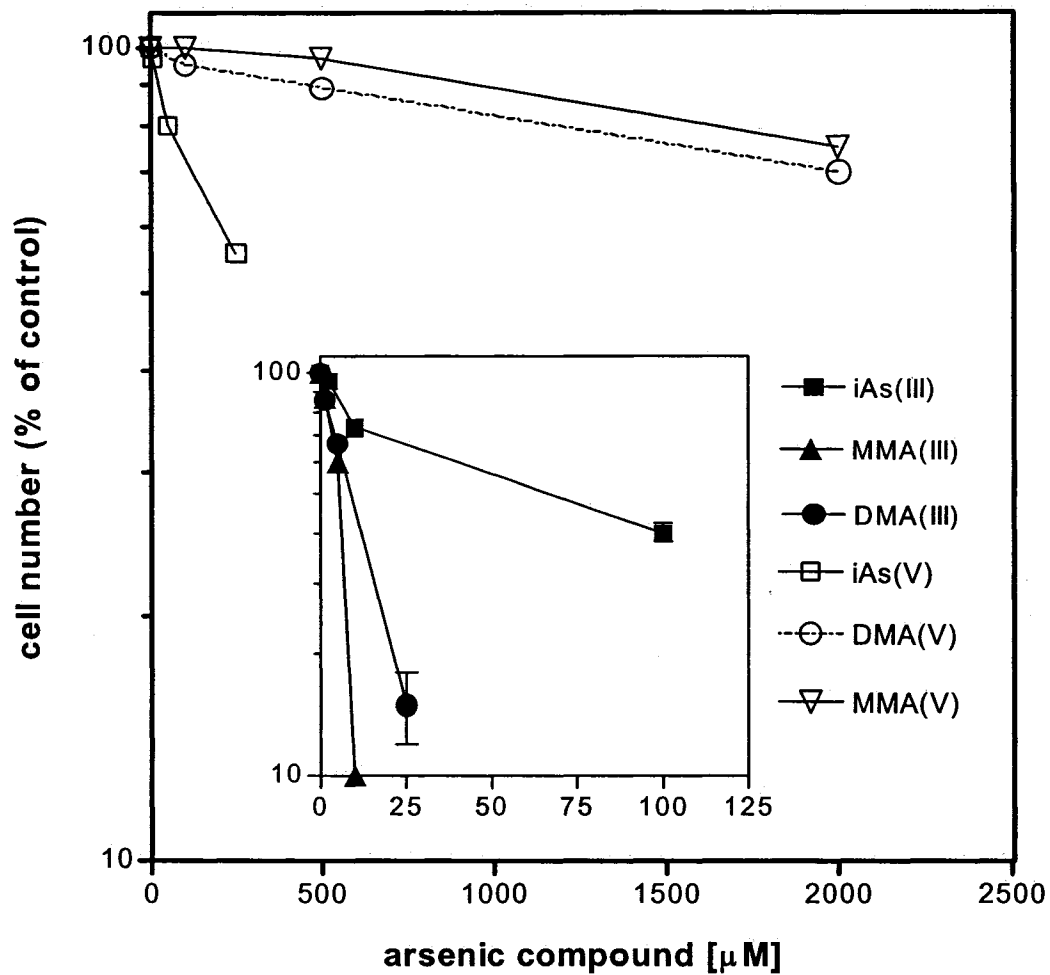


**Figure 3.10.** Effects of iAs(III), MMA(III), DMA(III), iAs(V), MMA(V) and DMA(V) on the cell numbers of GM04312C cells. 80-90% confluent cells were treated with various arsenic compounds for 24 h and then trypsinized and counted. Error bars indicate the standard error of four determinations from two experiments.

treatment between NER-proficient (GM00637) and NER-deficient (XP12BE) SV40 transformed human fibroblasts. It should be pointed out that in the studies of Hu et al. and Schwerdtle et al., a different treatment protocol than ours was used for the colony formation assay: exponentially growing cells were treated with arsenic, trypsinized, counted, and then reseeded for colony formation. Generally,  $IC_{50}$  values for clonal survival after re-plating following treatment in subconfluent monolayer cultures can be 10-fold higher than for direct exposure in a clonal culture (31).

#### **3.3.4 Time-dependence of enhancement of BPDE-DNA adduct formation**

The results in **Figures 3.3-3.8** show that the enhancement of BPDE-DNA adduct formation by arsenic compounds is dose-dependent. To determine if this enhancement is time-dependent, we pretreated cells with iAs(III) or MMA(III) for different time periods: 30 min, 6 h, or 24 h. We observed that both iAs(III) and MMA(III) increased adduct formation in a time-dependent manner, as shown in **Figures 3.11** and **3.12**. When the pretreatment time increased, the enhancement by 100  $\mu$ M iAs(III) or 5  $\mu$ M MMA(III) increased. After a 6-h or 24-h treatment with 5  $\mu$ M MMA(III), the formation of BPDE-DNA adducts was significantly enhanced. Only after 24 h of treatment did 10  $\mu$ M iAs(III) enhance the adduct formation significantly.

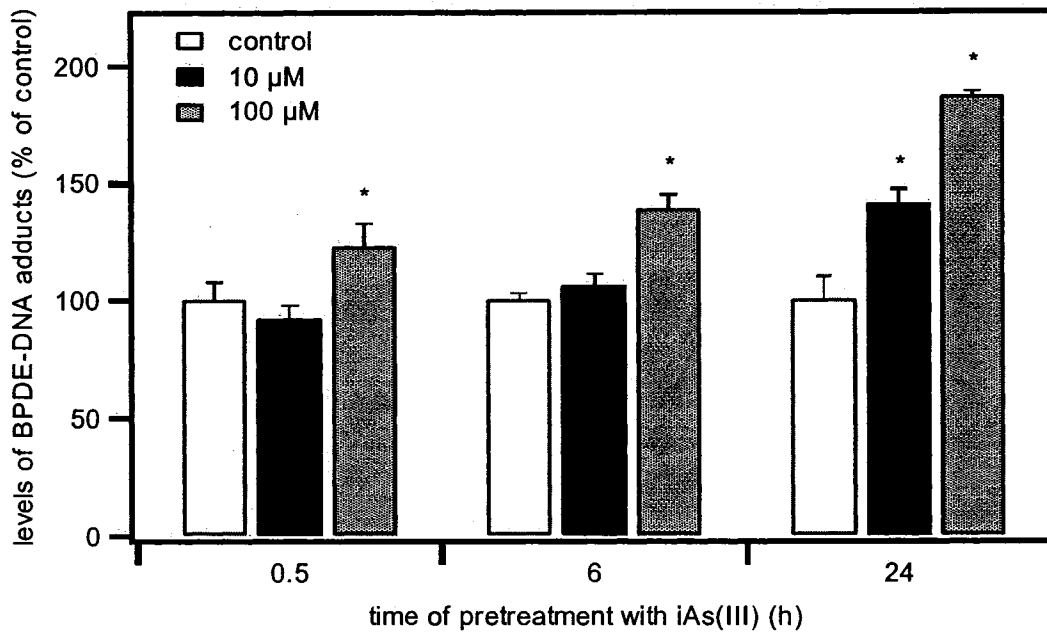


**Figure 3.11.** The effect of iAs(III) on the enhancement of BPDE-DNA adduct formation is time-dependent. \* $P < 0.05$  using one-way Student's test. Error bars indicate the standard deviation from three experiments.

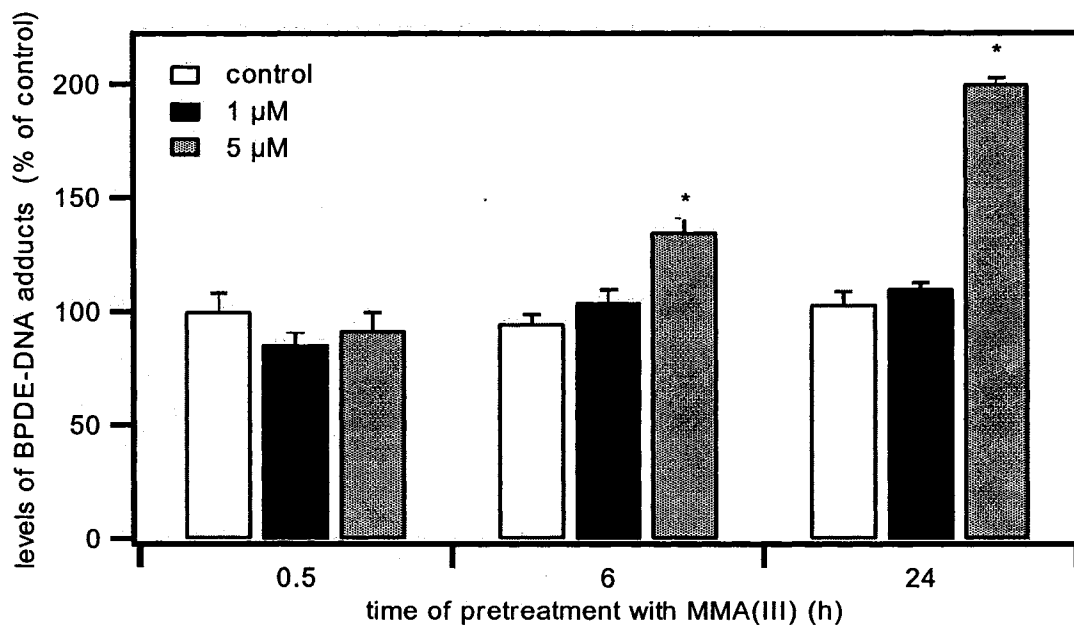


**Figure 3.12.** The effect of MMA(III) on the enhancement of BPDE-DNA adduct formation is time-dependent. \* $P < 0.05$  using one-way Student's test. Error bars indicate the standard deviation from three experiments.

### 3.3.5 Effects of arsenic on GSH-mediated inactivation of BPDE

GSH, a sulfhydryl tripeptide, is the single most abundant reducing agent within cells. It is synthesized from its three constituent amino acids by the combined activities of  $\gamma$ -glutamylcysteine synthetase ( $\gamma$ -GCS) and glutathione synthetase. GSH can also be generated by glutathione reductase (GR) from its oxidized form (GSSG). GSH and glutathione-related enzymes comprise a system that maintains an intracellular reducing environment and acts as a primary defense against excessive generation of reactive oxygen species (ROS). In ROS detoxification reactions, reduced GSH either directly scavenges oxygen radicals or acts as a substrate for glutathione peroxidase (GPx) and GST.

Arsenic has been shown to alter cellular redox status and to modify the expression of various stress-related genes through production of ROS, modulation of GSH, or binding to cysteine residues in proteins. Resistance to arsenic in mammalian cells is correlated with high levels of intracellular GSH and high GST activity (32-34). Depletion of GSH has been shown to block arsenic methylation (35) and result in increased cytotoxicity and clastogenicity of arsenic (36). GST-catalyzed GSH conjugation of BPDE is believed to be the most important enzymatic pathway to inactivate BPDE (37-39). Therefore, it is reasonable to suggest that arsenic may modulate BPDE-DNA adduct levels via its effects on GSH levels and GST activity.

GST is a family of isoenzymes, which can be grouped into seven classes, alpha, Mu, Pi, theta, sigma, zeta, and omega, on the basis of their structural and catalytic properties. Although studies have shown that the GST isoenzymes of different classes differ in their catalytic efficiency in the GSH conjugation of BPDE, the cytosolic GST

activity is due to multiple isoenzymes. Thus, the total GST activity was measured in our experiments.

Four arsenic compounds were examined for their effects on cellular GSH levels: iAs(III), DMA(III), MMA(V), and DMA(V), as shown in **Figure 3.13**. After a 30-min treatment with 50  $\mu\text{M}$  iAs(III), the GSH levels in GM04312C cells increased slightly from 6.2 nmol/ $10^6$  cells to 8.6 nmol/ $10^6$  cells (not statistically significant,  $P>0.05$ ). Further treatment with 50  $\mu\text{M}$  iAs(III) for 6 h or 24 h resulted in a statistically significant increase in the GSH levels (versus the time-matched controls). After a 24-h treatment, 10  $\mu\text{M}$  iAs(III) also increased the GSH levels. Treatment with 5  $\mu\text{M}$  or 10  $\mu\text{M}$  DMA(III) for 24 h led to a significant increase in the GSH levels. Although 2000  $\mu\text{M}$  DMA(V) did not increase the GSH levels at any of the time points under investigation, 2000  $\mu\text{M}$  MMA(V) increased the GSH levels when the treatment time was extended to 6 h or 24 h. After a 24-h treatment, MMA(V) appeared to increase the GSH levels in a concentration-dependent manner.

The results of our experiments (**Figure 3.13**) clearly indicated that arsenic compounds modulated GSH levels in a time-dependent manner, although each compound behaved distinctly. Similar observations have been made by Ochi (40) using Chinese hamster V79 cells. After 18 h of incubation, the GSH levels increased in proportion to iAs(III) concentrations up to 7.5  $\mu\text{M}$  and then plummeted at 20  $\mu\text{M}$  iAs(III). When treated with 5  $\mu\text{M}$  iAs(III), the GSH levels peaked after 8 h of exposure and kept declining when exposure times were prolonged up to 24 h. However, DMA(V) caused a time-dependent increase in the GSH levels up to 24 h at a concentration of 1 mM and caused a concentration-dependent increase up to 2 mM over a 24-h incubation. In the rat

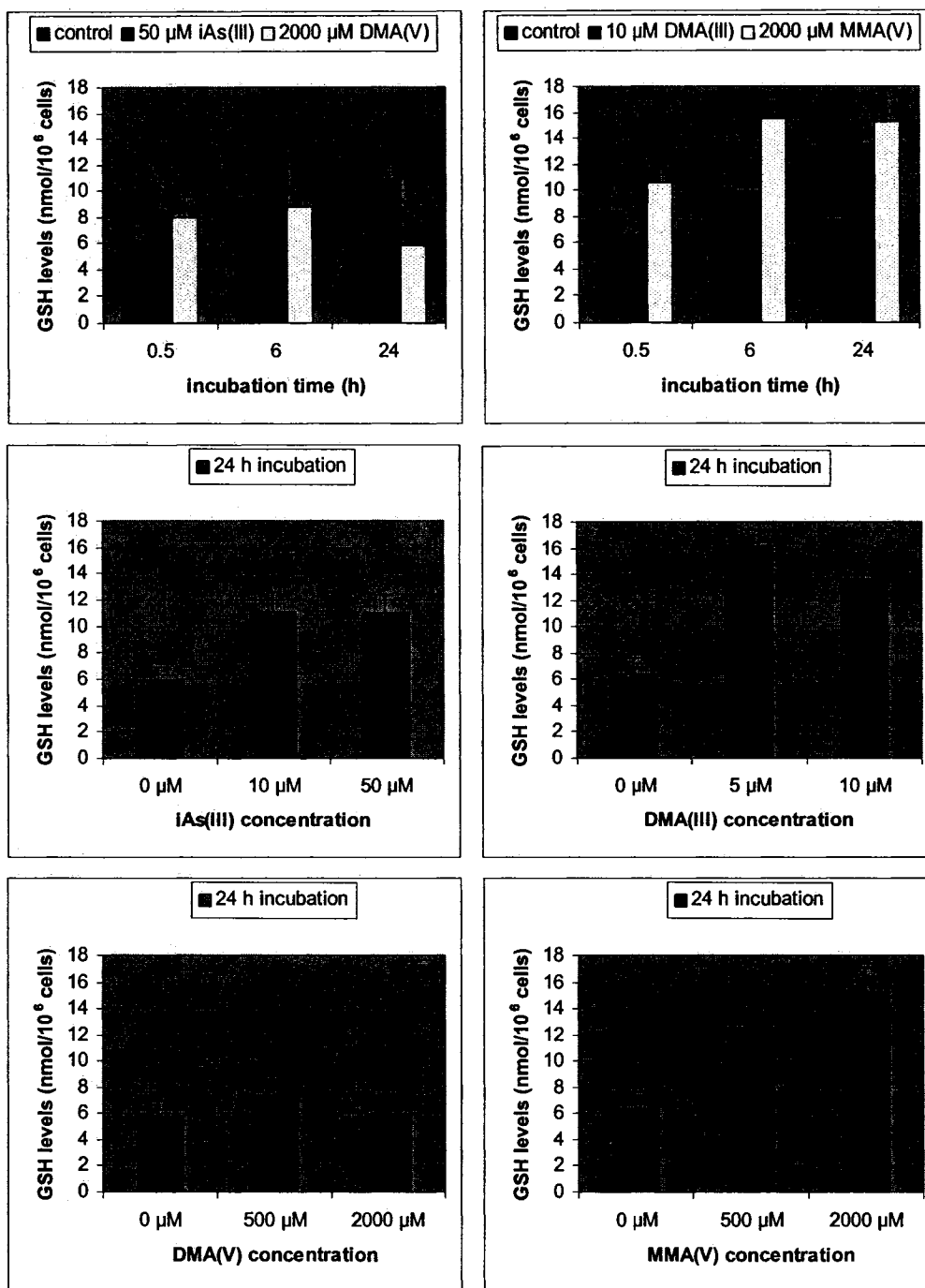


**Figure 3.13. Effects of arsenic compounds on cellular reduced GSH levels.** GM04312C cells that were 80-90% confluent were treated with arsenic compounds for the times indicated. Cells were homogenized for GSH detection. Error bars indicate the standard deviation from three experiments.

liver epithelial cell line TRL1215, this concentration-dependent increase of the GSH levels by DMA(V) treatment was also observed (41). When treated with 10 mM DMA(V), the GSH levels decreased slightly up to 12 h and then increased dramatically up to 48 h. Treatment of primary rat hepatocytes with 50  $\mu$ M iAs(III) for 30 min caused a decrease in the GSH levels from 27.1 nmol/ $10^6$  cells to 22 nmol/ $10^6$  cells (42). After a 30-min treatment, 5  $\mu$ M and 10  $\mu$ M MMA(III) decreased the GSH levels even more dramatically (42).

Ochi (40) reported no increase in the GSH levels by MMA(V) at any incubation time. By contrast, MMA(V) and DMA(V) were shown to decrease GSH in an *in vivo* study (43). Cellular GSH levels, therefore, may be significantly raised (44-49) or lowered (43, 50) depending on the arsenic speciation, the dose, the time after exposure, and the cell type.

Clearly, there is no correlation between cellular GSH levels and BPDE-DNA adduct levels after arsenic treatment. The arsenic compounds we have examined caused concentration-dependent increases in BPDE-DNA adducts (**Figure 3.3-3.8**). These increases are likely to be time-dependent as well, as manifested by iAs(III) and MMA(III). This lack of correlation is in agreement with the observation by Maier et al. (11). However, they treated cells with iAs(III) for 30 min before addition of BaP and determined the GSH levels after 1.5 h of iAs(III) and BaP co-treatment. They either depleted GSH with L-buthionine-S,R-sulfoximine (BSO) or replenished GSH with glutathione ethylester to modulate cellular GSH levels. The changes in the cellular GSH status led to noticeable effects on the yields of the BaP-induced BPDE-DNA adducts. However, those changes could not be achieved by arsenic treatment alone because of the

mM levels of cellular GSH. Their results did not suggest that iAs(III) increases BPDE-DNA adducts through direct competition with BaP metabolites for the cellular GSH pool.

The same four arsenic compounds were examined with regard to their effects on total GST activity. The results are shown in **Figure 3.14**. A 30-min treatment with each arsenic compound did not change GST activity. Treatment with 2000  $\mu$ M MMA(V) for 6 h led to a statistically significant decrease in GST activity. After a 24-h treatment with DMA(III) (5  $\mu$ M or 10  $\mu$ M), MMA(V) (2000  $\mu$ M), or DMA(V) (500  $\mu$ M or 2000  $\mu$ M) GST activity was increased.

So far, only a few studies have reported acute effects of arsenic on GST activity in cultured cells and all of them showed that iAs(III) increased GST activity (45, 48, 51, 52). In TRL1215 cells, MMA(V) significantly enhanced GST activity at concentrations over 2.5 mM. MMA(V) at a concentration of 5 mM increased GST activity in a time-dependent manner up to 48 h (47). In the same cell line, increased GST activity was observed after treatment with 2.5 mM DMA(V) for 24 h (41). This increase was suppressed at higher concentrations of DMA(V) (5 mM and 10 mM). Treatment with 2.5 mM DMA(V) resulted in a time-dependent increase in GST activity up to 24 h. Again, the effects of arsenic on GST activity might be tissue or cell-specific. iAs(III) caused an increase in GST activity in the guinea pig kidney but not the liver or lung (53). GST activity was also shown to increase slightly in keratinocytes (HaCaT and AG06), but not in fibroblasts (WI38) or breast tumor (PMC42) cells (46).

Obviously, no correlation could be established between GST activity and BPDE-DNA adduct levels after arsenic treatment. Both cellular GSH levels and GST activity

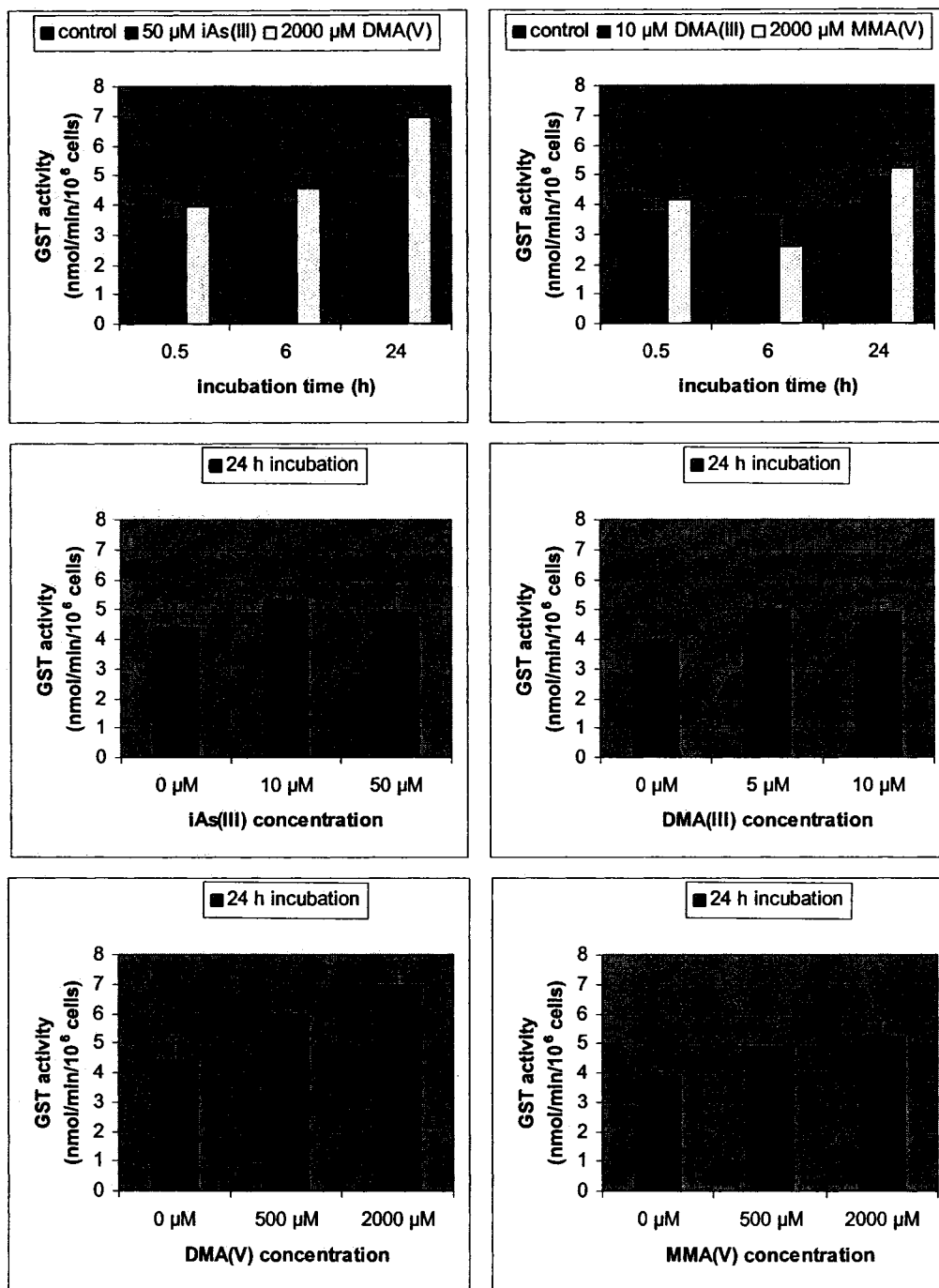


**Figure 3.14. Effects of arsenic compounds on the activity of GST. GM04312C cells that were 80-90% confluent were treated for the indicated times with arsenic compounds. Cells were homogenized for the GST activity assay. Error bars indicate the standard deviation from three experiments.**

failed to correlate with BPDE-DNA adduct levels after arsenic treatment. However, the possibility that inactivation of BPDE detoxification via direct disruption of GST-catalyzed GSH conjugation is a contributing factor of the enhancement of BPDE-DNA adduct formation by arsenic cannot be ruled out. CDNB is a general GST substrate and GST-CDNB activity is used to represent the integrated activity of various cytosolic GST isoforms. A convenient method adopted in our study, the CDNB colorimetric assay has been widely used to measure GST activity. Unfortunately, studies have shown that GST-CDNB activity may not reflect GST-BPDE activity (54-56).

Although at non-physiologically relevant millimolar concentrations arsenic has been shown to inhibit the activities of purified enzymes GR, GST, and GPx (42, 57, 58), in most cultured cell studies arsenic has been shown to upregulate the activity of  $\gamma$ -GCS (40, 45, 46, 59), GST (45-47, 49, 51, 52) and GR (46) but inhibit the activity of GPx (45). The rate of cystine uptake has also been shown to have increased after arsenic treatment (40, 46). All of these effects by arsenic promote the protective functions of GSH. Even so, if arsenic blocks the activities of GSH-conjugate transporters, the formation of BPDE-DNA adducts is likely to be facilitated because the intracellular accumulation of BPD-SG has been shown to be associated with increased formation of BPDE-DNA adducts in cells lacking a GSH-conjugate transporter multidrug resistance protein 2 (MRP2) (60). However, the evidence to date indicates that arsenic induces expression of MRP2 and other multidrug resistance transporters (61, 62).

### **3.3.6 Effects of arsenic on chromatin accessibility**

Chromatin relaxation carries an increased risk of certain types of DNA damage. Evidence has shown that compact chromatin is protective against DNA double strand

breaks and oxidative DNA damage. This protection is reduced after chromatin decondensation (63). Ultraviolet (UV)-induced global chromatin relaxation rendered DNA more susceptible to a number of DNA-damaging agents (64). Therefore, it is necessary to test whether arsenic affects chromatin accessibility, thereby enhancing DNA damage by BPDE.

A confocal microscopic technique was successfully employed to examine chromatin relaxation (27). After removal of RNA and partial denaturation of DNA by HCl, acridine orange (AO) was used to stain non-denatured, dsDNA sections and denatured ssDNA sections, resulting in green and red fluorescence, respectively. In general, DNA sensitivity to denaturation in cells is closely associated with the degree of chromatin condensation (65). Therefore, green fluorescence is associated with relaxed chromatin and red fluorescence with condensed chromatin. An important advantage of this method is its ability to detect extended and condensed chromatin *in situ*, without the need to extract DNA from cells. This avoids the alteration of chromatin morphology associated with manipulations such as isolation of nuclei and solubilization of chromatin (66).

UVC irradiation at  $4 \text{ J/m}^2$  reportedly led to chromatin relaxation in human normal diploid fibroblast GM00038B cells (27). To demonstrate our mastery of this new technique, we irradiated GM00038B and GM04312C cells with  $4 \text{ J/m}^2$  UVC and performed the same procedure as described in the original paper, with the exception that we used  $20 \text{ }\mu\text{g/ml}$  rather than  $100 \text{ }\mu\text{g/ml}$  AO to stain fixed cells. The reason we chose a lower concentration of AO solution is that we found that  $20 \text{ }\mu\text{g/ml}$  AO gave more reproducible results and uniformity from one sampling area to another on the coverslips.

In addition, AO itself at higher concentrations has the ability to denature DNA (67, 68), thus confounding the DNA stability changes incurred by the agents under investigation.

As demonstrated in **Figure 3.15**, after 4 J/m<sup>2</sup> UVC irradiation, the GM00038B cells showed chromatin relaxation. By contrast, no significant chromatin relaxation was observed in GM04312C cells. This observation agrees with Rubbi and Milner's results (27). They showed that UV-induced chromatin relaxation requires p53. The functionality of p53 is probably abrogated in GM04312C cells although SV40 immortalization may not completely eliminate p53 activity (69, 70).

Our results, shown in **Figure 3.16**, showed that although two pentavalent arsenic compounds (MMA(V) and DMA(V)) at very high concentrations (500-2000  $\mu$ M) relaxed the chromatin structure to some extent, none of the three trivalent arsenic compounds (iAs(III), MMA(III), DMA(III)) at much lower concentrations (1-50  $\mu$ M) relaxed the chromatin structure at all. High concentrations of the trivalent arsenic species were not included in this experiment because of their high cytotoxicity. In fact, a considerable number of cells treated with 50  $\mu$ M iAs(III) or 10  $\mu$ M DMA(III) appeared to be at the early apoptotic stage when observed under a microscope. Cells treated as such had more condensed chromatin than the controls. Unfortunately, using this technique alone we cannot evaluate separately the contributions from early apoptotic cells and from normal cells towards the observed chromatin structural changes.

Different structural changes triggered by different arsenic compounds may reveal that each arsenic species is distinctive in terms of its influence on chromatin structure. Chromatin relaxation may act as a contributing factor to enhance BPDE-DNA adduct formation by the pentavalent arsenic compounds MMA(V) and DMA(V).

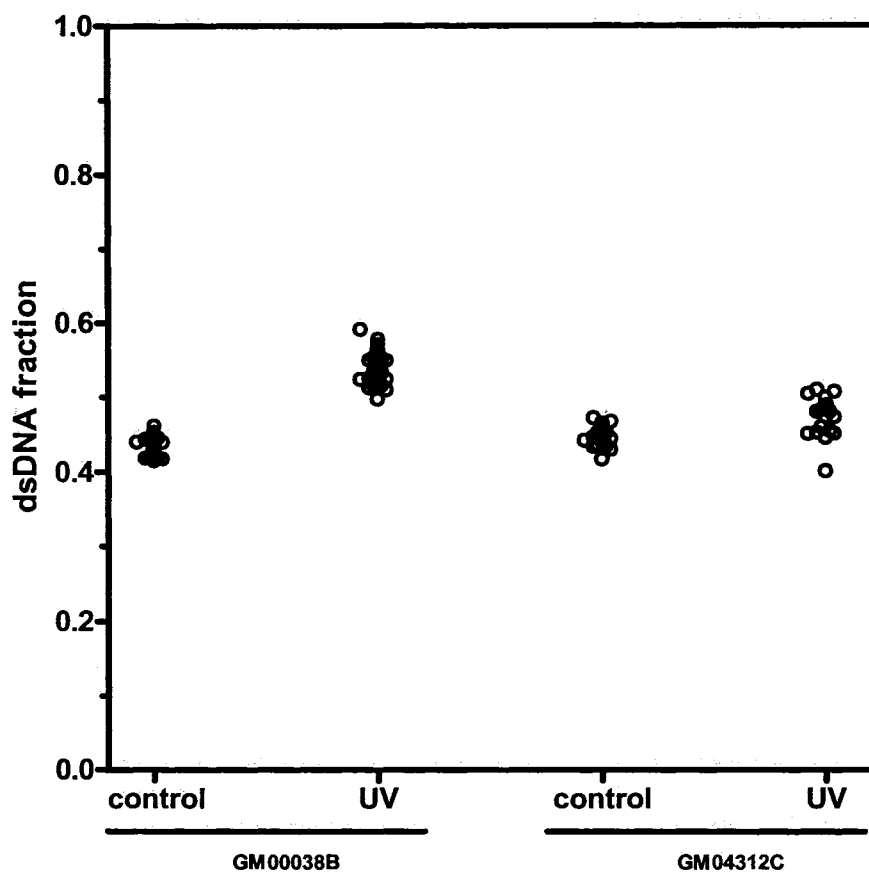


**Figure 3.15. DNA denaturation sensitivity of GM00038B and GM04312C cells with or without UVC irradiation. Cells were irradiated with UVC at 4 J/m<sup>2</sup> and incubated for 1 h in culture medium and then subjected to the HCl/AO assay.**

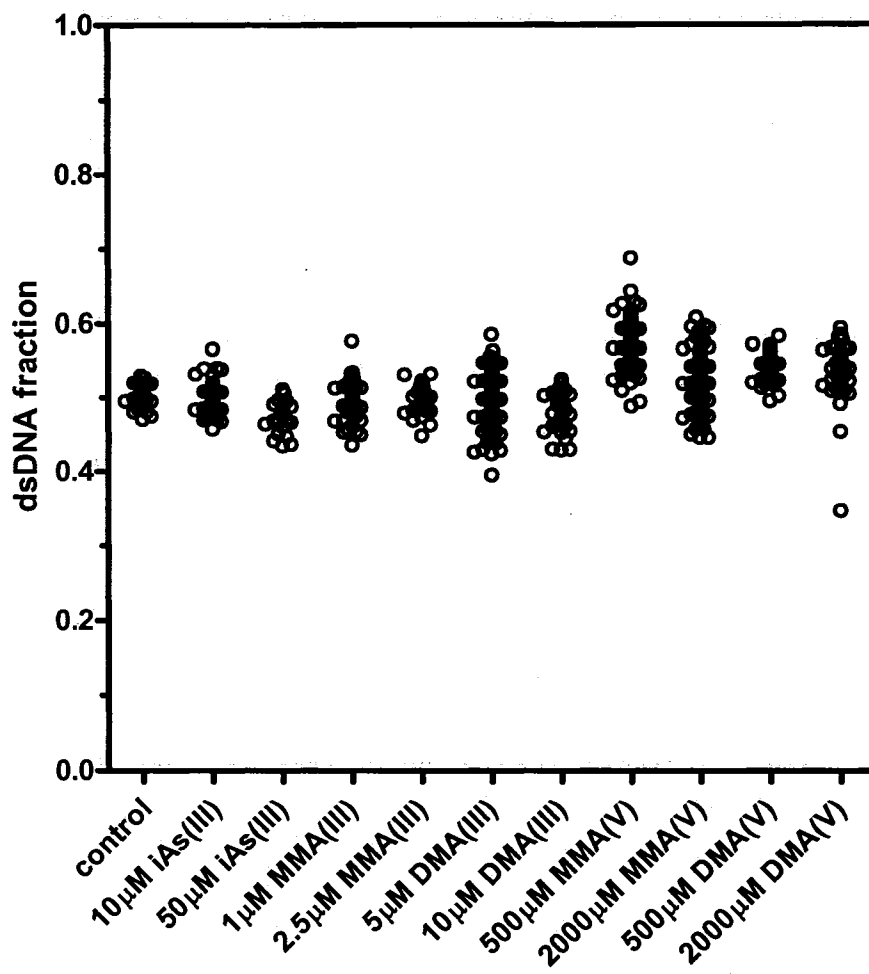


**Figure 3.16. DNA denaturation sensitivity measured by the HCl/AO assay on 80-90% confluent GM04312C cells after treatment with various arsenic compounds for 24 h.**

However, there was no clear-cut difference between cells treated with 500  $\mu\text{M}$  MMA(V) or DMA(V) and with 2000  $\mu\text{M}$  MMA(V) or DMA(V). Even for each specific arsenic species, a dose-response relationship could not be established because it is impossible to establish the exact relationship between DNA packing density and the proportion of red/green fluorescence of AO using this denaturation sensitivity assay (66).

Although arsenic pretreatment altered the chromatin structure at certain concentrations, it did not lead to a change in BPDE-DNA adduct formation at those concentrations. This means that BPDE forms DNA adducts regardless of chromatin accessibility. In line with this, no differences in the BPDE-DNA adduct levels were shown across different cell-cycle phases (71), although it is known that changes in chromatin structure are associated with different cell-cycle phases. Similarly, the BPDE-DNA adduct levels in quiescent cells were close to the levels in rapidly proliferating cells (72). More interestingly, histone hyperacetylation by butyrate treatment did not influence the initial levels of BPDE-DNA adducts, nor did it change the rate of removal of BPDE-DNA adducts from chromatin in either normal human fibroblasts or XP fibroblasts (73). The authors concluded that the subtle changes in chromatin brought about by histone acetylation had no influence on these processes. However, if changes in chromatin structure are sufficient, then changes in the levels of DNA modification would be observed. For instance, the inhibition of poly(ADP-ribosyl)ation by 3-aminobenzamide (3-AB) pretreatment has been shown to decrease BPDE-DNA adducts in both normal and XPA lymphoblastoid cells (74). Poly(ADP-ribosyl)ation of any chromatin protein might loosen the interaction between that protein and DNA and thus render more nucleotide residues accessible to carcinogens (75). However, at the concentration ranges examined,

arsenic failed to induce significant chromatin relaxation; rather, trivalent arsenic species led to chromatin condensation. Therefore, chromatin relaxation is not the main factor leading to the enhancement of BPDE-DNA adduct levels by arsenic pretreatment.

### 3.3.7 Effects of arsenic on the cellular uptake of BPDE

The attempt to correlate cellular GSH levels, GST activity, BPD-SG levels, or even chromatin accessibility with BPDE-DNA adduct levels is driven and justified by the assumption that cellular bioavailability of BPDE remained unchanged after arsenic treatment. However, arsenic might have enhanced the formation of BPDE-DNA adducts simply by increasing the stability of BPDE in aqueous medium or the uptake of BPDE by cells. In our treatment protocols, the cells were washed following arsenic treatment and then incubated with BPDE for 30 min, so the effect of arsenic on BPDE stability in aqueous medium is not a significant concern. However, the uptake of BPDE could most likely be affected by arsenic pretreatment. In addition, other known but less important mechanisms of BPDE inactivation, either spontaneous hydrolysis to tetrols and keto-diols or hydration by epoxide hydrolase (76-78), as well as covalent binding of BPDE to DNA could be affected by arsenic. To investigate these possibilities, radiolabelled BPDE was used to examine the cellular uptake of BPDE with and without arsenic treatment.

Figure 3.17 shows the effects of various arsenic compounds on the cellular uptake of BPDE. Cells exposed to [<sup>3</sup>H]-BPDE only had radioactivity of 55000 cpm/10<sup>6</sup> cells (assuming a counting efficiency of 100%, this corresponded to approximately 12.3 pmol of BPDE in 1 × 10<sup>6</sup> cells). When the uptake efficiency of the control cells was normalized to 1, the relative uptake efficiencies after arsenic pretreatment were: 10 μM iAs(III), 2.2; 1 μM MMA(III), 1.0; 5 μM DMA(III), 12.8; 250 μM iAs(V), 31.2;

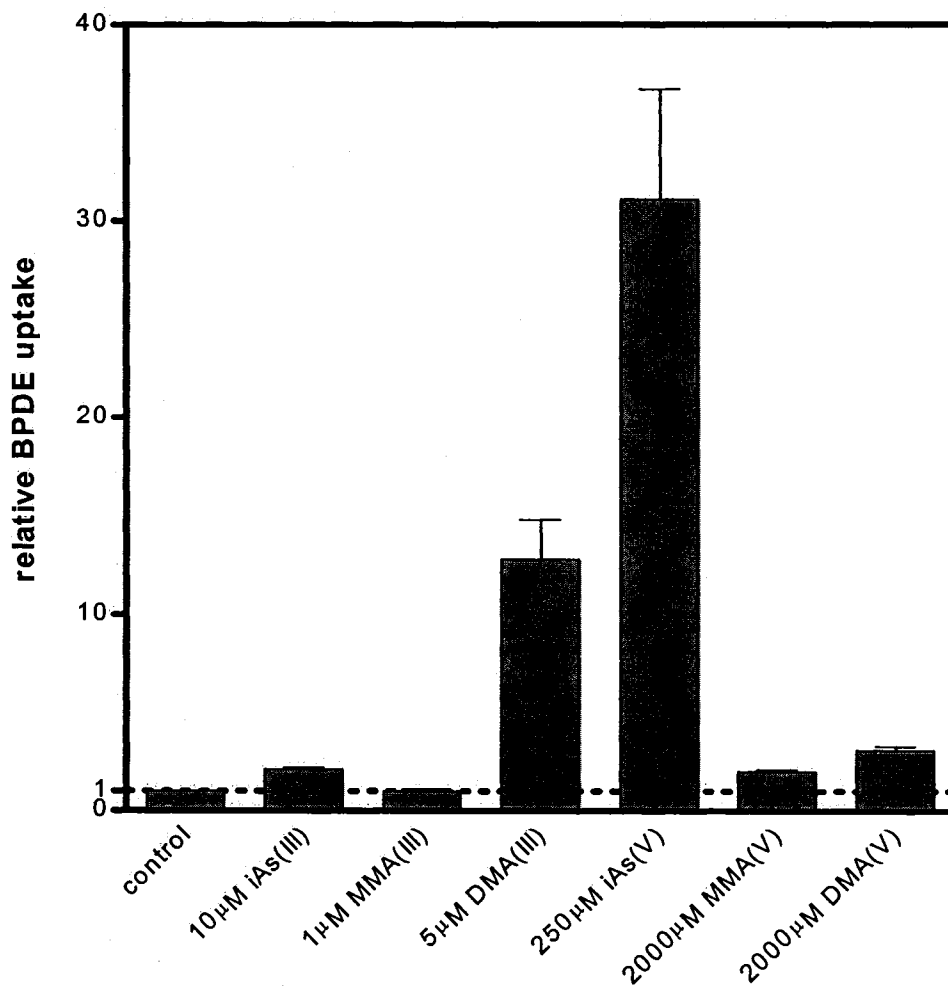


**Figure 3.17.** Effects of the pretreatment with various arsenic species on the cellular uptake of BPDE. GM04312 cells were pretreated with arsenic compounds at concentrations as indicated, and then incubated with 0.5 μM [<sup>3</sup>H]-BPDE for 30 min. After lysis, radioactivity was measured and normalized against the control. Error bars indicate the standard deviation of four determinations from two experiments.

2000  $\mu\text{M}$  MMA(V), 2.0; 2000  $\mu\text{M}$  DMA(V), 3.0. At their respective concentrations, these arsenic compounds were shown to enhance the formation of BPDE-DNA adducts, except for 1  $\mu\text{M}$  MMA(III), which we did not observe to have any enhancing effects on the adduct formation (Figure 3.4). In the study by Schwerdtle et al. (15), treatment with 10  $\mu\text{M}$  iAs(III) or 5  $\mu\text{M}$  DMA(III) did not lead to any enhancement of the formation of BPDE-DNA adducts. However, the enhancing effect on the formation of BPDE-DNA adducts by either 10  $\mu\text{M}$  iAs(III) or 5  $\mu\text{M}$  DMA(III) observed in our study can be accounted for by their promoting effect on the cellular uptake of BPDE. Therefore, our results suggested that arsenic enhanced the formation of BPDE-DNA adducts by increasing the cellular uptake of BPDE.

Currently, the data on the effects of arsenic on the uptake of other chemicals in human cells is limited. Ochi observed that micromolar concentrations of iAs(III) or millimolar concentrations of DMA(V) increased the uptake of cystine in Chinese hamster V79 cells (40). It was suggested that the cystine transport system was induced by iAs(III) or DMA(V) treatment. Similarly, micromolar concentrations of iAs(III) were shown to increase cystine uptake in AG06 keratinocytes (46). Low doses of iAs(III) (less than 1  $\mu\text{M}$ ) were also shown to increase neutral red dye uptake in the same cell line (45). However, in 3T3-L1 adipocytes, iAs(III), MMA(III), and DMA(III) each inhibited glucose uptake by interfering with a glucose transporter (79). As far as BPDE is concerned, no transporters have been reported for its cellular uptake. It is very likely that BPDE enters cells by passive diffusion, just like other polycyclic aromatic hydrocarbons (PAH). However, the efflux of BPDE is an adenosine-5'-triphosphate (ATP)-dependent transport process (80), which may be affected by arsenic pretreatment. Arsenic

compounds, especially iAs(V), are known to be effective energy depletors. This is a possible reason why 250  $\mu\text{M}$  iAs(V) greatly increased BPDE accumulation in the cells. Trivalent arsenic compounds may also affect the efflux system by inhibiting the activity of transport-related enzymes.

As shown in **Figure 3.18** and **Figure 3.19**, the increase in the uptake of BPDE by iAs(III) or MMA(III) treatment is concentration-dependent. At 10  $\mu\text{M}$  iAs(III) the uptake of BPDE increased by 1.2-fold while at 50  $\mu\text{M}$  iAs(III) the uptake increased by 8.6-fold. When the concentration of MMA(III) increased from 1  $\mu\text{M}$  to 2.5  $\mu\text{M}$ , we observed a 1.7-fold increase in the cellular uptake of BPDE. However, the increased uptake of BPDE did not translate into enhanced formation of BPDE-DNA adducts by the same order of magnitude (**Figures 3.3-3.8**). After entry into the cells, BPDE may be sequestered or inactivated by unknown pathways, which may be affected by arsenic. Further analysis of the subcellular distribution of [ $^3\text{H}$ ]-BPDE may help to resolve this question.

Taken together, the results suggested that arsenic increased the cellular uptake of BPDE, which is a major, if not the determining factor, leading to the observed enhancement of BPDE-DNA adduct formation.

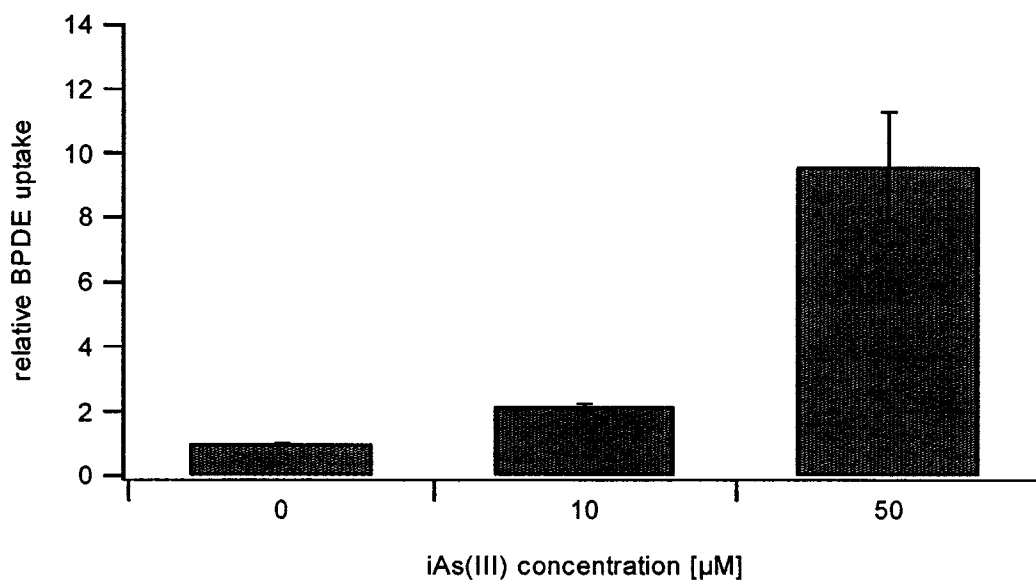


**Figure 3.18.** iAs(III) increased the cellular uptake of BPDE in a concentration-dependent manner. Error bars indicate the standard deviation of four determinations from two experiments.

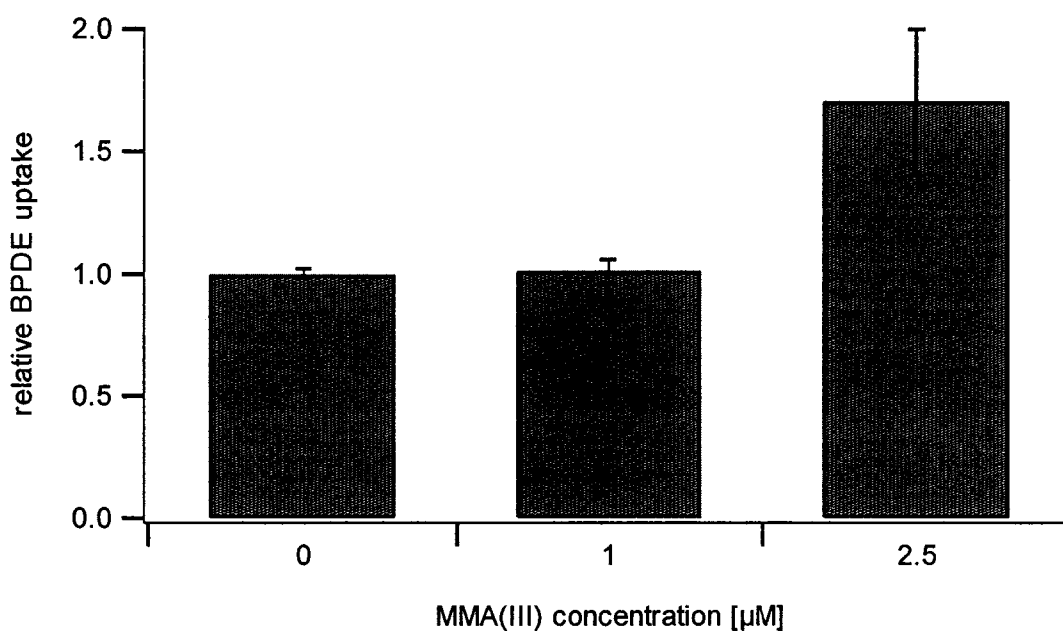


**Figure 3.19.** MMA(III) increased the cellular uptake of BPDE in a concentration-dependent manner. Error bars indicate the standard deviation of four determinations from two experiments.

### 3.4 Conclusions

By use of an SV40-transformed XPA cell line, we distinguished the effects of arsenic on the formation of BPDE-DNA adducts from its possible effects on the repair of BPDE-DNA adducts. We further demonstrated that all six arsenic species have the capability of enhancing the formation of BPDE-DNA adducts, although their enhancing efficiencies are largely dependent on their respective cytotoxicities, in a descending order of MMA(III)>DMA(III)>iAs(III)>iAs(V)>MMA(V)≈DMA(V). This enhancing effect of arsenic seems to be unrelated to changes in the GSH-related redox defense mechanism nor chromatin accessibility. Our results demonstrated that the efficiency of BPDE uptake was enhanced by arsenic pretreatment, which probably played a major role in the increased cellular formation of BPDE-DNA adducts.

### 3.5 References

1. Wild CP and Pisani P. (1997) Carcinogen-DNA and carcinogen-protein adducts in molecular epidemiology. In: Toniolo P, Boffetta P, Shuker DEG, Rothman N, Hulka B and Pearce N, eds. Application of Biomarkers in Cancer Epidemiology. IARC Scientific Publications No.142. Lyon, France. pp 43-158
2. Poirier MC. (1997) DNA adducts as exposure biomarkers and indicators of cancer risk. *Environ Health Perspect*, 105 (supplement 4), 907-912
3. Garner RC. (1998) The role of DNA adducts in chemical carcinogenesis. *Mutat Res*, 402, 67-75
4. Bartsch H. (1996) DNA adducts in human carcinogenesis: etiological relevance and structure-activity relationship. *Mutat Res*, 340, 67-79
5. Cooper CS, Grover PL, Sims P. (1983) The metabolism and activation of benzo[a]pyrene. *Prog Drug Metab*, 7, 295-396
6. Thakker DR, Yagi H, Levin W, Wood AW, Conney AH, Jerina DM. (1985) Polycyclic aromatic hydrocarbons: metabolic activation to ultimate carcinogens. In: Anders MW, ed. Bioactivation of Foreign Compounds. Academic Press, New York. pp 177-242
7. Sivarajah K, Lasker JM and Eling TE. (1981) Prostaglandin synthetase-dependent cooxidation of ( $\pm$ )-benzo[a]pyrene-7,8-dihydrodiol by human lung and other mammalian tissues. *Cancer Res*, 41, 1834-1839
8. Mallet WG, Mosebrook DR, and Trush MC. (1991) Activation of ( $\pm$ ) trans-7,8-dihydro-7,8-dihydrobenzo[a]pyrene to diol epoxides by human polymorphonuclear leukocytes or myeloperoxidase. *Carcinogenesis*, 12, 521-524

9. Sage E, Hasteltine WA. (1984) High ratio of alkali-sensitive lesions to total DNA modification induced by benzo[a]pyrene diol epoxide. *J Biol Chem*, 259, 11098-11102
10. Boysen G, Hecht SS. (2003) Analysis of DNA and protein adducts of benzo[a]pyrene in human tissues using structure-specific methods. *Mutat Res*, 543, 17-30
11. Maier A, Schumann BL, Chang X, Talaska G, Puga A. (2002) Arsenic co-exposure potentiates benzo[a]pyrene genotoxicity. *Mutat Res*, 517, 101-111
12. Evans CD, LaDow K, Schumann BL, Savage Jr RE, Caruso J, Vonderheide A, Succop P and Talaska G. (2004) Effects of arsenic on benzo[a]pyrene DNA adduct levels in mouse skin and lung. *Carcinogenesis*, 25, 493-497
13. Fischer JM, Robbins SB, Al-Zoughool M, Kannamkumarath SS, Stringer SL, Larson JS, Caruso JA, Talaska G, Stambrook PJ, Stringer JR. (2005) Co-mutagenic activity of arsenic and benzo[a]pyrene in mouse skin. *Mutat Res*, 588, 35-46
14. Tran H-P, Prakash AS, Barnard R, Chiswell B, Ng JC. (2002) Arsenic inhibits the repair of DNA damage induced by benzo(a)pyrene. *Toxicol Lett*, 133, 59-67
15. Schwerdtle T, Walter I, Hartwig A. (2003) Arsenite and its biomethylated metabolites interfere with the formation and repair of stable BPDE-induced DNA adducts in human cells and impair XPAzf and Fpg. *DNA Repair*, 2, 1449-1463
16. Lindahl T and Wood RD. (1999) Quality control by DNA repair. *Science*, 286, 1897-1905
17. Cleaver JE, Kraemer KH (1989) Xeroderma pigmentosum. In: Scriver CR, Beaudet AL, Sly WS, Valle D, eds. *The Metabolic Basis of Inherited Disease II*. Sixth ed. McGraw-Hill, New York. pp 2949-2971

18. Bowman KK, Sicard DM, Ford JM and Hanawalt PC. (2000) Reduced global genomic repair of UV light-induced cyclobutane pyrimidine dimers in simian virus 40-transformed human cells. *Mol Carcinog*, 29, 17-24
19. Elbekai RH, El-Kadi AO. (2004) Modulation of aryl hydrocarbon receptor-regulated gene expression by arsenite, cadmium, and chromium. *Toxicology*, 202, 249-269
20. Iwanari M, Nakajima M, Kizu R, Hayakawa K, Yokoi T. (2002) Induction of CYP1A1, CYP1A2, and CYP1B1 mRNAs by nitropolycyclic aromatic hydrocarbons in various human tissue-derived cells: chemical-, cytochrome P450 isoform-, and cell-specific differences. *Arch Toxicol*, 76, 287-298
21. Spink DC, Katz BH, Hussain MM, Spink BC, Wu SJ, Liu N, Pause R, Kaminsky LS. (2002) Induction of CYP1A1 and CYP1B1 in T-47D human breast cancer cells by benzo[a]pyrene is diminished by arsenite. *Drug Metab Dispos*, 30, 262-269
22. Vernhet L, Allan N, Le Vee M, Morel F, Guillouzo A and Fardel O. (2003) Blockage of multidrug resistance-associated proteins potentiates the inhibitory effects of arsenic trioxide on CYP1A1 induction by polycyclic aromatic hydrocarbons. *J Pharmacol Exp Ther*, 304, 145-155
23. Vakharia DD, Liu N, Pause R, Fasco M, Bessette E, Zhang Q-Y, Kaminsky LS. (2001) Effects of metals on polycyclic aromatic hydrocarbon induction of CYP1A1 and CYP1A2 in human hepatocyte cultures. *Toxicol Appl Pharmacol*, 170, 93-103
24. Vakharia DD, Liu N, Pause R, Fasco M, Bessette E, Zhang Q-Y, Kaminsky LS. (2001) Polycyclic aromatic hydrocarbon (PAH)/metal mixtures: Effects on PAH induction of CYP1A1 in human HepG2 cells. *Drug Metab Dispos*, 29, 999-1006

25. Ho I-C, Lee T-C. (2002) Arsenite pretreatment attenuates benzo[a]pyrene cytotoxicity in a human lung adenocarcinoma cell line by decreasing cyclooxygenase-2 levels. *J Toxicol Environ Health Part A*, 65, 245-263
26. Han S, Kim K, Hahm E, Park CH, Kimler BF, Lee SJ, Lee S, Kim WS, Jung CW, Park K, Kim J, Yoon S, Lee J, Park S. (2005) Arsenic trioxide represses constitutive activation of NF- $\kappa$ B and COX-2 expression in human acute myeloid leukemia, HL-60. *J Cell Biochem*, 94, 695-707
27. Rubbi CP and Milner J. (2003) p53 is a chromatin accessibility factor for nucleotide excision repair of DNA damage. *EMBO J*, 22, 975-986
28. Dopp E, Hartmann LM, Florea A-M, von Recklinghausen U, Pieper R, Shokouhi B, Rettenmeier AW, Hirner AV, Obe G. (2004) Uptake of inorganic and organic derivatives of arsenic associated with induced cytotoxic and genotoxic effects in Chinese hamster ovary (CHO) cells. *Toxicol Appl Pharmacol*, 201, 156-165
29. Hamdan S, Morse B, and Reinhold D. (1999) Nickel subsulfide is similar to potassium dichromate in protecting normal human fibroblasts from mutagenic effects of benzo[a]pyrene diolepoxide. *Environ Mol Mutagen*, 33, 211-218
30. Hu W, Feng Z and Tang M-S. (2004) Nickel(II) enhances benzo[a]pyrene diol epoxide-induced mutagenesis through inhibition of nucleotide excision repair in human cells: a possible mechanism for nickel(II)-induced carcinogenesis. *Carcinogenesis*, 25, 455-462
31. Rossman TG. (2003) Mechanism of arsenic carcinogenesis: an integrated approach. *Mutat Res*, 533, 37-65

32. Lo JF, Wang HF, Tam MF and Lee TC. (1992) Glutathione S-transferase in an arsenic-resistant Chinese hamster ovary cell line. *Biochem J*, 288, 977-981
33. Lee TC, Wei ML, Chang WJ, Ho IC, Lo JF, Jan KY and Huang H. (1989) Elevation of glutathione levels and glutathione S-transferase activity in arsenic-resistant Chinese hamster ovary cells. *In Vivo Cell Dev Biol*, 25, 442-448
34. Brambila EM, Achanzar WE, Qu W, Webber MM, Waalkes MP. (2002) Chronic arsenic-exposed human prostate epithelial cells exhibit stable arsenic tolerance: mechanistic implication of altered cellular glutathione and glutathione S-transferase. *Toxicol Appl Pharmacol*, 183, 99-107
35. Buchet JP and Lauwreys RR. (1987) Study of factors influencing the in vivo methylation of inorganic arsenic in rats. *Toxicol Appl Pharmacol*, 91, 65-74
36. Oya-Ohta Y, Kaise T, Ochi T. (1996) Induction of chromosomal aberrations in cultured human fibroblasts by inorganic and organic arsenic compounds and the different roles of glutathione in such induction. *Mutat Res*, 357, 123-129
37. Robertson IG, Jansson H, Mannervik B, Jernstrom B. (1986) Glutathione transferases in rat lung: The presence of transferase 7-7, highly efficient in the conjugation of glutathione with the carcinogenic (+)-7 $\beta$ , 8 $\alpha$ -dihydroxy-9 $\alpha$ ,10 $\alpha$ -oxy-7,8,8,10-tetrahydrobenzo(a)pyrene. *Carcinogenesis*, 7, 295-299
38. Robertson IG, Guthenberg C, Mannervik B, Jernstrom B. (1986) Differences in stereoselectivity and catalytic efficiency of three human glutathione transferases in the conjugation of glutathione with 7 $\beta$ , 8 $\alpha$ -dihydroxy-9 $\alpha$ ,10 $\alpha$ -oxy-7,8,8,10-tetrahydrobenzo(a)pyrene. *Cancer Res*, 46, 2220-2224

39. Hu X, Srivastava SK, Xia H, Awasthi YC, Singh SV. (1996) An alpha class mouse glutathione S-transferase with exceptional catalytic efficiency in the conjugation of glutathione with 7 $\beta$ , 8 $\alpha$ -dihydroxy-9 $\alpha$ ,10 $\alpha$ -oxy-7,8,8,10-tetrahydrobenzo(a)pyrene. *J Biol Chem*, 271, 32684-32688
40. Ochi Y. (1997) Arsenic compound-induced increases in glutathione levels in cultured Chinese hamster V79 cells and mechanisms associated with changes in  $\gamma$ -glutamylcysteine synthase activity, cystine uptake and utilization of cysteine. *Arch Toxicol*, 71, 730-740
41. Sakurai T, Ochiai M, Kojima C, Ohta T, Sakurai MH, Takada N, Qu W, Waalkes MP and Fujiwara K. (2004) Role of glutathione in dimethylarsinic acid-induced apoptosis. *Toxicol Appl Pharmacol*, 198, 354-365
42. Thomas DJ, Styblo M and Lin S. (2001) The cellular metabolism and systemic toxicity of arsenic. *Toxicol Appl Pharmacol*, 176, 122-144
43. Brown JL, Kitchin KT, George M. (1997) Dimethylarsinic acid treatment alters six different rat biochemical parameters: relevance to arsenic carcinogenesis. *Teratog Carcinog Mutagen*, 17, 71-84
44. Lee TC and Ho IC. (1995) Modulation of cellular antioxidant defense activities by sodium arsenite in human fibroblasts. *Arch Toxicol*, 69, 498-504
45. Snow ET, Hu Y, Yan CC and Chouchane S. (1999) Modulation of DNA repair and glutathione levels in human keratinocytes by micromolar arsenite. In: Chappell WR, Abernathy CO and Calderon RL, eds. *Arsenic Exposure and Health Effects*. Oxford, Elsevier. pp 243-251

46. Schuliga M, Chouchane S and Snow ET. (2002) Upregulation of glutathione-related genes and enzyme activities in cultured human cells by sublethal concentrations of inorganic arsenic. *Toxicol Sci*, 70, 183-192
47. Sakurai T, Kojima C, Ochiai M, Ohta T, Sakurai MH, Waalkes MP, and Fujiwara K. (2004) Cellular glutathione prevents cytolethality of monomethylarsonic acid. *Toxicol Appl Pharmacol*, 195, 129-141
48. Li W, Chou I-N. (1992) Effects of sodium arsenite on the cytoskeleton and cellular glutathione levels in cultured cells. *Appl Pharmacol*, 114, 132-139
49. Yeh JY, Cheng LC, Ou BR, Whanger DP, Chang LW. (2002) Differential influences of various arsenic compounds on glutathione redox status and antioxidative enzymes in porcine endothelial cells. *Cell Mol Life Sci*, 59, 1972-1982
50. Szinicz L, Forth W. (1988) Effect of  $As_2O_3$  on gluconeogenesis. *Arch Toxicol*, 61, 444-449
51. Bergelson S, Pinkus R and Daniel V. (1994) Induction of AP-1 (Fos/Jun) by chemical agents mediates activation of glutathione S-transferase and quinone reductase gene expression. *Oncogene*, 9, 565-571
52. Daniel V, Bergelson S and Pinkus R. (1993) The role of AP-1 transcription factor in the regulation of glutathione S-transferase Ya subunit gene expression by chemical agents. In: Tew KD, Pickett CB, Mentle TJ, Mannervik B and Hayes JD, eds. *Structure and Function of Glutathione S-Transferase*. CRC Press, Boca Raton, FL. pp 129-136.
53. Falkner KC, McCallum GP, Cherian MG and Bend JR. (1993) Effects of acute sodium arsenite administration on the pulmonary chemical metabolizing enzymes,

- cytochrome p-450 monooxygenase, NAD(P)H: quinone acceptor oxidoreductase and glutathione S-transferase in guinea pig: comparison with effects in liver and lung. *Chem Biol Interact*, 86, 51-68
54. Hu X, Herzog C, Zimniak P and Singh SV. (1999) Differential protection against benzo[a]pyrene-7,8-dihydrodiol-9,10-epoxide-induced DNA damage in HepG2 cells stably transfected with allelic variants of  $\pi$  class human glutathione S-transferase. *Cancer Res*, 59, 2358-2362
55. Henson KL, Stauffer G and Gallagher EP. (2001) Induction of glutathione S-transferase activity and protein expression in brown bullhead (*Ameiurus nebulosus*) liver by ethoxyquin. *Toxicol Sci*, 62, 54-60
56. Gallagher EP, Sheehy KM, Janssen PL, Eaton DL, Collier TK. (1999) Isolation and cloning of homologous glutathione S-transferase cDNA from English sole and starry flounder liver. *Aquatic Toxicol*, 44, 171-182
57. Chouchane S and Snow ET. (2001) In vitro effect of arsenical compounds on glutathione-related enzymes. *Chem Res Toxicol*, 14, 517-522
58. Styblo M, Serves SV, Cullen WR and Thomas DJ. (1997) Comparative inhibition of yeast glutathione reductase by arsenicals and arsenothiols. *Chem Res Toxicol*, 10, 27-33
59. Li M, Cai JF, Chiu JF. (2002) Arsenic induces oxidative stress and activates stress expressions in cultured lung epithelial cells. *J Cell Biochem*, 87, 29-38
60. Srivastava SK, Watkins SC, Schuetz E, Singh SV. (2002) Role of glutathione conjugate efflux in cellular protection against benzo[a]pyrene-7,8-diol-9,10-epoxide-induced DNA damage. *Mol Carcinog*, 93, 156-162

61. Vernhet L, Seite MP, Allain N, Guillouzo A, Fardel O. (2001) Arsenic induces expression of the multidrug resistance-associated protein 2 (MRP2) gene in primary rat and human hepatocytes. *J Pharmacol Exp Ther*, 298, 234-239
62. Chin KV, Tanaka S, Darlington G, Pastan I, Gottesmen MM. (1990) Heat shock and arsenite increase expression of the multidrug resistance (MDR1) gene in human renal carcinoma cells. *J Biol Chem*, 265, 221-226
63. Ljungman M and Hanawalt PC. (1992) Efficient protection against oxidative DNA damage in chromatin. *Mol Carcinog*, 5, 264-269
64. Ljungman M. (1989) Pretreatment with UV light renders the chromatin in human fibroblasts more susceptible to the DNA-damaging agents bleomycin,  $\gamma$  radiation and 8-methoxypsoralen. *Carcinogenesis*, 10, 447-451
65. Darzynkiewicz Z. (1994) Acid-induced denaturation of DNA in situ as a probe for chromatin structure. *Methods Cell Biol*, 41, 527-541
66. Dobrucki J and Darzynkiewicz Z. (2001) Chromatin condensation and sensitivity of DNA in situ to denaturation during cell cycle and apoptosis—a confocal microscopy study. *Micron*, 32, 645-652
67. Darzynkiewicz Z, Evenson D, Kapuscinski J and Melamed MR. (1983) Denaturation of RNA and DNA in situ induced by acridine orange. *Exp Cell Res*, 148, 31-46
68. Darzynkiewicz Z, Traganos F, Kapuscinski J and Melamed MR. (1985) Denaturation and condensation of DNA in situ induced by acridine orange in relation to chromatin changes during growth and differentiation of Friend erythroleukemia cells. *Cytometry*, 6, 195-207

69. Segawa K, Minowa A, Sugasawa K, Takano T and Hanaoka F. (1993) Abrogation of p53-mediated transactivation by SV40 large T antigen. *Oncogene*, 8, 543-548
70. Kohli M and Jorgensen TJ. (1999) The influence of SV40 immortalization of human fibroblasts on p53-dependent radiation responses. *Biochem Biophys Res Commun*, 257, 168-176
71. Shinozaki R, Inoue S and Choi K-S. (1998) Flow cytometric measurement of benzo[a]pyrene-diol-epoxide-DNA adducts in normal human peripheral lymphocytes and cultured human lung cancer cells. *Cytometry*, 31, 300-306
72. Cunningham MJ, Kurian P and Milo GE. (1989) Metabolism and binding of benzo[a]pyrene in randomly-proliferating, confluent and S-phase human skin fibroblasts. *Cell Biol Toxicol*, 5, 155-168
73. Kootstra A. (1982) Effect of histone acetylation on the formation and removal of B(a)P chromatin adducts. *Nucleic Acids Res*, 10, 2775-2789
74. Venkatachalam S, Denissenko M and Wani AA. (1997) Modulation of ( $\pm$ )-anti-BPDE mediated p53 accumulation by inhibitors of protein kinase C and poly(ADP-ribose) polymerase. *Oncogene*, 14, 801-809
75. Kurian P, Kumari HL and Milo GE. (1992) Selective inhibition of the BPDE-I-induced modification of the replicating DNA of S-phase cells, by benzamide and 3-aminobenzamide. *Carcinogenesis*, 13, 489-491
76. Yang SK, Gelboin HV. (1976) Nonenzymatic reduction of benzo(a)pyrene diol epoxides to trihydroxypentahydrobenzo(a)pyrenes by reduced nicotinamide adenine dinucleotide phosphate. *Cancer Res*, 36, 4185-4189

77. Dock L, Waern F, Martinez M, Grover PL, Jernstrom B. (1986) Studies on the further activation of benzo[a]pyrene diolepoxides by rat liver microsomes and nuclei. *Chem Biol Interact*, 58, 301-318
78. Thakker DR, Yagi H, Levin W, Lu AYH, Conney AH, Jerina DM. (1977) Stereospecificity of microsomal and purified epoxide hydrase from rat liver. *J Biol Chem*, 252, 6328-6334
79. Walton FS, Harmon AW, Paul DS, Drobna Z, Patel YM and Styblo M. (2004) Inhibition of insulin-dependent glucose uptake by trivalent arsenicals: possible mechanism of arsenic-induced diabetes. *Toxicol Appl Pharmacol*, 198, 424-433
80. Srivastava SK, Hu X, Xia H, Bleicher RJ, Zaren HA, Orchard JL, Awasthi S and Singh SV. (1998) ATP-dependent transport of glutathione conjugate of 7 $\beta$ , 8 $\alpha$ -dihydroxy-9 $\alpha$ , 10 $\alpha$ -oxy-7,8,9,10-tetrahydrobenzo[a]pyrene in murine hepatic canalicular plasma membrane vesicles. *Biochem J*, 332, 799-805

## **Chapter Four**

### **Effects of Arsenic on the Repair of Benzo(a)pyrene Diol Epoxide-DNA Adducts**

#### **4.1 Introduction**

Although it is not itself mutagenic, arsenite (iAs(III)) increased the mutation frequency in *E. coli* when combined with ultraviolet (UV) light (1). Arsenic compounds have also been shown to enhance the persistence of DNA damage induced by UV light, benzo[a]pyrene (BaP), X-rays, alkylating agents, and DNA crosslinking compounds in cultured mammalian cells and to potentiate cytotoxicity, mutagenicity, and clastogenicity of the damaging agents. Inhibition of DNA repair has been suggested as one possible mechanism for arsenic co-mutagenicity. The first evidence to support this suggestion was documented by Okui and Fujiwara (2). They showed that iAs(III) and arsenate (iAs(V)) at micromolar concentrations increased the sensitivity of normal human fibroblasts to UV light, but had no effect on repair-deficient xeroderma pigmentosum complementation group A (XPA) cells. Furthermore, arsenic reduced unscheduled DNA synthesis (UDS) and the excision of cyclobutane pyrimidine dimers (CPD) after UV irradiation. Inhibition of CPD excision was also demonstrated in HeLa cells (3). Lee-Chen et al. (4) observed an inhibition of the repair of methylmethane sulfonate (MMS)-induced DNA damage in Chinese hamster ovary (CHO) cells. They found that low doses of MMS and iAs(III) were associated with an increased frequency of alkali-labile sites in CHO cells. In a separate study, they showed that micromolar concentrations of iAs(III) caused a delayed rejoining of repair-mediated DNA strand breaks after UV irradiation in CHO cells (5). They proposed that arsenic might inhibit the repair of DNA damage by impairing the

DNA ligation step. Li and Rossman observed that in Chinese hamster V79 cells, iAs(III) enhanced the mutagenicity of UVC (6) as well as of N-methyl-N-nitrosourea (MNU) (7). UVC caused DNA lesions that were repairable by nucleotide excision repair (NER) (Figure 4.1) while MNU caused DNA adducts that were repairable by base excision repair (BER) (Figure 4.2) (V79 cells lack the O<sup>6</sup>-methylguanine DNA methyltransferase, so all premutagenic MNU adducts would be subjected to BER). This strongly suggested that iAs(III) might inhibit a late step in DNA repair shared by both DNA excision repair pathways. DNA strand breaks persisted longer in MNU-treated cells in the presence of iAs(III) (10  $\mu$ M) than in the absence of iAs(III), indicating that either the polymerase or the ligase step was blocked by iAs(III). In subsequent experiments, nuclear extracts of iAs(III)-treated cells were found to have a decreased total ligase activity. iAs(III) inhibited DNA ligase III more specifically and DNA ligase I to a lesser extent (8). Surprisingly, the inhibition of the activity of DNA ligase III extracted from untreated cells required 1,000-fold higher concentrations of iAs(III) than needed to inhibit the ligase activity inside the cells (8), indicating that iAs(III) did not directly inhibit DNA ligase III activity. This was confirmed by using purified DNA ligase III (9). DNA polymerases are not sensitive to inhibition by iAs(III) either (9, 10). DNA polymerase  $\alpha$  (pol  $\alpha$ ) requires >1 mM iAs(III) to be inhibited and DNA polymerase  $\beta$  (pol  $\beta$ ) is stimulated by iAs(III) up to at least 12 mM. Based on these observations, it was suggested that the effects of arsenic on ligation are not caused by direct inhibition of DNA repair enzymes (9).

When the effects of iAs(III) on NER in UV-irradiated repair-proficient fibroblasts and repair-deficient xeroderma pigmentosum complementation group C (XPC) cells were

studied, inhibition of the ligation step within the repair machinery was observed. Additionally, inhibition of the damage incision step of the NER process by iAs(III) was observed at much lower concentrations (as low as 2.5  $\mu$ M) (11). This suggests that inhibition of damage recognition/incision may be a more biologically relevant factor that contributes to arsenic-associated carcinogenesis. This latter effect would somehow shift the center of attention from the ligation step, which was previously believed to be the major target for arsenic-induced repair inhibition. However, the enzymatic activities of some repair proteins involved in early stages of BER and NER pathways such as formamidopyrimidine-DNA glycosylase (Fpg) and XPA, which were believed to be biochemically plausible targets for arsenic, were not inhibited by iAs(III) at concentrations up to 1 mM (12). Recently, poly(ADP-ribosyl)ation was shown to be suppressed by iAs(III) at concentrations as low as 10 nM in HeLa cells (13). Poly(ADP-ribosyl)ation is mediated by poly(ADP-ribose) polymerase (PARP) and plays a major role in the detection of DNA single strand breaks (SSB) that initiates BER. In terms of effects on PARP activity, both stimulation and inhibition by iAs(III) were reported (14, 15).

Apparently, direct enzymatic activity inhibition by arsenic still seems uncertain and in some cases controversial. Under such circumstances, an indirect action of arsenic by interfering with signal transduction pathways that regulate DNA repair has been proposed. For example, arsenic could downregulate the synthesis of DNA repair enzymes (16) or inhibit the induction of accessory or other key proteins involved in cellular control of DNA repair pathways (17). The inhibitory mechanism of DNA repair by arsenic remains unknown and deserves further investigation.

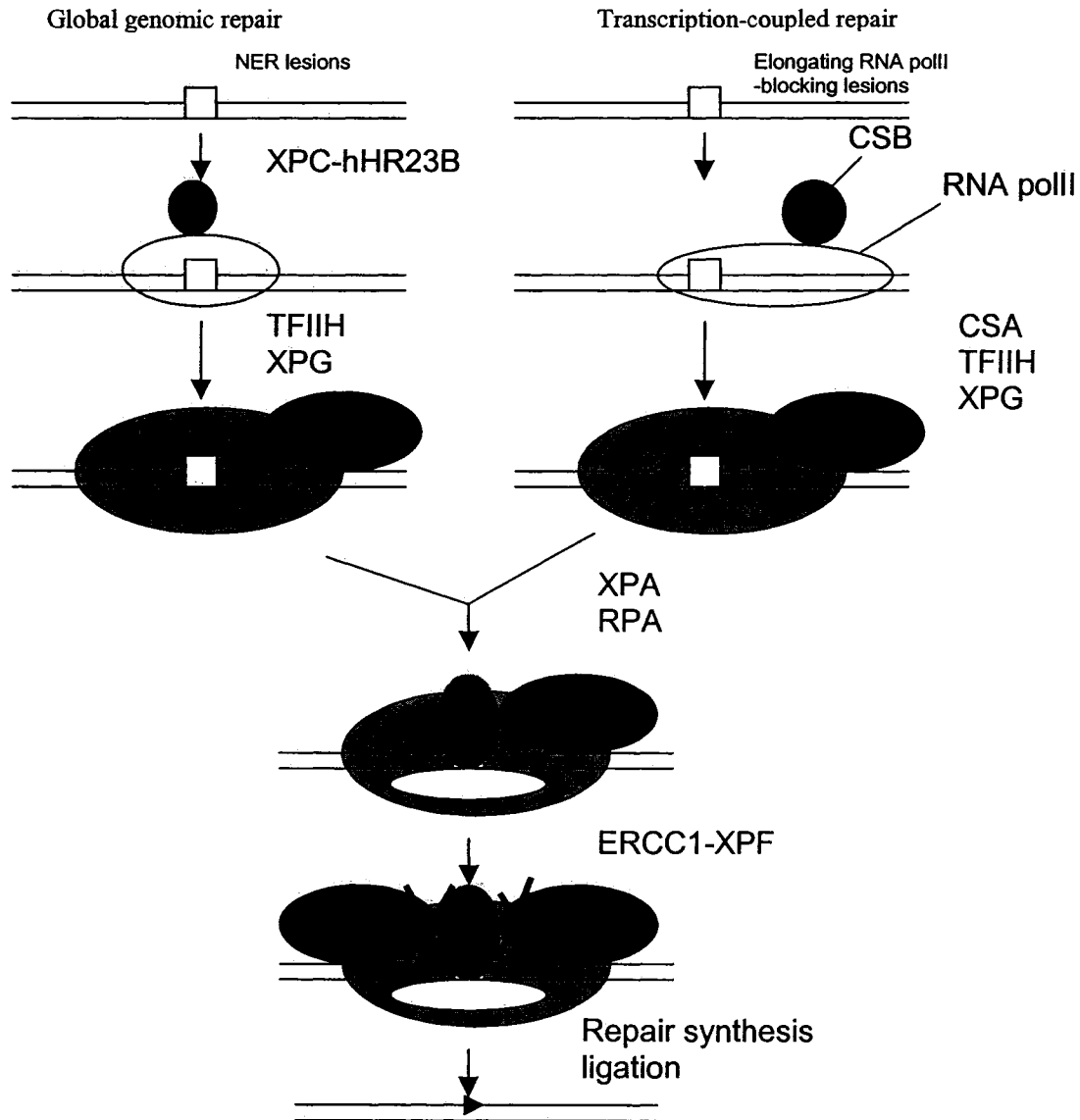


**Figure 4.1. Proposed model for mammalian nucleotide excision repair (NER). NER consists of two subpathways: global genome repair (GGR) and transcription-coupled repair (TCR). They differ only in DNA damage recognition. In GGR, XPC/hHR23B binds to the damaged DNA site whereas in TCR, a stalled RNA polymerase II is displaced with the help of CSA and CSB to initiate the repair. After DNA damage recognition, the DNA lesion is opened by the concerted action of XPA, RPA, and the bi-directional XPB/XPD helicase subunits of TFIIH. XPG and ERCC1-XPF are recruited to incise the damaged DNA. Then DNA synthesis and ligation are followed to fill the gap (adapted from [18]).**

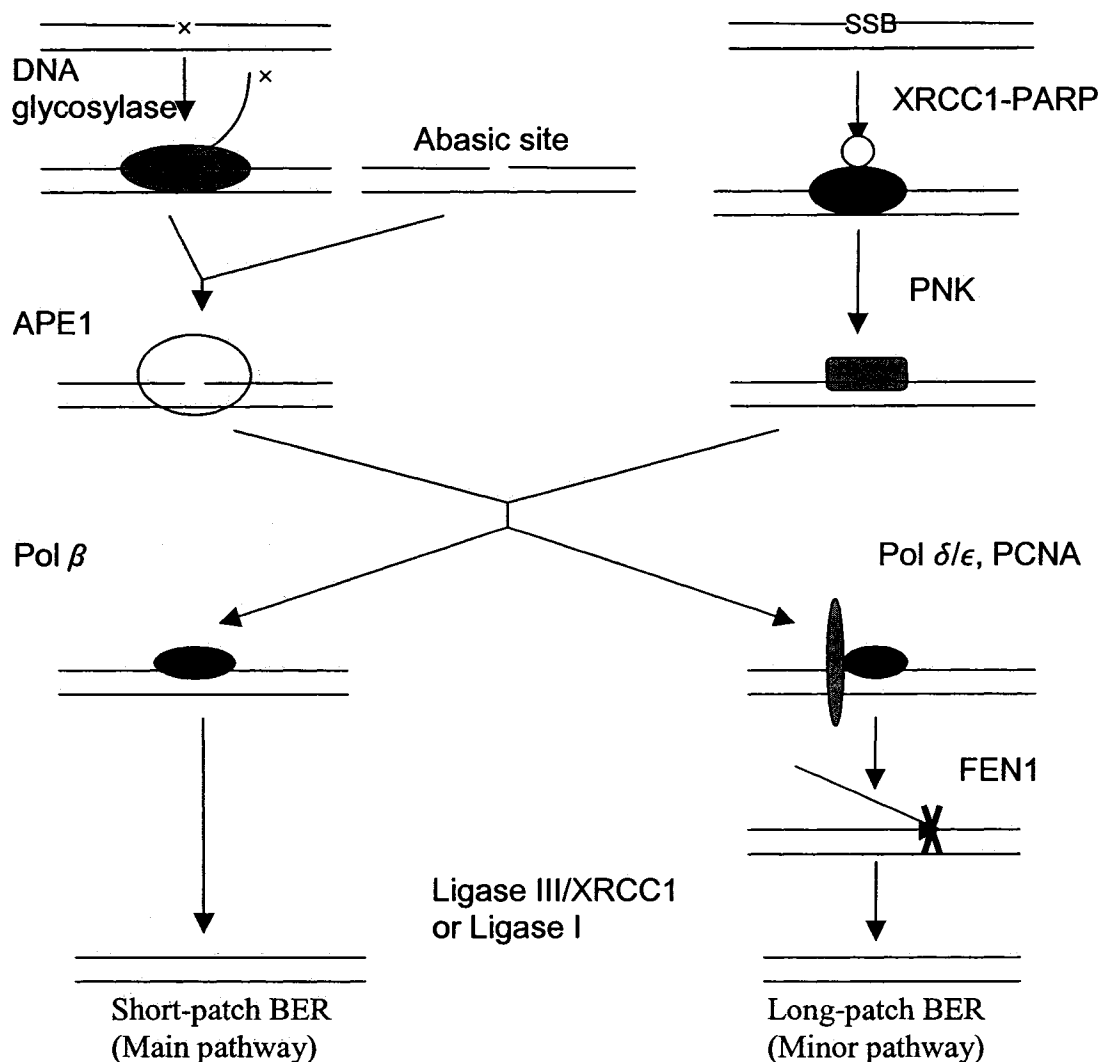


**Figure 4.2. Proposed model for mammalian base excision repair (BER).** Many distinct DNA glycosylases recognize and remove damaged bases to generate a central apurinic/apyrimidinic (AP) site intermediate. Subsequently, the AP site products (which can occur spontaneously by hydrolysis) are processed by 5'-AP endonuclease (APE1) to provide a free 3'OH for repair synthesis and ligation. If BER is initiated by a bifunctional DNA glycosylase/AP lyase, excision is mainly by short-batch BER; if BER is initiated by a monofunctional DNA glycosylase, excision is via either short-batch BER or long-batch BER. Poly(ADP-ribose)polymerase (PARP) and polynucleotide kinase (PNK) are involved in SSB-initiated BER (adapted from [18]).

NER is the major pathway responsible for repairing DNA damage induced by BaP or its metabolite benzo(a)pyrene diol epoxide (BPDE). iAs(III) was shown to inhibit the repair of BaP-induced DNA damage both in Sprague-Dawley rats (19) and in human cell cultures (20). In the human cell culture study, an alkaline comet assay was employed to investigate DNA repair, while a  $^{32}\text{P}$ -postlabelling assay was used for DNA adduct measurement in the rat bioassay. The  $^{32}\text{P}$ -postlabelling assay was also used by Maier et al. (21), but they did not observe changes in adduct removal kinetics in BaP-treated cells by iAs(III). Recently, five arsenic species — iAs(III), monomethylarsonous acid (MMA(III)), dimethylarsinous acid (DMA(III)), monomethylarsonic acid (MMA(V)), and dimethylarsinic acid (DMA(V)) — have been examined by Schwerdtle et al. (22) for their effects on the formation and repair of BPDE-DNA adducts in A549 human lung cancer cells. They observed that all arsenic species under investigation diminished DNA repair at non-cytotoxic concentrations of arsenic.

Although these studies are very useful, they have several drawbacks. Firstly, the effects in the comet assay can be influenced by DNA repair processes in a rather complex way: DNA repair eliminates DNA lesions, which results in a decreased DNA migration. Furthermore, excision repair itself leads to strand break formation, which may cause DNA migration in the comet assay. Secondly, coexposure to BaP and arsenic is a very complex system because both BaP and arsenic generate other alkali labile sites and DNA strand breaks (14, 23, 24), which make the interpretation of the comet assay results difficult. In addition, the use of either an animal model or human tumor cells (Hepa-1, c37, CX4 in Maier et al.'s study and A549 in Schwerdtle et al.'s study) was equally inappropriate for extrapolation to normal human cells in an attempt to elucidate the

carcinogenic mechanism of arsenic as a human carcinogen. Moreover, in these cell culture studies, either a 30-min arsenic treatment prior to BaP or a 16-h arsenic treatment prior to BPDE was applied. The effects of arsenic on adduct repair could not be distinguished from its effects on adduct formation. The DNA repair kinetics are known to be dependent on the initial DNA damage level. Finally, Schwerdtle et al. used exponentially growing A549 cells, and their observation of repair inhibition by arsenic could be confounded by possible replication inhibition by arsenic. Different observations from Maier et al.'s and Schwerdtle et al.'s studies are most likely due to different carcinogens (BaP versus BPDE) and different treatment protocols used.

To confirm whether or not arsenic has an effect on the repair of BPDE-DNA adducts, a repair-proficient human normal foreskin fibroblast cell line CRL2522 was chosen in our study. It is non-SV40 transformed and its intrinsic repair capacity is intact. BPDE was used to induce BPDE-DNA adducts. Therefore, the change in adduct levels at a certain post-treatment time-point could be unambiguously attributed to the effect of arsenic on adduct repair. In all of our repair experiments, cells were grown to almost 100% confluence in order to prevent post-treatment replication.

## 4.2 Experimental

### 4.2.1 Materials

Racemic anti-BPDE was supplied by the NCI Chemical Carcinogen Repository (Midwest Research Institute, Kansas City, MO). To avoid hydrolysis of the epoxide, a stock of BPDE was always prepared fresh by dissolving BPDE in anhydrous tetrahydrofuran (THF) (>99.9% purity, Sigma-Aldrich, St. Louis, MO) immediately before use. iAs(III) (99.4% purity) was obtained as an arsenic atomic absorption standard solution from Aldrich (Milwaukee, WI) and used as a stock solution with a concentration of 13.3 mM. iAs(V) (99.4% purity) and DMA(V) (98% purity) were obtained from Sigma (St. Louis, MO). MMA(V) was purchased from Chem Service (West Chester, PA) and its purity was determined to be approximately 85% using an Elan 6100 DRC<sup>plus</sup> inductively coupled argon plasma mass spectrometer (PE Sciex, Concord, ON). Methylarsine oxide ( $\text{CH}_3\text{As}^{\text{III}}\text{O}$ ) and dimethyliodoarsine ( $(\text{CH}_3)_2\text{As}^{\text{III}}\text{I}$ ) were kindly provided by Dr. WR Cullen (University of British Columbia, Vancouver, BC) and were used as the precursors to MMA(III) and DMA(III), respectively. Stock solutions of iAs(V), MMA(V), and DMA(V) were prepared in deionized water at concentrations of 1 M, and stock solutions of MMA(III) and DMA(III) were prepared by dissolving the precursors in deionized water to a final concentration of 10 mM. When preparing the stock solution of DMA(III), 3 volumes of dimethylsulfoxide (DMSO) were used to dissolve  $(\text{CH}_3)_2\text{As}^{\text{III}}\text{I}$  before adding deionized water. To prevent oxidation of the trivalent methylated arsenic species, their stock solutions were prepared shortly before the experiment.

#### **4.2.2 Cells and cell cultures**

CRL2522 cells (normal human foreskin fibroblasts (NHF)) were obtained from the American Type Culture Collection (Rockville, MD). This cell line has a great growth potential (>60 doublings). CRL2522 cells were grown in Dulbecco's modified Eagle's medium/nutrient mixture F-12 (DMEM/F12) supplemented with 5% fetal bovine serum plus 5% bovine growth supplements. The cells were seeded in 100-mm dishes at a density of  $1 \times 10^6$  cells per dish and maintained at 37 °C in humidified air containing 5% CO<sub>2</sub>. The cells were grown to almost 100% confluence to prevent post-treatment replication. The passage numbers of CRL2522 in use for experiments were less than 22 to ensure clone integrity throughout the experiments.

#### **4.2.3 Treatment of cells**

At almost 100% confluence, CRL2522 cells were washed once with phosphate-buffered saline (PBS). BPDE in serum-free medium was added to a final concentration of 1 μM. After a 30-min incubation, BPDE was removed and the cells were washed twice with PBS and exposed to arsenic species of different concentrations in complete growth medium for 24 h. The concentrations of organic solvents used to dissolve BPDE and (CH<sub>3</sub>)<sub>2</sub>As<sup>III</sup>I did not exceed 0.001%, to avoid the direct influence of DMSO or THF on the cells. The cells were then washed three times with PBS before DNA was extracted for measurement of BPDE-DNA adducts.

#### **4.2.4 DNA isolation**

Cells were lysed in DNAzol® reagent (Invitrogen Life Technologies). Genomic DNA was precipitated with ice-cold 99.9% ethanol and washed twice with cold 70% ethanol. The DNA pellet was air-dried and then resuspended in deionized water, and the solution was placed in an incubator at 37 °C overnight to facilitate the redissolution of

DNA. DNA concentrations were measured at 260 nm using a SmartSpec™ 3000 spectrometer (Bio-Rad Laboratories, Cambridge, MA).

#### 4.2.5 Detection of BPDE-DNA adducts

A capillary electrophoresis laser-induced detection (CE-LIF) immunoassay, described in **Chapters 2** and **3**, was used to detect BPDE-DNA adducts. Typically, an aliquot of DNA was heat-denatured at 100 °C for 5 min followed by cooling on ice for 3 min. Denatured DNA was incubated with a mouse anti-BPDE antibody (Clone 8E11, isotype IgG<sub>1</sub>, Trevigen, Gaithersburg, MD), and a fluorescently-labelled goat anti-mouse antibody. The primary antibody 8E11 was raised against BPDE-modified guanosine coupled to bovine serum albumin. The goat anti-mouse antibody was received as a Zenon™ Alexa Fluor® 546 mouse IgG<sub>1</sub> labelling kit (Molecular Probes, Eugene, OR). This secondary antibody was a F<sub>ab</sub> fragment directed against the F<sub>c</sub> portion of a whole IgG primary antibody. It was labelled with a fluorophore Alexa Fluor® 546 whose optimum excitation wavelength was 553 nm, which was close to the He-Ne laser wavelength of 543.5 nm in the CE-LIF instrument being used. To the mixture of the DNA sample and the antibodies, an incubation buffer was added to bring the total sample volume to 20 µL. The incubation buffer contained 10 mM Tris and 80 mM glycine, and its pH was adjusted to pH 7.8 with acetic acid. After overnight incubation on ice in the dark, samples were electrokinetically injected into the capillary using an injection voltage of 10 kV for 10 s. The separation was carried out at room temperature with a separation voltage of 20 kV. The running buffer was a Tris-glycine mixture containing 30 mM Tris and 170 mM glycine, at pH 8.3. Between runs, the capillary was rinsed for 5 min electrophoretically with 0.02 M NaOH and 5 min with the running buffer.

#### **4.2.6 Cell cycle analysis**

Cells were incubated with 1  $\mu$ M BPDE for 30 min, and then allowed to repair in complete medium in the absence or presence of MMA(III). The cells were washed and trypsinized. After centrifugation at 1000 rpm, the cells were resuspended in 300  $\mu$ L of PBS, fixed with 3 mL of ice-cold 70% ethanol, and stored at  $-20$  °C until analysis. After removal of ethanol, the cells were stained with propidium iodide (5  $\mu$ g/ml, Sigma # P4170) and RNase (0.1 mg/ml, Sigma # R6513) at room temperature for 1 h. The DNA content in  $2 \times 10^5$  cells was determined using a FACSort flow cytometer (Becton Dickinson, San Jose, CA) equipped with CellQuest and ModFit software (Becton Dickinson).

#### **4.2.7 Western blotting assay**

>90% confluent CRL2522 cells were washed with PBS and exposed to 1  $\mu$ M BPDE in serum-free medium for 30 min. BPDE was removed and the cells were washed with PBS twice before adding 5  $\mu$ M MMA(III) in complete medium for different times as indicated. The cells were recovered by gentle trypsinization and whole cell extracts were prepared. Twenty-five  $\mu$ g of protein samples was resolved by 10% SDS-PAGE and electroblotted onto nitrocellulose membranes. The membranes were subjected to immunoblotting with the mouse monoclonal antibodies to XPA (clone 12F5 from Abcam; 1:500), p62 (clone 3C9 from Euromedex; 1:500), p53 (clone DO-1 from Santa Cruz, 1:500), and p21 (clone EA10 from Zymed; 1:200) and the polyclonal antibody to XPC (GTX70308 from Gene Tex, 1:500) in 5% non-fat milk in PBST, followed by incubation with a horseradish-peroxidase-conjugated secondary antibody (1:10000 in 5% non-fat milk/PBST). Proteins were detected by enhanced chemiluminescence (Roche).

## 4.3 Results and Discussion

### 4.3.1 Effects of arsenic compounds on the repair of BPDE-DNA adducts

All six arsenic compounds under investigation were shown to be capable of inhibiting the repair of BPDE-DNA adducts (**Figures 4.3-4.8**) although the minimum concentrations of the arsenic species starting the inhibition differed substantially. iAs(III) inhibited the adduct repair by 18% at 5  $\mu\text{M}$  and by 32% at 25  $\mu\text{M}$  (**Figures 4.3a and 4.3b**). MMA(III) and DMA(III) started to inhibit the adduct repair at a much lower concentration (**Figures 4.4 and 4.5**). MMA(III) at 1  $\mu\text{M}$  inhibited the repair by 45%, and DMA(III) at 1  $\mu\text{M}$  inhibited the repair by 37%. Pentavalent arsenic compounds exerted their inhibitory effects at higher concentrations. iAs(V) inhibited the repair by 24% at 25  $\mu\text{M}$  (**Figure 4.6**) and MMA(V) inhibited the repair by 26% at 500  $\mu\text{M}$  (**Figure 4.7**), while DMA(V) started to inhibit the repair at 100  $\mu\text{M}$  and achieved inhibition of 30% at 500  $\mu\text{M}$  (**Figure 4.8**).

Inhibitory effects by various arsenic species were also observed by Schwerdtle et al. (22). In their study, iAs(III) inhibited the adduct repair by about 15% at 5  $\mu\text{M}$  and 40% at 25  $\mu\text{M}$ . At 5  $\mu\text{M}$ , MMA(III) and DMA(III) inhibited the repair by 62% and 43%, respectively. At 500  $\mu\text{M}$ , MMA(V) and DMA(V) were shown to inhibit the repair by ~30% and ~15%, respectively. The difference in the magnitude of inhibition between their study (22) and ours might be due to the different treatment protocols and different cell lines used. Schwerdtle et al. (16) pre-incubated exponentially growing A549 cells with arsenic for 16 h and co-incubated the cells with 50 nM BPDE and arsenic for 2 h before repair in the presence of arsenic for 8 h was assessed.

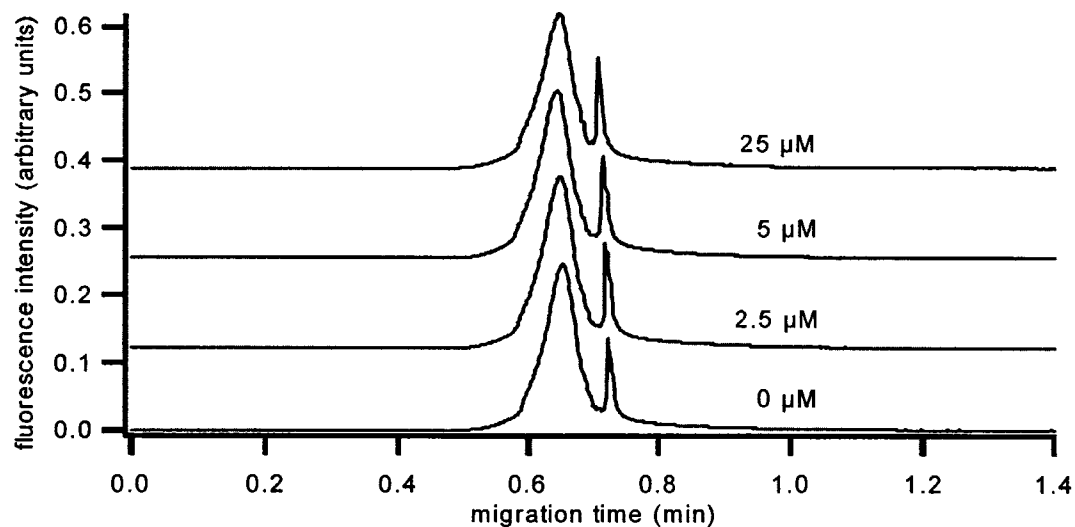


**Figure 4.3a.** Electropherograms obtained from DNA extracted from HNF cells incubated with 1  $\mu\text{M}$  BPDE for 30 min followed by repair for 24 h in the presence of different concentrations of iAs(III) as indicated. The ratio of peak areas between the two peaks indicates the level of DNA adducts.

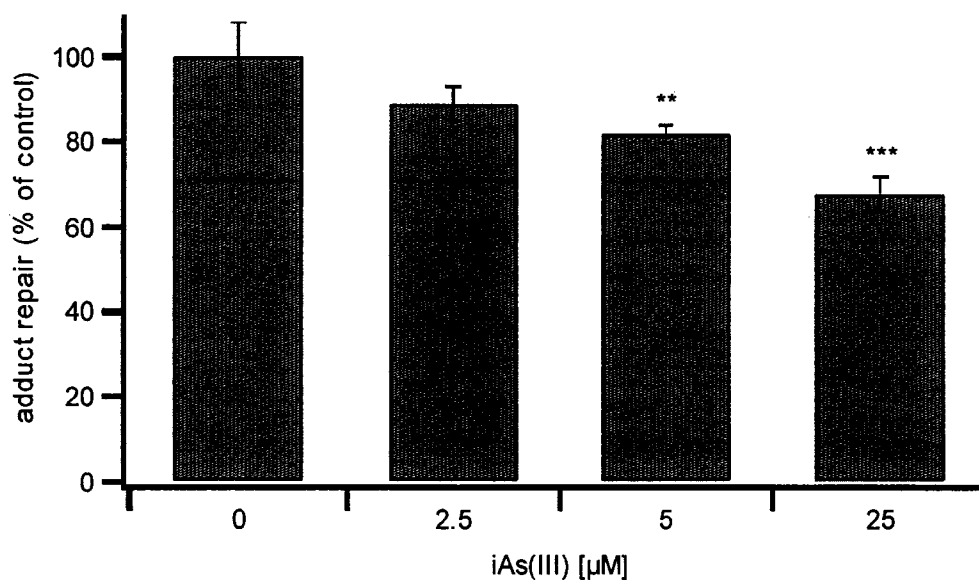


**Figure 4.3b.** Histograms representing the relative adduct levels after repair for 24 h in the presence of different iAs(III) concentrations. Adduct levels obtained from cells repaired in the absence of iAs(III) were used as controls. \*\* $P < 0.05$ , \*\*\* $P < 0.01$  using one-way Student's test. Error bars indicate the standard deviation from three experiments.

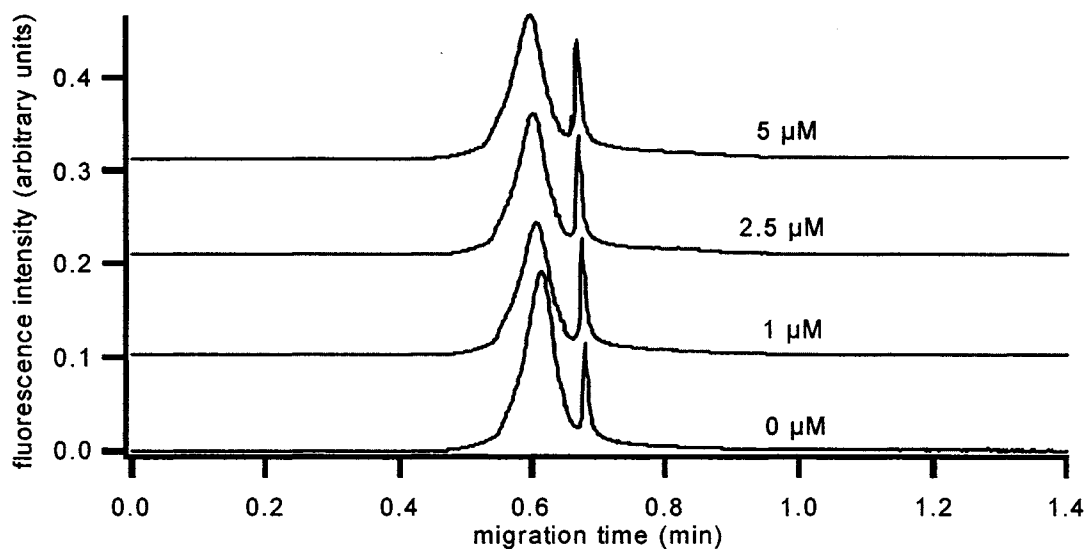


**Figure 4.4a. Electropherograms obtained from DNA extracted from HNF cells incubated with 1  $\mu\text{M}$  BPDE for 30 min followed by repair for 24 h in the presence of different concentrations of MMA(III) as indicated. The ratio of peak areas between the two peaks indicates the level of DNA adducts.**

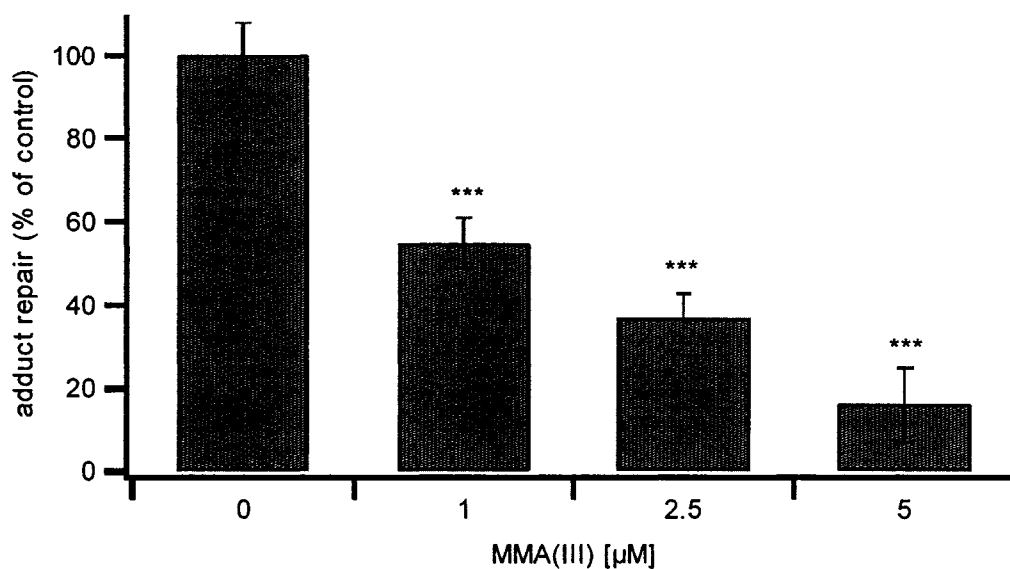


**Figure 4.4b. Histograms representing the relative adduct levels after repair for 24 h in the presence of different MMA(III) concentrations. Adduct levels obtained from cells repaired in the absence of MMA(III) were used as controls. \*\*\* $P < 0.01$  using one-way Student's test. Error bars indicate the standard deviation from three experiments.**

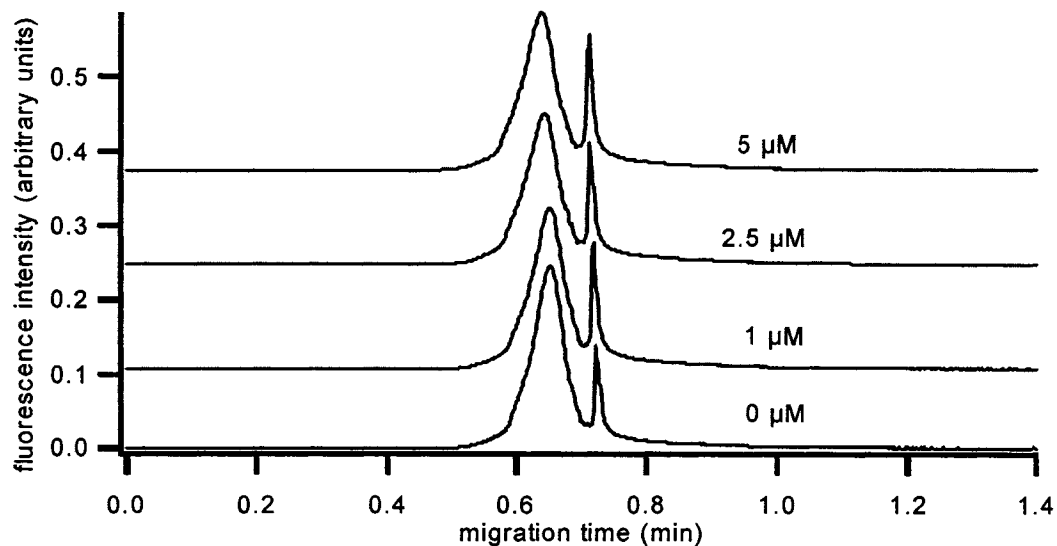


**Figure 4.5a.** Electropherograms obtained from DNA extracted from HNF cells incubated with 1  $\mu\text{M}$  BPDE for 30 min followed by repair for 24 h in the presence of different concentrations of DMA(III) as indicated. The ratio of peak areas between the two peaks indicates the level of DNA adducts.

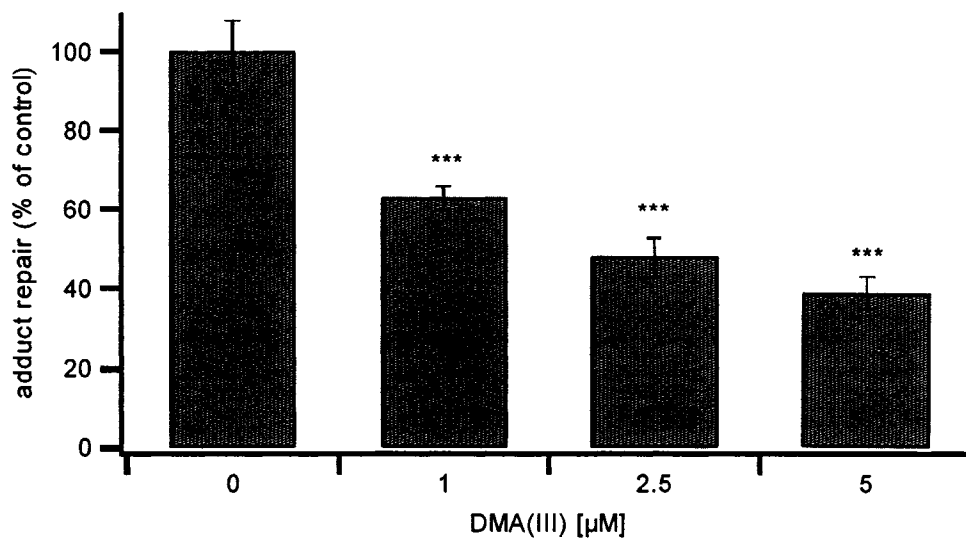


**Figure 4.5b.** Histograms representing the relative adduct levels after repair for 24 h in the presence of different DMA(III) concentrations. Adduct levels obtained from cells repaired in the absence of DMA(III) were used as controls. \*\*\* $P < 0.01$  using one-way Student's test. Error bars indicate the standard deviation from three experiments.

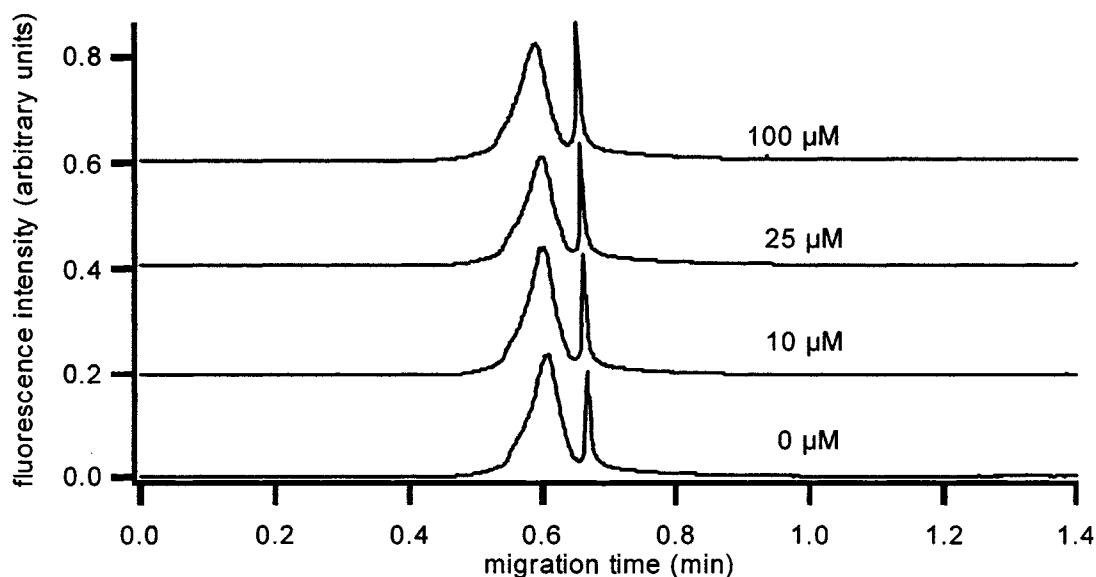


**Figure 4.6a.** Electropherograms obtained from DNA extracted from HNF cells incubated with 1 μM BPDE for 30 min followed by repair for 24 h in the presence of different concentrations of iAs(V) as indicated. The ratio of peak areas between the two peaks indicates the level of DNA adducts.

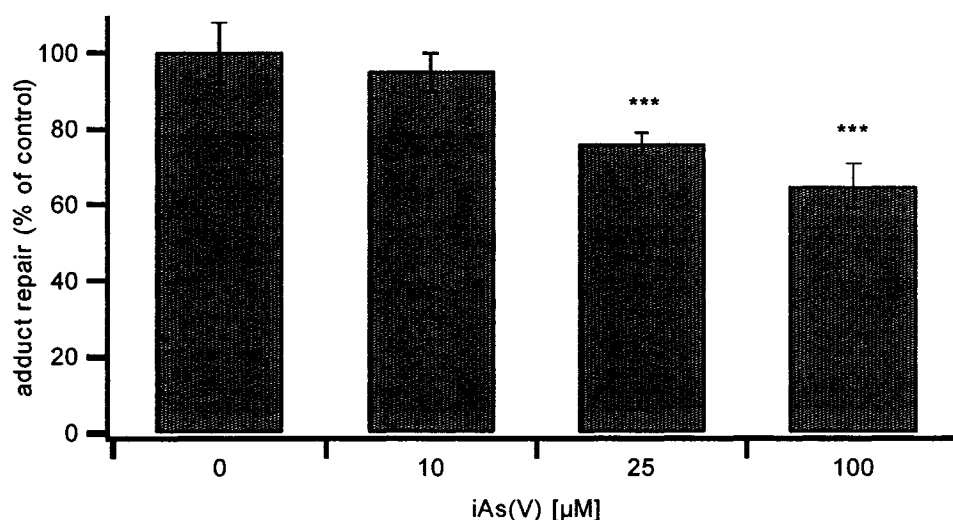


**Figure 4.6b.** Histograms representing the relative adduct levels after repair for 24 h in the presence of different iAs(V) concentrations. Adduct levels obtained from cells repaired in the absence of iAs(V) were used as controls. \*\*\*P<0.01 using one-way Student's test. Error bars indicate the standard deviation from three experiments.

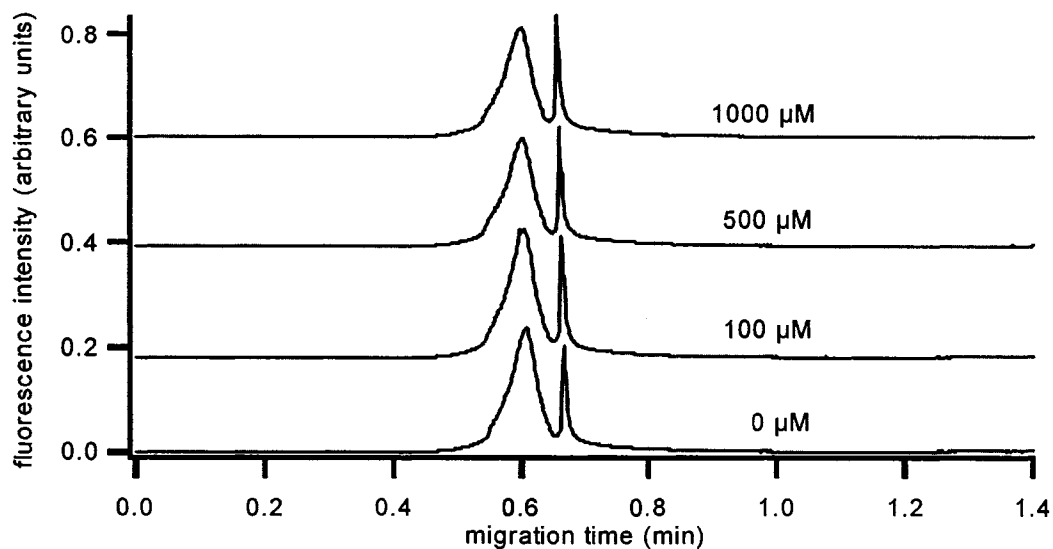


**Figure 4.7a. Electropherograms obtained from DNA extracted from HNF cells incubated with 1  $\mu\text{M}$  BPDE for 30 min followed by repair for 24 h in the presence of different concentrations of MMA(V) as indicated. The ratio of peak areas between the two peaks indicates the level of DNA adducts.**

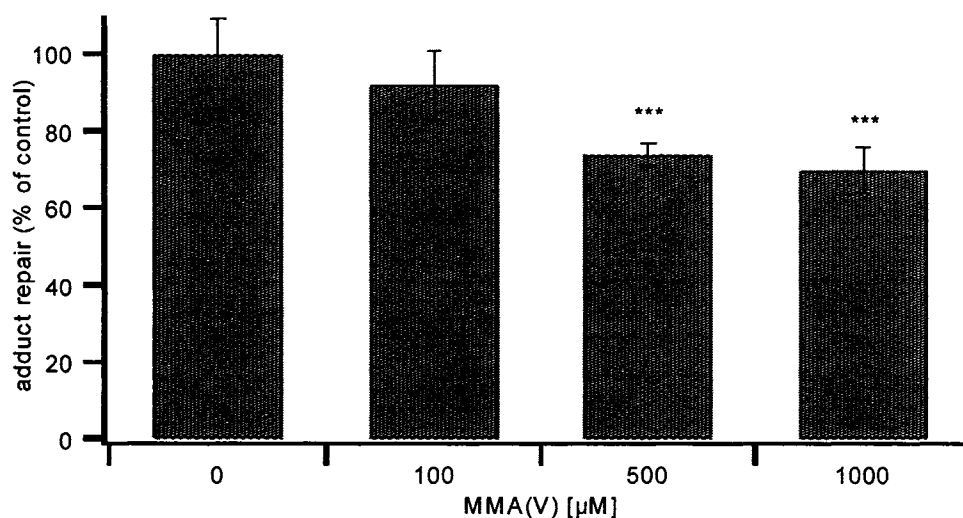


**Figure 4.7b. Histograms representing the relative adduct levels after repair for 24 h in the presence of different MMA(V) concentrations. Adduct levels obtained from cells repaired in the absence of MMA(V) were used as controls. \*\*\* $P < 0.01$  using one-way Student's test. Error bars indicate the standard deviation from three experiments.**

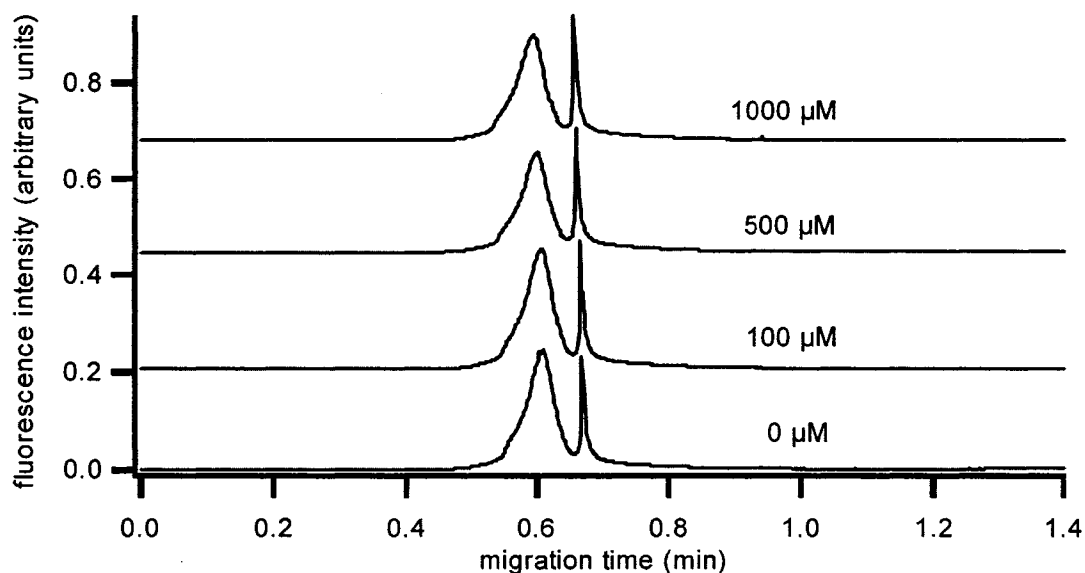


**Figure 4.8a.** Electropherograms obtained from DNA extracted from HNF cells incubated with 1  $\mu\text{M}$  BPDE for 30 min followed by repair for 24 h in the presence of different concentrations of DMA(V) as indicated. The ratio of peak areas between the two peaks indicates the level of DNA adducts.

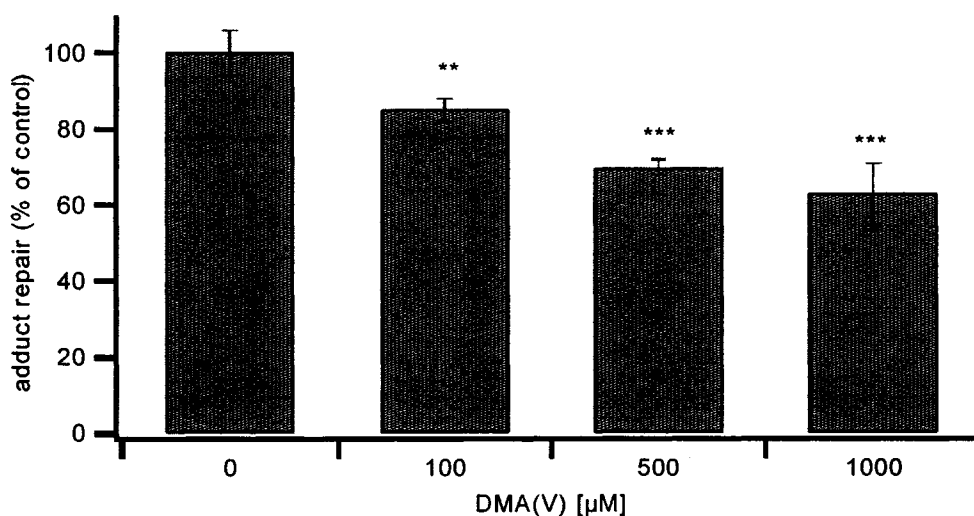


**Figure 4.8b.** Histograms representing the relative adduct levels after repair for 24 h in the presence of different DMA(V) concentrations. Adduct levels obtained from cells repaired in the absence of DMA(V) were used as controls. \*\* $P < 0.05$ , \*\*\* $P < 0.01$  using one-way Student's test. Error bars indicate the standard deviation from three experiments.

### 4.3.2 Time-dependence of inhibition of BPDE-DNA adduct repair

Of the six arsenic compounds we examined, MMA(III) was the most potent inhibitor of BPDE-DNA adduct repair. To determine if this inhibition is time-dependent, we allowed cells to stay in MMA(III)-containing media for different time periods after BPDE treatment. The levels of BPDE-DNA adducts in the cells after varying repair times were determined and the results are shown in **Figure 4.9**. Incubation for 24 h in the presence of MMA(III) after BPDE treatment was demonstrated to inhibit the repair of BPDE-DNA adducts to the largest extent when compared to respective time-matched controls. Therefore, the apparent extent of inhibition can be affected by the time allowed for repair before assessment. Our observation of repair inhibition by 5  $\mu\text{M}$  MMA(III) at 8 h post-treatment was comparable to the result of Schwerdtle et al. (22).

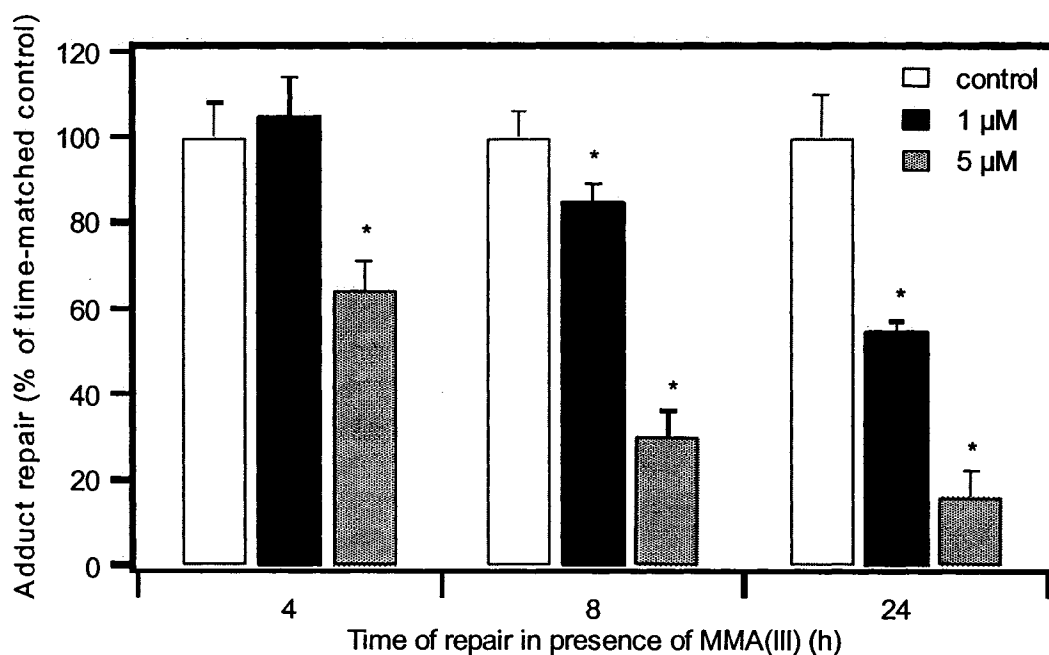


**Figure 4.9. Inhibition of BPDE-DNA adduct repair by MMA(III) is time-dependent. \*P<0.05 using one-way Student's test. Error bars indicate the standard deviation from three experiments.**

### 4.3.3 Kinetics of BPDE-DNA adduct repair

To ensure that our study reveals the effects of arsenic on the repair of BPDE-DNA adducts and to minimize any confounding effects from arsenic influence on the formation of BPDE-DNA adducts, we monitored the BPDE-DNA adduct levels in cells that were treated with BPDE and were allowed to repair in the absence or presence of MMA(III) over a 24-h period. There was no arsenic treatment prior to BPDE exposure. However, there could conceivably be a delay for cellular BPDE to accumulate in the nucleus and generate the maximum BPDE-DNA adducts, during which time MMA(III) might have an effect. To examine whether the apparent repair inhibition was due either to the difference in the kinetics of BPDE-DNA adduct formation, or the difference in the maximum adduct levels in the absence or presence of MMA(III) after BPDE exposure, or both, the repair kinetics of BPDE-DNA adducts over time were obtained both in the absence and presence of 5  $\mu$ M MMA(III), shown in **Figure 4.10**.

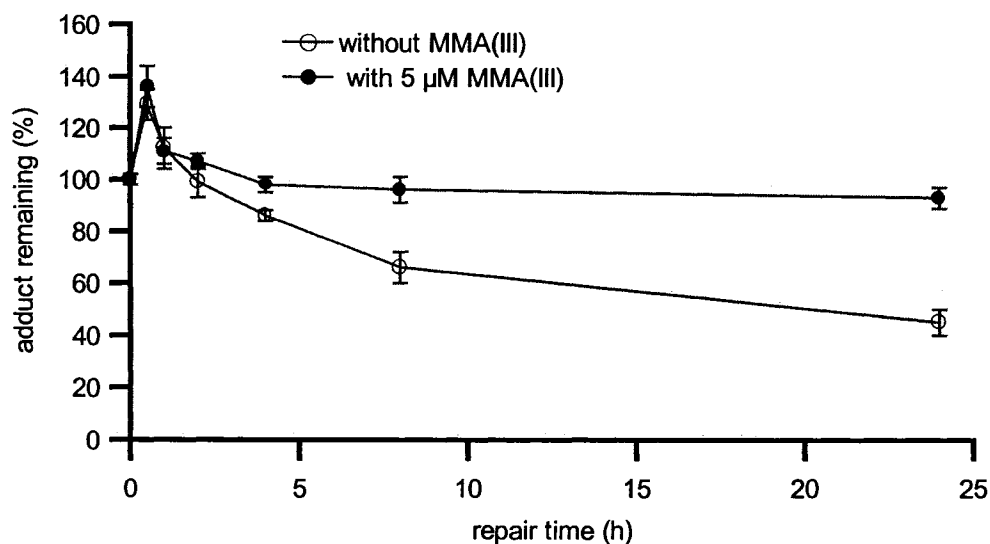


**Figure 4.10.** Repair kinetics of BPDE-DNA adducts in CRL2522 cells in the absence (open circle) and presence (filled circle) of 5  $\mu$ M MMA(III). Error bars indicate the standard deviation of four determinations from two experiments.

As expected, an abrupt increase in adduct levels after 30 min following BPDE exposure was observed regardless of whether the repair was in the presence or absence of MMA(III). This might indicate that BPDE was sequestered and stabilized in lipids within cells and released slowly, thereby extending the period of exposure to the BPDE after its withdrawal from the culture medium. This similar “jump” was observed in some other *in vitro* cultured cell studies when short repair time points were included (25-29) and is probably a general phenomenon in repair studies of chemically induced DNA adducts. For this reason, DNA damage immediately after treatment (0 h) cannot reliably indicate the “initial” levels of DNA damage.

Our results showed that BPDE-DNA adducts peaked at 30 min regardless of the absence or presence of 5  $\mu$ M MMA(III). The difference in the peak levels between the absence and the presence of MMA(III) was not statistically significant (mean value 129% vs 136%). In the absence of MMA(III), the cellular repair of BPDE-DNA adducts resulted in approximately 45% of the adducts remaining after 24 h. In the presence of MMA(III) treatment, the cells seemed to lose completely the momentum to remove BPDE-DNA adducts after the initial 4 h (93% of adducts remained unrepaired 24 h after BPDE exposure). This graph explains why the repair inhibition observed in the present work is time-dependent and is determined by the sampling time for assessment. These results further suggest that the observed difference in BPDE-DNA adduct levels between the presence and absence of MMA(III) during repair is due to repair inhibition by MMA(III), not due to the effect of MMA(III) on the adduct formation.

Another possibility for this apparent repair inhibition–replication inhibition can also be dismissed. There was no difference in DNA yield between the MMA(III)-treated

group and the control group over time until after 24 h of incubation, when approximately one-third of the amount of DNA obtained from the 24 h controls was harvested from the group incubated with 5  $\mu$ M MMA(III). The cells used were confluent, contact-inhibited normal fibroblasts. Typically, normal fibroblasts have no tendency to undergo apoptosis after DNA damage (30-32); rather, they exhibit only an increase in cellular size resembling large senescent cells (30). In our experiment, we indeed observed some larger cells but no considerable cell detachment in growth media or in media containing 5  $\mu$ M MMA(III) for up to 24 h. The loss of DNA after 24 h of incubation with MMA(III) was probably due to removal of cells with senescence-like changes during three PBS washes. By using almost 100% confluent normal fibroblasts in our experiment, the possibility of cell division was sharply reduced. The absence of DNA replication in confluent normal human foreskin fibroblasts after BPDE treatment at various repair times up to 24 h was clearly shown in the study by Venkatachalam et al. (33). To further confirm that DNA replication inhibition was not responsible for the observed repair inhibition by MMA(III), the cell cycle distribution of confluent CRL2522 cells in the absence or presence of 5  $\mu$ M MMA(III) following BPDE treatment was analyzed by flow cytometry (**Table 4.1**). There was no difference between these two groups nor was there any difference ( $G_1$  or  $G_2/M$ ) over time within each group. Therefore, the repair inhibition we observed was not an artifactual effect from replication inhibition by arsenic, but reflected arsenic modulation of DNA repair.

**Table 4.1. The cell cycle analysis of confluent CRL2522 cells during repair in the presence or absence of 5  $\mu$ M MMA(III) following treatment with 1  $\mu$ M BPDE for 30 min. After the indicated times, cells were subjected to flow cytometry.**

	<b>G<sub>0</sub>/G<sub>1</sub></b>	<b>S</b>	<b>G<sub>2</sub>/M</b>
Control (no treatment)	72	19	9
BPDE	74	18	8
<b>BPDE+MMA(III)</b>			
0.5h -	70	20	10
+	77	12	11
1h -	70	18	12
+	73	19	8
4h -	76	20	4
+	79	21	0
8h -	80	12	8
+	80	11	9
24h -	76	14	10
+	82	7	11

#### 4.3.4 Repair inhibition in exponentially growing cells

By using confluent cells, we observed that arsenic inhibited the repair of BPDE-DNA adducts. We confirmed that this repair inhibition was not due to replication inhibition by arsenic. Other studies of repair inhibition by arsenic, such as the one by Schwerdtle et al. (22), where exponentially growing cells were used, could be confounded by DNA replication. This is because without correction for parental, adduct-containing DNA by density labelling, adduct reduction in exponentially growing cells could be merely the artifact of dilution effects by DNA replication. To further explore this issue, the cell cycle distribution in exponentially growing CRL2522 cells was examined.

To achieve an exponentially growing stage, cells were synchronized by holding confluency for 3 days to bring them to the G<sub>0</sub> phase, as described for the synchronization of human fibroblast cells (34, 35). The cells were split at a ratio of 1:3 and incubated for 18 h to allow the cells to re-enter the G<sub>1</sub> phase. The cells were then treated with 1  $\mu$ M BPDE in serum-free medium for 30 min, followed by replacement with complete medium containing 1  $\mu$ M MMA(III) for 24 h.

Cell cycle profiles are shown in **Figure 4.11** and the percentages of cells in different phases of the cell cycle are tabulated in **Table 4.2**. To the best of our knowledge, this is the first report of the effects of arsenic on the cell cycle distribution following BPDE treatment.

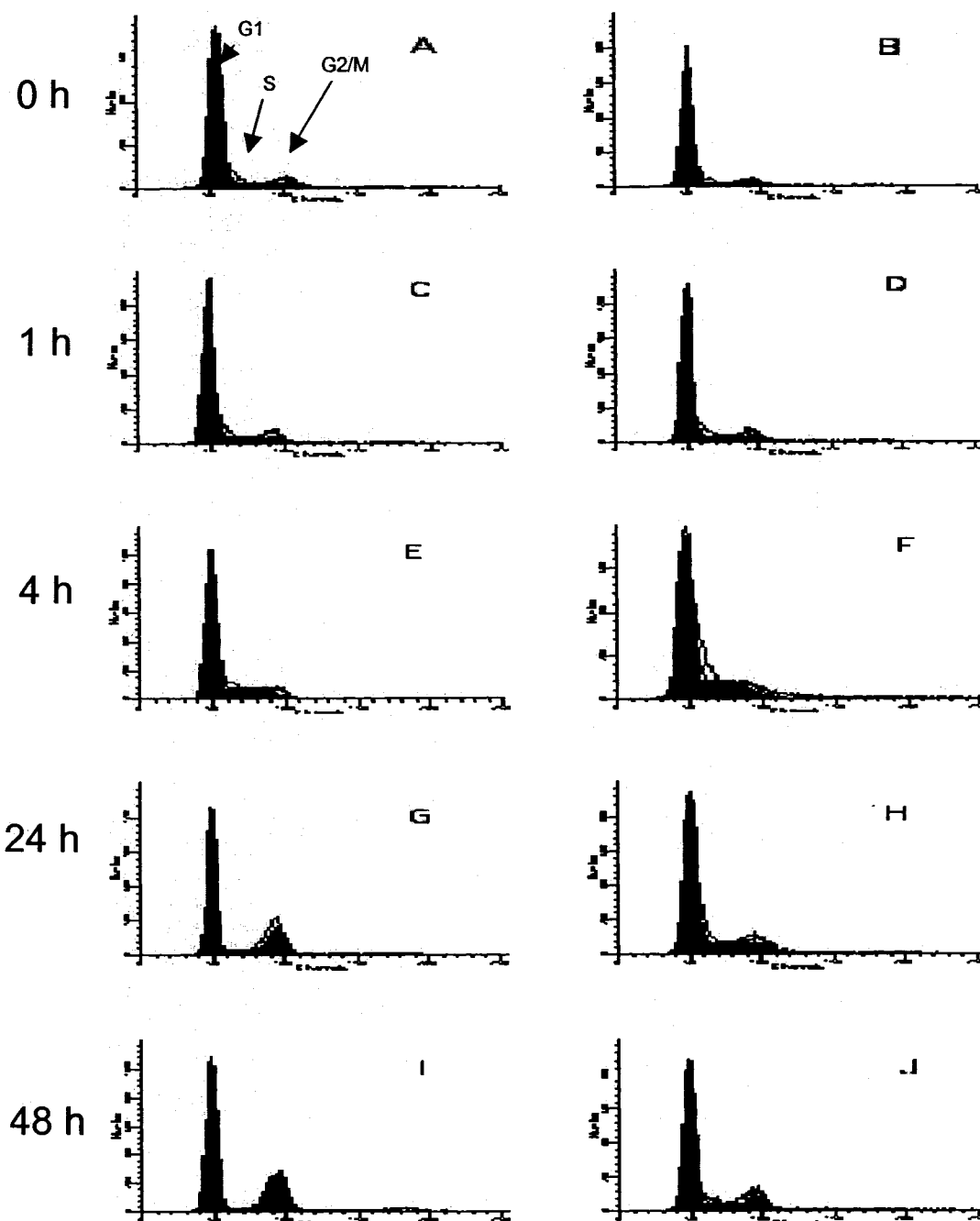


**Figure 4.11.** The cell cycle profiles of BPDE-treated exponentially growing CRL2522 cells for control (A) and cells treated with 1.0  $\mu\text{M}$  BPDE for 30 min (B) and incubated in fresh media in the absence (C, E, G, I) or presence of 1  $\mu\text{M}$  MMA(III) (D, F, H, J) for the indicated times. The cell numbers are plotted on the *y-axis*; the DNA content is plotted on the *x-axis*.

**Table 4.2. Summary of the cell cycle analysis data from Figure 4.11 showing the percentage of cells in G<sub>1</sub>, S and G<sub>2</sub>/M phases. The data represent the means ( $\pm$  SE) of four determinations from two experiments.**

		<b>G<sub>1</sub></b>	<b>S</b>	<b>G<sub>2</sub>/M</b>
Control (no treatment)		81.8 $\pm$ 4.2	12.2 $\pm$ 3.2	6.0 $\pm$ 1.9
BPDE		83.2 $\pm$ 5.8	12.3 $\pm$ 1.2	4.5 $\pm$ 2.2
<b>BPDE+MMA(III)</b>				
1h	-	77.5 $\pm$ 4.4	15.7 $\pm$ 0.8	6.8 $\pm$ 2.1
	+	78.2 $\pm$ 5.1	15.1 $\pm$ 2.2	6.7 $\pm$ 2.4
4h	-	69.6 $\pm$ 3.8	25.6 $\pm$ 2.9	4.8 $\pm$ 2.8
	+	67.2 $\pm$ 4.6	28.8 $\pm$ 3.3	4.0 $\pm$ 1.5
24h	-	62.9 $\pm$ 3.8	15.1 $\pm$ 2.5	22.0 $\pm$ 2.3
	+	67.2 $\pm$ 4.7	23.1 $\pm$ 2.0	9.7 $\pm$ 1.3
48h	-	63.7 $\pm$ 2.1	5.6 $\pm$ 1.5	30.7 $\pm$ 3.4
	+	65.7 $\pm$ 1.3	19.8 $\pm$ 3.6	14.5 $\pm$ 2.3

We found that MMA(III) retarded the release from G<sub>1</sub> arrest caused by BPDE. More obvious retardation would have been expected if recovery time had been allowed after treatment. G<sub>1</sub> arrest caused by treatment for 30 min with 1  $\mu$ M BPDE or for 90 min with 0.5  $\mu$ M BPDE was previously observed in human normal fibroblasts (30, 35). In contrast to arsenic, cadmium was shown to abrogate G<sub>1</sub> arrest caused by BPDE in human fibroblasts (35). Our results suggest that replication inhibition by arsenic may be a concern in Schwerdtle et al.'s study (22). However, the contribution of replication inhibition to the repair inhibition that they observed cannot be assessed, because they

used a different cell line (A549). A very recent study showed that trivalent arsenic overrode the growth arrest caused by UV treatment leading to a concentration-dependent increase in proliferation in primary normal human epidermal keratinocytes (NHEK) cells (36). Therefore, caution should be exercised when interpreting results from DNA repair studies on exponentially growing cells. For an accurate determination, information on cell numbers or direct measurements of cellular DNA replication after prelabelling DNA with [<sup>3</sup>H]thymidine during the periods of repair analysis in exponentially growing cells is needed.

#### **4.3.5 Altered expression of repair-related proteins**

Previous studies suggested that arsenic might not directly inhibit the enzymatic activity of repair proteins. To understand why arsenic inhibited DNA repair in our study, it is reasonable and worthwhile to determine if the expression of repair proteins involved is downregulated by arsenic. Although gene expression profiling after arsenic treatment has been explored in various types of cells (16, 37-48), studies of the protein expression of repair-related genes are rather limited. Complete NER involves the coordinated action of more than 25–30 proteins. It includes two partially overlapping pathways, as shown in **Figure 4.1**. Transcription-coupled repair (TCR) deals with the DNA damage in the transcribed strand of actively transcribing genes whereas global genome repair (GGR) removes lesions from the entire genome, including the non-transcribed strand of active genes. The minimal set of GG-NER components is comprised of XPA, XPC-hHR23B, XPG, RPA, ERCC1-XPF, TFIIH, proliferating cell nuclear antigen (PCNA), pol  $\delta$  or  $\epsilon$ , and DNA ligase I (49). Since our measurement of DNA repair is lesion-removal-based, only the repair proteins that are involved upstream of the dual incision step in GG-NER

are relevant in our study. These proteins and the sequence of their assembly are shown in **Figure 4.12**. So far, only two studies have touched on the expression of the repair genes relevant to our study. In one study, arsenic in drinking water was shown to decrease the mRNA expression of *XPB*, *XPF*, and *ERCC1* but not of *XPA* and *XPG* (48). The other study showed that iAs(III) downregulated the mRNA expression of *XPC* and some other repair-related genes including damage-specific DNA-binding protein 2 (*DDB2*), *pol δ*, *pol ε*, and *p53* but upregulated *p21* (also known as *Waf1*, *Cip1*, or *Sid1*) (16). It should be pointed out that the correlation between mRNA levels and protein levels is usually poor except for the most highly expressed genes and that this correlation was shown to be problematic in cases of NER genes (50).

It is worthwhile to systematically examine all the repair proteins directly involved upstream of the dual incision step in GG-NER, including *XPA*, *XPC*, hHR23B, *ERCC1*, *XPF*, *XPG*, *RPA*, and *TFIIH*; however, it is beyond the scope of this work for practical reasons. Although antibodies to most of those proteins are commercially available and of varying degrees of performance, the fact that *TFIIH* alone has ten subunits means that this undertaking is daunting and expensive. Therefore, only the expressions of three critical proteins that are indispensable for NER incision, *XPA*, *TFIIH* p62 subunit (p62-*TFIIH*), and *XPC*, were examined in our study. In addition, the expression of *p53* and its effector molecule *p21* was also investigated.

As seen in **Figure 4.10**, 5  $\mu$ M MMA(III) did not affect DNA repair until 1 h post-treatment and completely suppressed repair efficiency after 4 h post-treatment. Western blot analysis of proteins was carried out on the time scale up to 4 h, as shown in **Figure 4.13**.

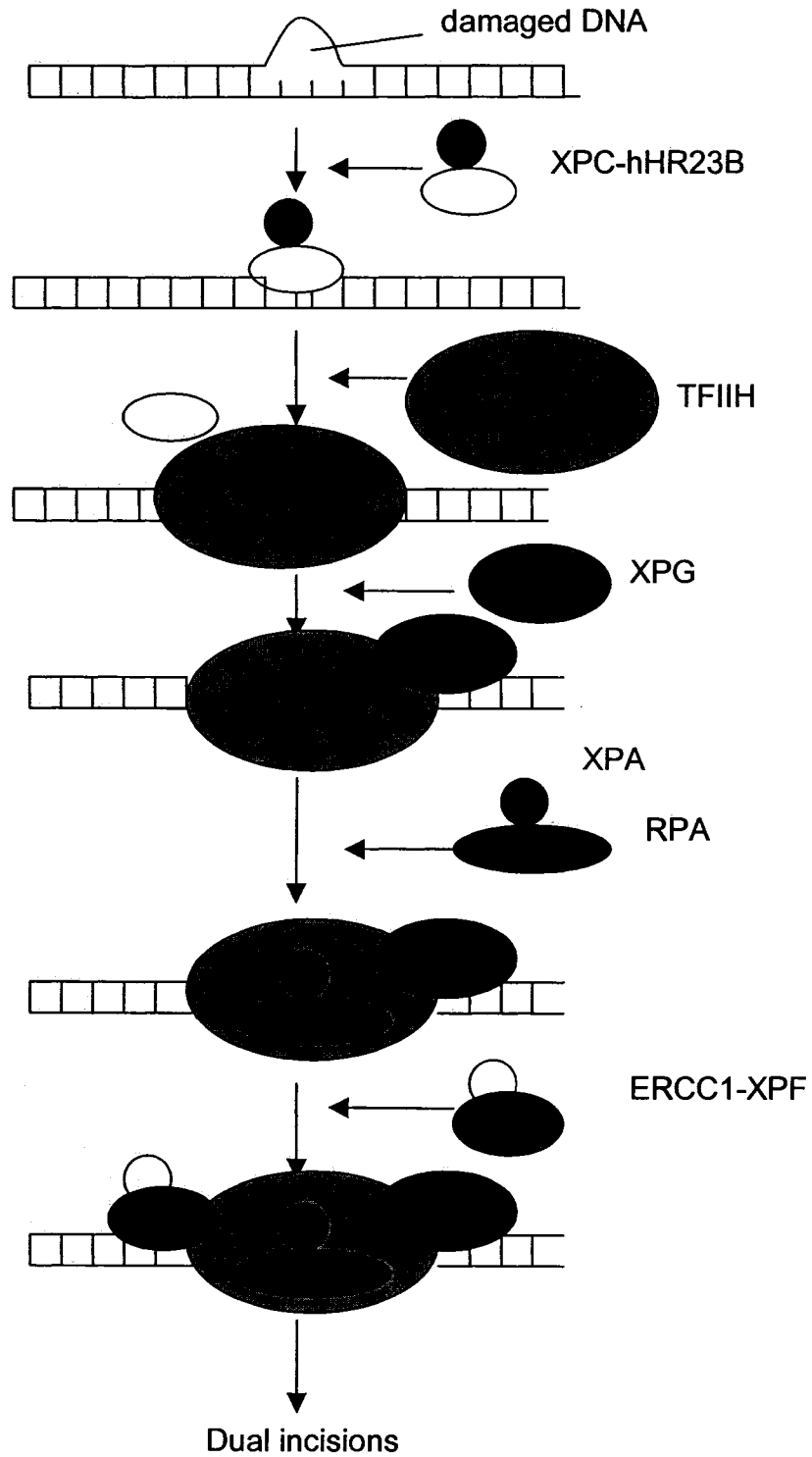
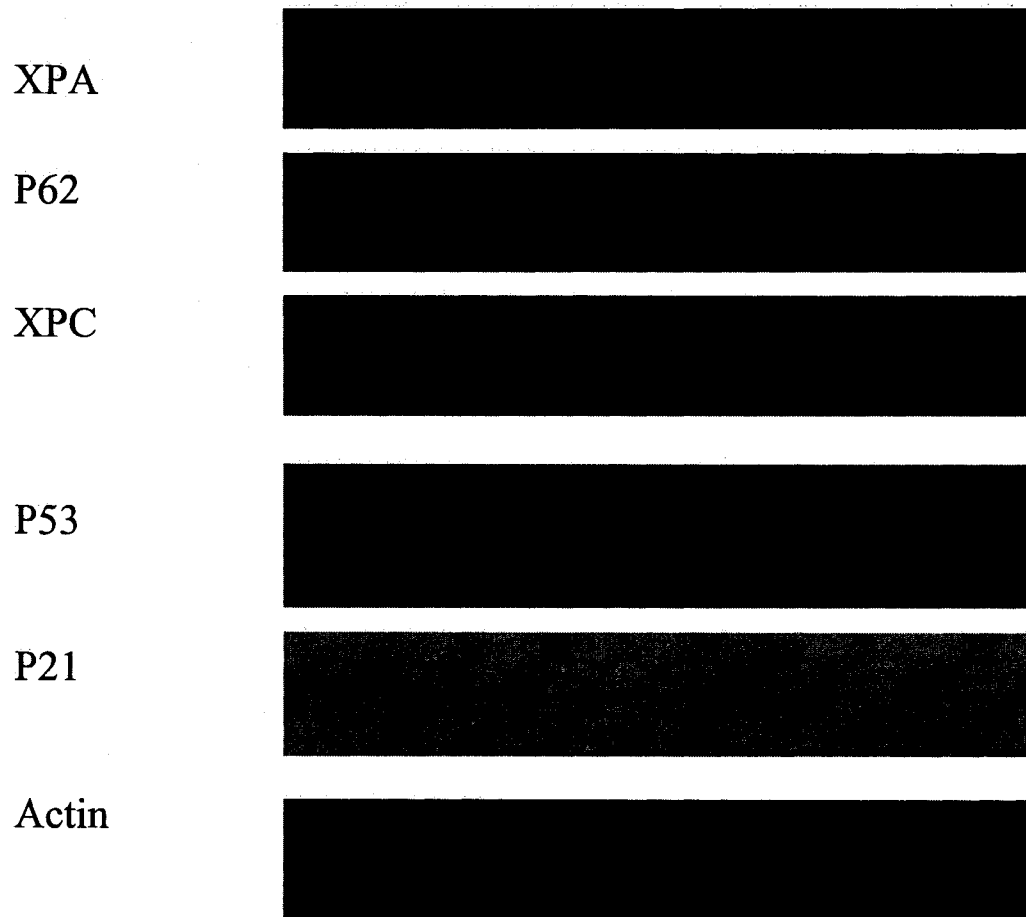


**Figure 4.12. Model of the assembly of the repair proteins involved upstream of GG-NER incision (adapted from [51]).**



Lane	1	2	3	4	5	6
1 $\mu$ M BPDE	-	+	+	+	+	+
5 $\mu$ M MMA(III)	-	-	-	-	+	+
Repair time	control	0 h	1 h	4 h	1 h	4 h

**Figure 4.13. Effects of 5  $\mu$ M MMA(III) on the expression of repair-related proteins XPA, p62, XPC, p53, and p21 during the repair of BPDE-DNA adducts over time.**

As seen in **Figure 4.13**, after BPDE treatment, the expression levels of XPA and p62 remained similar to their basal levels. Moreover, there was no marked difference in the expression levels of XPA and p62 in cells with subsequent repair both in the presence and in the absence of MMA(III). By contrast, BPDE treatment increased p53 expression and led to its accumulation over time up to 4 h post-treatment (the longest repair time period examined). In agreement with Lloyd and Hanawalt's work (27), our observation of p53 induction in confluent contact-inhibited cells indicated that this induction was shared by both confluent and exponentially growing cells wild-type for p53, in which induction of p53 by BPDE in both a dose-dependent and a time-dependent manner has been well-documented (30, 52, 53). It suggests that the induced response of p53 to BPDE treatment is independent of the cell cycle. In the presence of MMA(III), this time-dependent accumulation was markedly reduced and the trend was even reversed. The same effect by MMA(III) on p21 was also observed. This abrogation could not be an artifact resulting from cell death caused by the cytotoxicity of MMA(III), because no significant cell loss was seen within 4 h after BPDE treatment. Although the effect of iAs(III) on p53 expression has been intensively examined by a plethora of studies (54-65), yielding results ranging from increasing expression, decreasing expression, to no effect at all, only marginal efforts have been made to examine the effect of MMA(III) on p53 expression (65). MMA(III) is more toxic than iAs(III) and far more toxic than iAs(V), and it is the most relevant metabolite responsible for toxicity caused by inorganic arsenic (iAs) in human cells. Therefore, to study this single metabolite and its modulation of protein expression may simplify the situation surrounding iAs and reveal the predominant mechanism that is responsible for arsenic toxicity.

When comparing **Figure 4.13** with **Figure 4.10**, we found a striking temporal correlation between DNA repair efficiency and the expression levels of p53, as shown in **Figure 4.14**. The relative repair efficiency refers to the ratio of the percentage of adducts removed in the presence of MMA(III) to that of adducts removed in the absence of MMA(III) at the same time points after BPDE treatment. p53 levels were estimated using Photoshop 7.0 software and the relative p53 level refers to the ratio of the p53 level in the presence of MMA(III) to that in the absence of MMA(III) at the same points after BPDE treatment. This correlation cannot be dismissed as coincidental. Most likely, it suggests that MMA(III) inhibited the global NER of BPDE-DNA adducts via the suppression of p53 expression. p53, as a tumor suppressor, is known to play an important role in cell-cycle control, apoptosis, and control of DNA repair. There is accumulating evidence for a role of p53 in NER (27, 29, 52,53, 66-77). However, the precise molecular mechanism for p53 involvement is not completely understood. It has been suggested that p53 may regulate NER through transcriptional activation of downstream NER genes (78-86), through modulating chromatin accessibility of damaged DNA (87,88), or through protein-protein interactions to alter the activity of NER gene products (89-93).

Although there were relatively high basal levels for XPA and p62 in CRL2522 cells, the basal level for XPC was extremely low. This constitutively low expression of XPC was also observed in some other studies (82, 94). High levels of XPC were shown to be toxic and can interfere with other vital processes like DNA metabolism (94). Keeping XPC at low levels may reduce the untargeted repair of normally occurring DNA conformations, which might resemble DNA lesions. In agreement with Adimoolam et al.'s work (82), our study showed that XPC expression was inducible in a very weak p53-

dependent manner. After 4 h following BPDE treatment in the absence of MMA(III), XPC was highly induced, in parallel with the highest expression of p53 at that time point (**Figure 4.13**). The inducible response was presumably intended to replenish the levels of the repair protein degraded during the repair process, to ensure maintenance of the lesion repair process, and direct the slow kinetics of GG-NER (95,96). However, in both Adimoolam et al.'s and our studies, XPC induction took a longer time when most of the repair had been initiated and completed. Therefore, it seemed that the regulatory role of p53 in NER might not be via the induction of XPC, although our results gave the impression that MMA(III) inhibited NER through p53-mediated XPC downregulation. Most likely, the role of p53 on NER is through the recruitment of NER proteins like XPC and TFIIH (97-100).

In our study we also observed that p21 was induced following BPDE treatment and abrogated by MMA(III), following exactly the same trend as p53 (**Figure 4.13**). Because p21 is a downstream effector molecule for p53 action, our study indicated that p53 is still transcriptionally active and therefore its wild type conformation remained intact even in the presence of MMA(III). The suppression of p21 by MMA(III) was probably through the depletion of p53. The fact that p21 can sequester PCNA, a DNA polymerase processivity factor that is essential for NER, led to studies revealing the potential involvement of p21 in NER (101, 102). However, the role of p21 in DNA repair is still controversial but an increasing body of evidence appears to favour a negative role or even no involvement of p21 in NER (84, 101-114). Our results could not confirm or negate the inhibitory role of p21 in NER, because we used an immunoassay to detect global genomic repair.

Taken together, our studies suggested that MMA(III) inhibited the repair of BPDE-DNA adducts through abrogating the accumulation of p53 induced by BPDE treatment. Our results implied that the p53 protein conformation and DNA-binding activity were not functionally affected. However, this p53-dependent abrogation of p21 in confluent cells did not translate into an overriding of G1/S arrest induced by BPDE in exponentially growing counterparts, implying that cell cycle modulation was not relevant to repair inhibition by MMA(III). Therefore, we suggest that this abrogation may be due to destabilization of p53 by means of inhibition of PARP activity by MMA(III). Poly(ADP-ribosylation) of p53 was indicated to be an important factor in stabilizing p53 levels after BPDE treatment (30, 115) and increased PARP activity was observed during repair of BPDE-DNA adducts (116). In addition, iAs(III) was shown to be able to inhibit PARP activity (13, 15), although it remains to be seen whether MMA(III) has such a capability. In support of our suggestion, cells lacking PARP had defective induction but normal activation and function of p53 (117).

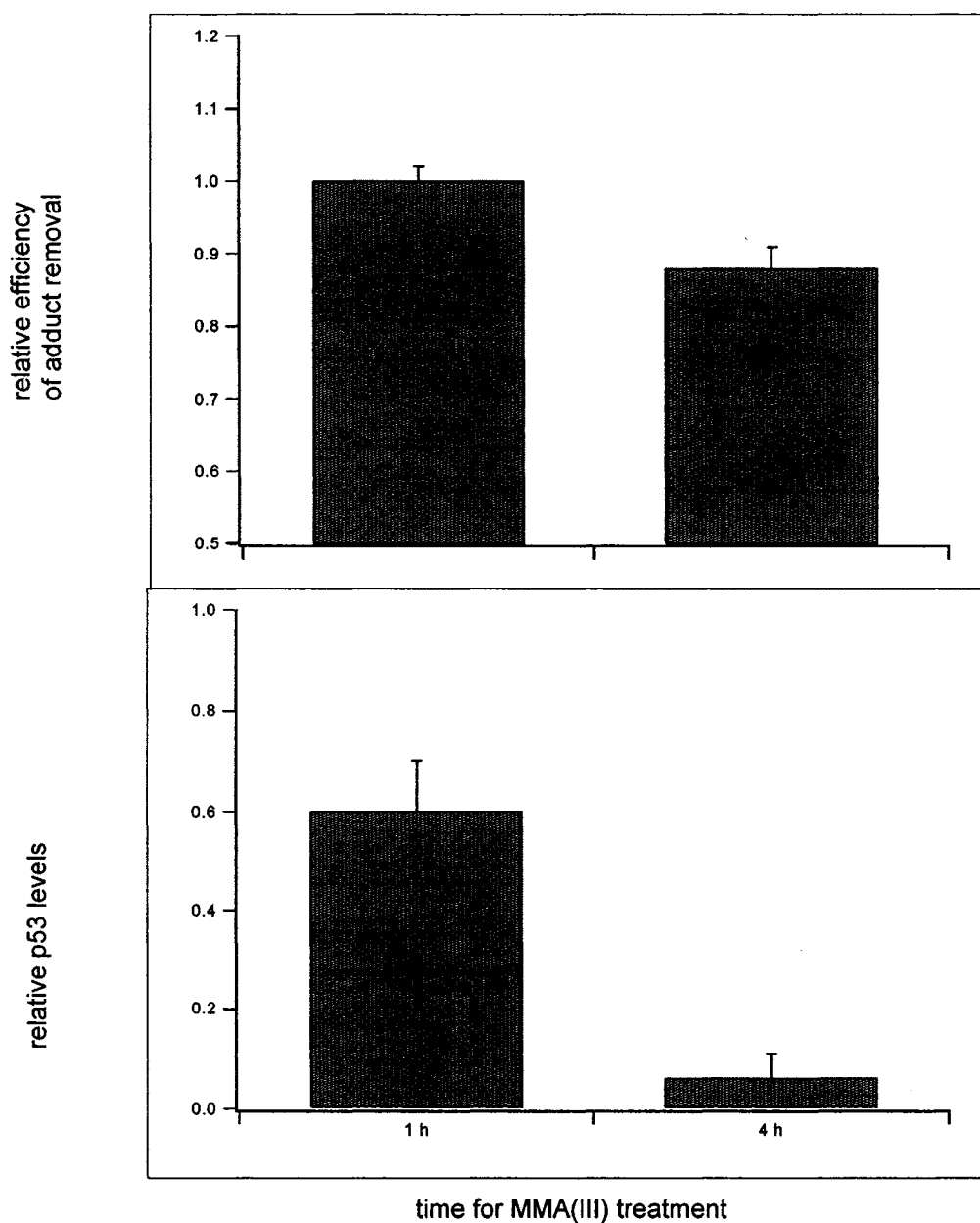


**Figure 4.14. Temporal correlation between p53 levels and DNA repair efficiency after MMA(III) treatment. The percentage of adducts removed in the presence of MMA(III) was divided by that of adducts removed in the absence of MMA(III) at the same time point and the ratio was referred to as the relative repair efficiency. p53 expression levels were estimated and the relative p53 level refers to the ratio of the p53 level in the presence of MMA(III) to that in the absence of MMA(III) at the same time point. Error bars indicate the standard deviation of four determinations from two experiments.**

#### 4.4 Conclusions

By use of confluent human normal fibroblasts we demonstrated that each of the six arsenic species has the capability of inhibiting the repair of BPDE-DNA adducts with a descending order of potency of MMA(III)>DMA(III)>iAs(III)>iAs(V)>DMA(V)≈MMA(V). MMA(III), the most relevant metabolite of iAs, was shown to sharply attenuate the accumulation of p53 induced by BPDE treatment. The comparison of the p53 expression level and DNA repair efficiency revealed a striking temporal correlation between these two. Our study suggested that arsenic inhibited the excision repair via modulation of p53 induction in response to DNA damage. Therefore, for the first time, we have linked arsenic with DNA repair inhibition through p53, an intensively studied repair-related protein with a well-established role in NER. However, the general question of how p53 is involved in NER remains unresolved. Further mechanistic studies in that respect will facilitate our understanding of the underlying mechanism of arsenic carcinogenesis through DNA repair inhibition.

## 4.5 References

1. Rossman TG. (1981) Enhancement of UV-mutagenesis by low concentrations of arsenite in *E. coli*. *Mutat Res*, 91, 207-211
2. Okui T and Fujiwara Y. (1986) Inhibition of human excision DNA repair by inorganic arsenic and the co-mutagenic effect in V79 Chinese hamster cells. *Mutat Res*, 172, 69-76
3. Snyder RD, Davis GF, and Lachmann PJ. (1989) Inhibition by metals of X-ray and ultraviolet-induced DNA repair in human cells. *Biol Trace Element Res*, 21, 389-398
4. Lee-Chen SF, Gurr JR, Lin IB, Jan KY. (1993) Arsenite enhances DNA double-strand breaks and cell killing of methylmethanesulfonate-treated cells by inhibiting the excision of alkali-labile sites. *Mutat Res*, 294, 21-28
5. Lee-Chen SF, Yu CT, Jan KY. (1992) Effect of arsenite on the DNA repair of UV-irradiated Chinese hamster ovary cells. *Mutagenesis*, 7, 51-55
6. Li J-H, Rossman TG. (1991) Comutagenesis of sodium arsenite with ultraviolet radiation in Chinese hamster V79 cells. *Biol Met*, 4, 197-200
7. Li J-H and Rossman TG. (1989) Mechanism of comutagenesis of sodium arsenite with N-methyl-N-nitrosourea. *Biol Trace Elem Res*, 21, 373-381
8. Li J-H, Rossman TG. (1989) Inhibition of DNA ligase activity by arsenite: a possible mechanism of its comutagenesis. *Mol Toxicol*, 2, 1-9
9. Hu Y, Su L, Snow ET. (1998) Arsenic toxicity is enzyme specific and its effects on ligation are not caused by the direct inhibition of DNA repair enzymes. *Mutat Res*, 408, 203-218

10. Li J-H. (1989) The molecular mechanism of arsenic carcinogenesis [PhD Thesis].  
New York University.
11. Hartwig A, Groblinghoff UD, Beyersmann D, Natarajan AT, Filon R, Mullenders LHF. (1997) Interaction of arsenic(III) with nucleotide excision repair in UV-irradiated human fibroblasts. *Carcinogenesis*, 18, 399-405
12. Asmuss M, Mullenders LH, Eker A, Hartwig A. (2000) Differential effects of toxic metal compounds on the activities of Fpg and XPA, two zinc finger proteins involved in DNA repair. *Carcinogenesis*, 21, 2097-2104
13. Hartwig A, Pelzer A, Asmuss M and Burkle A. (2003) Very low concentrations of arsenite suppress poly(ADP-ribosyl)ation in mammalian cells. *Int J Cancer*, 104, 1-6
14. Lynn S, Shiung JN, Gurr JR and Jan KY. (1998) Arsenite stimulates poly(ADP-ribosylation) by generation of nitric oxide. *Free Radical Biol Med*, 24, 442-449
15. Yager JW, Wiencke JK. (1997) Inhibition of poly(ADP-ribose) polymerase by arsenite. *Mutat Res*, 386, 345-351
16. Hamadeh HK, Trouba KJ, Amin RP, Afshari CA, Germolec D. (2002) Coordination of altered DNA repair and damage pathways in arsenic-exposed keratinocytes. *Toxicol Sci*, 69, 306-316
17. Clewell HJ, Gentry PR, Barton HA, Shipp AM, Yager JW, Andersen ME. (1998) Requirements for a biologically realistic cancer risk assessment for inorganic arsenic. *Int J Toxicol*, 18, 1-17
18. Hoeijmakers JHJ. (2001) Genome maintenance mechanisms for preventing cancer. *Nature*, 411, 366-374

19. Tran H-P, Prakash AS, Barnard R, Chiswell B, Ng JC. (2002) Arsenic inhibits the repair of DNA damage induced by benzo(a)pyrene. *Toxicol Lett*, 133, 59-67
20. Hartmann A and Speit G. (1996) Effect of arsenic and cadmium on the persistence of mutagen-induced DNA lesions in human cells. *Environ Mol Mutagen*, 27, 98-104
21. Maier A, Schumann BI, Chang X, Talaska G, Puga A. (2002) Arsenic co-exposure potentiates benzo[a]pyrene genotoxicity. *Mutat Res*, 517, 101-111
22. Schwerdtle T, Walter I, Hartwig A. (2003) Arsenite and its biomethylated metabolites interfere with the formation and repair of stable BPDE-induced DNA adducts in human cells and impair XPAzf and Fpg. *DNA repair*, 2, 1449-1463
23. Ochi T, Ishiguro T, Ohsawa M. (1986) Induction of alkaline-labile sites in DNA by benzo(a)pyrene and the repair of those lesions in cultured Chinese hamster cells. *Mutat Res*, 165, 31-38
24. Dong J-T and Luo X-M. (1993) Arsenic-induced DNA strand breaks associated with DNA-protein crosslinks in human fetal lung fibroblasts. *Mutat Res*, 302, 97-102
25. Kootstra A. (1982) Formation and removal of B[a]P diol epoxide-DNA adducts in human fibroblasts. *Carcinogenesis*, 3, 953-955
26. Kootstra A. (1986) The dynamics of chromatin carcinogen interactions in human cells. *Nucleic Acid Res*, 14, 9897-9909
27. Lloyd DR and Hanawalt PC. (2000) p53-dependent global genomic repair of benzo[a]pyrene-7,8-diol-9,10-epoxide adducts in human cells. *Cancer Res*, 60, 517-521
28. Luch A, Kudla K, Seidel A, Doehmer J, Greim H and Baird WM. (1999) The level of DNA modification by (+)-syn-(11S, 12R, 13S, 14R)- and (-)-anti-(11R, 12S, 13S,

- 14R)-dihydrodiol epoxides of dibenzo[a,l]pyrene determined by the effect on proteins p53 and p21<sup>WAF1</sup> in the human mammary carcinoma cell line MCF-7. *Carcinogenesis*, 20, 859-865
29. Lloyd DR and Hanawalt PC. (2002) p53 controls global nucleotide excision repair of low levels of structurally diverse benzo(g)chrysene-DNA adducts in human fibroblasts. *Cancer Res*, 62, 5288-5294
30. Venkatachalam S, Denissenko M and Wani AA. (1997) Modulation of (±)-anti-BPDE mediated p53 accumulation by inhibitors of protein kinase C and poly(ADP-ribose) polymerase. *Oncogene*, 14, 801-809
31. Canman CE, Chen C-Y, Lee M-H and Kastan MB. (1994) DNA damage responses: p53 induction, cell cycle perturbations and apoptosis. *Cold Spring Harbor Symp Quant Biol*, 59, 277-286
32. Di Leonardo A, Linke SP, Clarkin K and Wahl GM. (1994) DNA damage triggers a prolonged p53-dependent G<sub>1</sub> arrest and long-term induction of Cip1 in normal human fibroblasts. *Genes Dev*, 8, 2540-2551
33. Venkatachalam S, Denissenko M and Wani AA. (1995) DNA repair in human cells: quantitative assessment of bulky anti-BPDE-DNA adducts by non-competitive immunoassays. *Carcinogenesis*, 16, 2029-2036
34. Mahadevan B, Luch A, Seidel A, Pelling JC and Baird WM. (2001) Effects of the (-)-anti-11R, 12S-dihydrodiol 13S, 14R-epoxide of dibenzo[a,l]pyrene on DNA adduct formation and cell cycle arrest in human diploid fibroblasts. *Carcinogenesis*, 22, 161-169

35. Mukherjee JJ, Gupta SK, Kumar S and Sikka HC. (2004) Effects of cadmium(II) on ( $\pm$ )-anti-benzo[a]pyrene-7,8-diol-9,10-epoxide-induced DNA damage response in human fibroblasts and DNA repair: a possible mechanism of cadmium's cogenotoxicity. *Chem Res Toxicol*, 17, 287-293
36. Mudipalli A, Owen RD, Preston RJ. (2005) The effect of arsenicals on ultraviolet-radiation-induced growth arrest and related signaling events in human keratinocytes. *Int J Oncol*, 27, 769-77
37. Zheng XH, Watts GS, Vaught S, Gandolfi AJ. (2003) Low-level arsenite induced gene expression in HEK293 cells. *Toxicology*, 187, 39-48
38. Trouba KJ, Geisenhoffer KM and Germolec DR. (2002) Sodium arsenite-induced stress-related gene expression in normal human epidermal, HaCaT, and HEL30 keratinocytes. *Environ Health Perspect*, 110 (Suppl 5), 761-766
39. Schuliga M, Chouchane S and Snow ET. (2002) Upregulation of glutathione-related genes and enzyme activities in cultured human cells by sublethal concentrations of inorganic arsenic. *Toxicol Sci*, 70, 183-192
40. Yih L-H, Peck K and Lee TC. (2002) Changes in gene expression profiles of human fibroblasts in response to sodium arsenite treatment. *Carcinogenesis*, 23, 867-876
41. Beyersmann D. (2002) Effects of carcinogenic metals on gene expression. *Toxicol Lett*, 127, 63-68
42. Liu J, Kadiiska MB, Liu Y, Lu T, Qu W, Waalkes MP. (2001) Stress-related gene expression in mice treated with inorganic arsenicals. *Toxicol Lett*, 61, 314-320
43. Ahn WS, Bae SM, Lee KH, Kim YW, Lee JM, Namkoong SE, Lee IP, Kim CK, Seo JS, Sin JI, Kim YW. (2004) Comparison of effects of As<sub>2</sub>O<sub>3</sub> and As<sub>4</sub>O<sub>6</sub> on cell

- growth inhibition and gene expression profiles by cDNA microarray analysis in SiHa cells. *Oncol Rep*, 12, 573-580
44. Burnichon V, Jean S, Bellon L, Maraninchi M, Bideau C, Orsiere T, Margotat A, Gerolami V, Botta A, Berge-Lefranc JL. (2003) Patterns of gene expressions induced by arsenic trioxide in cultured human fibroblasts. *Toxicol Lett*, 143, 155-162
45. Tully DB, Collins BJ, Overstreet JD, Smith CS, Dinse GE, Mumtaz MM and Chapin RE. (2000) Effects of arsenic, cadmium, chromium, and lead on gene expression regulated by a battery of 13 different promoters in recombinant HepG2 cells. *Toxicol Appl Pharmacol*, 168, 79-90
46. Sen B, Wang A, Hester SD, Rebertson JL, Wolf DC. (2005) Gene expression profiling of responses to dimethylarsinic acid in female F344 rat urothelium. *Toxicology*, 215, 214-226
47. Bae DS, Hanneman WH, Yang RSH and Campain JA. (2002) Characterization of gene expression changes associated with MNNG, arsenic, or metal mixture treatment in human keratinocytes: application of cDNA microarray technology. *Environ Health Perspect*, 110 (Suppl 6), 931-941
48. Andrew AS, Karagas MR and Hamilton JW. (2003) Decreased DNA repair gene expression among individuals exposed to arsenic in United States drinking water. *Int J Cancer*, 104, 263-268
49. Araujo SJ, Tirode F, Colin F, Pospiech H, Syvaioja JE, Stucki M, Hubscher U, Egly JM, Wood RD. (2000) Nucleotide excision repair of DNA with recombinant human proteins: definition of the minimal set of factors, active forms of TFIIH, and modulation by CAK. *Genes Dev*, 14, 349-359

50. Vogel U, Dybdahl M, Frentz G, Nexø BA. (2000) DNA repair capacity: inconsistency between effect of over-expression of five NER genes and the correlation to mRNA levels in primary fibroblasts. *Mutat Res*, 461, 197-210
51. Volker M, Mone MJ, Karmakar P, van Hoffen A, Schul W, Vermeulen W, Hoeijmakers JHJ, van Driel R, van Zeeland AA and Mullenders LHF. (2001) Sequential assembly of the nucleotide excision repair factors in vivo. *Mol Cell*, 8, 213-224
52. Wani MA, El-Mahdy M, Hamada EM, Wani G, Zhu Q, Wang Q and Wani AA. (2002) Efficient repair of bulky anti-BPDE DNA adducts from non-transcribed DNA strand requires functional p53 but not p21<sup>waf1/cip1</sup> and pRb. *Mutat Res*, 505, 13-25
53. Wani MA, Zhu QZ, El-Mahdy M, Venkatachalam S and Wani AA. (2000) Enhanced sensitivity to anti-benzo(a)pyrene-diol-epoxide DNA damage correlates with decreased global genomic repair attributable to abrogated p53 function in human cells. *Cancer Res*, 60, 2273-2280
54. Salazar AM, Ostrosky-Wegman P, Menendez D, Miranda E, Garcia-Carranca A, Rojas E. (1997) Induction of p53 protein expression by sodium arsenite. *Mutat Res*, 381, 259-265
55. Yih LH, Lee TC. (2000) Arsenite induces p53 accumulation through an ATM-dependent pathway in human fibroblasts. *Cancer Res*, 60, 6346-6352
56. Yih LH, Ho IC and Lee TC. (1997) Sodium arsenite disturbs mitosis and induces chromosome loss in human fibroblasts. *Cancer Res*, 57, 5051-5059

57. Yih LH and Lee TC. (1999) Effects of exposure protocols on induction of kinetochore-plus and -minus micronuclei by arsenite in diploid human fibroblasts. *Mutat Res*, 440, 75-82
58. Hamadeh HK, Vargas M, Lee E, Menzel DB. (1999) Arsenic disrupts cellular levels of p53 and mdm2: a potential mechanism of carcinogenesis. *Biochem Biophys Res Commun*, 263, 446-449
59. Hernandez-Zavala A, Cordova E, Del Razo LM, Cebrian ME, Garrido E. (2005) Effects of arsenite on cell cycle progression in a human bladder cancer cell line. *Toxicology*, 207, 49-57
60. Shen L, Chen TX, Wang YP, Lin Z, Zhao HJ, Zu YZ, Wu G, Ying DM. (2000) As<sub>2</sub>O<sub>3</sub> induces apoptosis of the human B lymphoma cell line MBC-1. *J Biol Regul Homeost Agents*, 14, 116-119
61. Zhao S, Tsuchida T, Kawakami K, Shi C, Kawamoto K. (2002) Effect of As<sub>2</sub>O<sub>3</sub> on cell cycle progression and cyclins D1 and B1 expression in two glioblastoma cell lines differing in p53 status. *Int J Oncol*, 21, 49-55
62. Jiang XH, Wong BC, Yuen ST, Jiang SH, Cho CH, Lai KC, Lin MC, Kung HF, Lam SK. (2001) Arsenic trioxide induces apoptosis in human gastric cancer cells through up-regulation of p53 and activation of caspase-3. *Int J Cancer*, 91, 173-179
63. Vogt BL, Rossman TG. (2001) Effects of arsenite on p53, p21 and cyclin D expression in normal human fibroblasts—a possible mechanism for arsenite's comutagenicity. *Mutat Res*, 478, 159-168

64. Huang C, Ma MY, Li J, Dong Z. (1999) Arsenic induces apoptosis through a c-Jun NH2-terminal kinase-dependent, p53-independent pathway. *Cancer Res*, 59, 3053-3058
65. Filippova M and Duerksen-Hughes PJ. (2003) Inorganic and dimethylated arsenic species induce cellular p53. *Chem Res Toxicol*, 16, 423-431
66. McKay BC, Ljungman M and Rainbow AJ. (1999) Potential roles of p53 in nucleotide excision repair. *Carcinogenesis*, 20, 1389-1396
67. Wani MA, Zhu QZ, El-Mahdy M and Wani AA. (1999) Influence of p53 tumor suppressor protein on bias of DNA repair and apoptotic response in human cells. *Carcinogenesis*, 20, 765-772
68. El-Mahdy MA, Hamada FM, Wani MA, Zhu QZ and Wani AA. (2000) P53-degradation by HPV-16 E6 preferentially affects the removal of cyclobutane pyrimidine dimers from non-transcribed strand and sensitizes mammary epithelial cells to UV-irradiation. *Mutat Res (DNA Repair)*, 459, 135-145
69. Zhu Q, Wani MA, El-Mahdy M and Wani AA. (2000) Decreased DNA repair efficiency by loss or disruption of p53 function preferentially affects removal of cyclobutane pyrimidine dimers from non-transcribed strand and slow repair sites in transcribed strand. *J Biol Chem*, 275, 11492-11497
70. Ford JM, Baron El and Hanawalt PC. (1998) Human fibroblasts expressing the human papillomavirus E6 gene are deficient in global genomic nucleotide excision repair and sensitive to ultraviolet irradiation. *Cancer Res*, 58, 599-063

71. Ford JM and Hanawalt PC. (1995) Li-Fraumeni syndrome fibroblasts homozygous for p53 mutations are deficient in global DNA repair but exhibit normal transcription coupled repair and enhanced UV resistance. *Proc Natl Acad Sci USA*, 92, 8876-8880
72. Bowman KK, Sicard DM, Ford JM and Hanawalt PC. (2000) Reduced global genomic repair of ultraviolet light-induced cyclobutane pyrimidine dimers in simian virus 40-transformed human cells. *Mol Carcinog*, 29, 17-24
73. Ford JM and Hanawalt PC. (1997) Expression of wild-type p53 is required for efficient global genomic nucleotide excision repair in UV-irradiated human fibroblasts. *J Biol Chem*, 272, 28073-28080
74. Swaminathan S, Torino JL and Burger MS. (2002) Human urinary bladder epithelial cells lacking wild-type p53 function are deficient in the repair of 4-aminobiphenyl-DNA adducts in genomic DNA. *Mutat Res*, 499, 103-117
75. Torino JL, Burger MS, Reznikoff CA, Swaminathan S. (2001) Role of TP53 in repair of N-(deoxyguanosin-8-yl)-4-aminobiphenyl in human transitional cell carcinoma of the urinary bladder. *Carcinogenesis*, 22, 143-154
76. Therrien JP, Drouin R, Baril C and Drobetsky EA. (1999) Human cells compromised for p53 function exhibit defective global and transcription-coupled nucleotide excision repair, whereas cells compromised for pRb function are defective only in global repair. *Proc Natl Acad Sci USA*, 96, 15038-15043
77. Smith ML, Chen IT, Zhan Q, O'Connor PM, Fornace AJ. (1995) Involvement of the p53 tumor suppressor in repair of u.v.-type DNA damage. *Oncogene*, 10, 1053-1059

78. Kastan MB, Zhan Q, El-Deiry WS, Carrier F, Jacks T, Walsh WV, Plunkett BS, Vogelstein B, Fornace AJ. (1992) A mammalian cell cycle checkpoint pathway utilizing p53 and GADD45 is defective in ataxia-telangiectasia. *Cell*, 71, 587-597
79. Hwang BJ, Ford JM, Hanawalt PC, Chu G. (1999) Expression of the p48 xeroderma pigmentosum gene is p53-dependent and is involved in global genomic repair. *Proc Natl Acad Sci USA*, 96, 424-428
80. Itoh T, O'Shea C and Linn S. (2003) Impaired regulation of tumor suppressor p53 caused by mutations in the xeroderma pigmentosum DDB2 gene: mutual regulatory interaction between p48 (DDB2) and p53. *Mol Cell Biol*, 23, 7540-7553
81. Tan T, Chu G. (2002) p53 binds and activates the xeroderma pigmentosum DDB2 gene in human but not mice. *Mol Cell Biol*, 22, 3247-3254
82. Adimoolam S, Ford JM. (2002) p53 and DNA damage-inducible expression of the xeroderma pigmentosum group C gene. *Proc Natl Acad Sci USA*, 99, 12985-12990
83. Smith ML, Chen IT, Zhan Q, Bae I, Chen CY, Gilmer TM, Kastan MB, O'Connor PM and Fornace AJ. (1994) Interaction of the p53-regulated protein Gadd45 with proliferating cell nuclear antigen. *Science*, 266, 1376-1380
84. Smith ML, Ford JM, Hollander MC, Bortnick RA, Amundson SA, Seo YR, Deng CX, Hanawalt PC, Fornace AJ. (2000) P53-mediated DNA repair responses to UV radiation: studies of mouse cells lacking p53, p21, and/or GADD45 genes. *Mol Cell Biol*, 20, 3705-3714
85. Shivakumar CV, Brown DR, Deb S and Deb SP. (1995) Wild-type p53 transactivates the human proliferating cell nuclear antigen promoter. *Mol Cell Biol*, 15, 6785-6793

86. Amundson SA, Patterson A, Do KT, Fornace AJ. (2002) A nucleotide excision repair master-switch: p53 regulated coordinated induction of global genomic repair genes. *Cancer Biol Ther*, 1, 145-149
87. Rubbi CP, Milner J. (2003) p53 is a chromatin accessibility factor for nucleotide excision repair of DNA damage. *EMBO J*, 22, 975-986
88. Datta A, Bagchi S, Nag A, Shiyanov P, Adami GR, Yoon T, Raychaudhuri P. (2001) The p48 subunit of the damaged-DNA binding protein DDB associated with the CBP/p300 family of histone acetyltransferase. *Mutat Res*, 486, 89-97
89. Wang XW, Yeh H, Schaeffer L, Roy R, Moncollin V, Egly JM, Wang Z, Freidberg EC, Evans MK, Taffe BG. (1995) p53 modulation of TFIIH-associated nucleotide excision repair activity. *Nat Genet*, 10, 188-195
90. Dutta A, Ruppert JM, Aster JC, Winchester E. (1993) Inhibition of DNA replication factor RPA by p53. *Nature*, 365, 79-83
91. Leveillard T, Andrea L, Bissonnette N, Schaeffer L, Bracco L, Egly JM, Wasyluk B. (1996) Functional interactions between p53 and TFIIH complex are affected by tumour-associated mutations. *EMBO J*, 15, 1615-1624
92. Marmorstein LH, Ouchi T and Aaronson SA. (1998) The BRAC2 gene product functionally interacts with p53 and RAD51. *Proc Natl Acad Sci USA*, 95, 13869-13874
93. Zhang H, Somasundaram K, Peng Y, Tian H, Zhang H, Bi D, Weber BL and El-Deiry WS. (1998) BRAC1 physically associated with p53 and stimulates its transcriptional activity. *Oncogene*, 16, 1713-1721

94. Ng JM, Vermeulen W, van der Horst GT, Bergink S, Sugasawa K, Vrieling H and Hoeijmakers JHJ. (2003) A novel regulation mechanism of DNA repair by damage-induced and RAD23-dependent stabilization of xeroderma pigmentosum group C protein. *Genes Dev*, 17, 1630-1645
95. Adimoolam S, Ford JM. (2003) p53 and regulation of DNA damage recognition during nucleotide excision repair. *DNA Repair*, 2, 947-954
96. Ford JM. (2005) Regulation of DNA damage recognition and nucleotide excision repair: another role for p53. *Mutat Res*, 577, 195-202
97. Wang QE, Zhu MA, Wani MA, Wani G, Chen J, Wani AA. (2003) Tumor suppressor p53 dependent recruitment of nucleotide excision repair factors XPC and TFIIH to DNA damage. *DNA Repair*, 2, 483-499
98. Wang QE, Zhu Q, Wani G, Chen J and Wani AA. (2004) UV radiation-induced XPC translocation within chromatin is mediated by damaged-DNA binding protein, DDB2. *Carcinogenesis*, 25, 1033-1043
99. Fitch ME, Cross IV, Ford JM. (2003) p53 responsive nucleotide excision repair gene products p48 and XPC, but not p53, localize to sites of UV-irradiated-induced DNA damage, in vivo. *Carcinogenesis*, 24, 843-850
100. Fitch ME, Nakajima S, Yasui A, Ford JM. (2003) In vivo recruitment of XPC to UV-induced cyclobutane pyrimidine dimers by the DDB2 gene product. *J Biol Chem*, 278, 46906-46910
101. Li R, Waga S, Hannon GJ, Beach D, Stillman B. (1996) Differential effects by the p21 CDK inhibitor on PCNA-dependent DNA replication. *Nature*, 371, 534-537

102. Shivji MK, Grey SJ, Strausfeld UP, Wood RD, Blow JJ. (1994) Cip inhibits DNA replication but not PCNA-dependent nucleotide excision repair. *Curr Biol*, 4, 1062-1068
103. Chen J, Chen S, Saha P and Dutta A. (1996) p21<sup>Cip1</sup>/Waf1 disrupts the recruitment of human Fen1 by proliferating-cell nuclear antigen into the DNA replication complex. *Proc Natl Acad Sci USA*, 93, 11597-11602
104. Wani MA, Wani G, Yao J, Zhu Q and Wani AA. (2002) Human cells deficient in p53 regulated p21<sup>waf1/cip1</sup> expression exhibit normal nucleotide excision repair of UV-induced DNA damage. *Carcinogenesis*, 23, 403-410
105. Shivji MK, Ferrari E, Ball K, Hubscher U and Wood RD. (1998) Resistance of human nucleotide excision repair synthesis in vitro to p21<sup>Cdn1</sup>. *Oncogene*, 17, 2827-2838
106. Maeda T, Espino RA, Chomey EG, Luong L, Bano A, Meakins D and Tron VA. (2005) Loss of p21<sup>WAF1/Cip1</sup> in Gadd45-deficient keratinocytes restores DNA repair capacity. *Carcinogenesis*, 26, 1804-1810
107. Pan ZQ, Reardon JT, Li L, Flores-Rozas H, Legerski R, Sancar A, Hurwitz J (1995). Inhibition of nucleotide excision repair by the cyclin-dependent kinase inhibitor p21. *J Biol Chem*, 270, 22008-22016
108. Sheikh MS, Chen YQ, Smith ML, Fornace AJ, (1997) Role of p21<sup>waf1/cip1/sd1</sup> in cell death and DNA repair as studied using a tetracycline-inducible system in p53-deficient cells. *Oncogene*, 14, 1875-1882
109. Adimoolan S, Lin CX, Ford JM. (2001) The p53-regulated cyclin-dependent proteins kinases inhibitor, p21<sup>(waf1, cip1, sid1)</sup>, is not required for global genomic and

- transcription-coupled nucleotide excision repair of UV-induced DNA photoproducts.  
*J Biol Chem*, 276, 25813-25822
- 110.Cooper MP, Balajee AS and Bohr VA. (1999) The C-terminal domain of p21 inhibits nucleotide excision repair in vitro and in vivo. *Mol Biol Cell*, 10, 2119-2129
- 111.Bendjennat M, Boulaire J, Jascur T, Brickner H, Barbier V, Sarasin A, Fotedar A and Fotedar R. (2003) UV irradiation triggers ubiquitin-dependent degradation of p21(WAF1) to promote DNA repair. *Cell*, 114, 599-610
- 112.Stivala LA, Riva F, Cazzalini O, Savio M and Prosperi E. (2001) p21 (waf1/cip1)-null human fibroblasts are deficient in nucleotide excision repair downstream the recruitment of PCNA to DNA repair sites. *Oncogene*, 20, 563-570
- 113.Therrien JP, Loignon M, Drouin R and Drobetsky EA. (2001) Ablation of p21waf1cip1 expression enhances the capacity of p53-deficient human tumor cells to repair UVB-induced DNA damage. *Cancer Res*, 61, 3781-3786
- 114.McDonald ER III, Wu GS, Waldman T and El-Deiry WS. (1996) Repair defect in p21 WAF1/CIP1-/- human cancer cells. *Cancer Res*, 56, 2250-2255
- 115.Wesierska-Gadek J, Schmid G. (2001) Poly(ADP-ribose) polymerase-1 regulates the stability of the wild-type p53 protein. *Cell Mol Biol Lett*, 6, 117-140
- 116.Stierum RH, van Herwijnen MH, Hageman GJ, Kleinjans JC. (1994) Increased poly(ADP-ribose)polymerase activity during repair of (+/-)-anti-benzo[a]pyrene diolepoxide-induced DNA damage in human peripheral blood lymphocytes in vitro. *Carcinogenesis*, 15, 745-751

117. Agarwal ML, Agarwal A, Taylor WR, Wang ZQ, Wagner EF and Stark GR. (1997)  
Defective induction but normal activation and function of p53 in mouse cells lacking  
poly-ADP-ribose polymerase. *Oncogene*, 15, 1035-1041

# **Chapter Five**

## **Conclusions and Synthesis**

### **5.1 Introduction**

A well-defined dose-response relationship of arsenic at environmentally relevant concentrations is desperately needed in order to establish a rational and reliable cancer risk assessment. This will help to develop appropriate risk management measures to adequately protect people from the detrimental effects incurred by exposure to arsenic, especially the cancerous effects from chronic exposure to arsenic in drinking water. Epidemiological studies provide evidence that the dose-response relationship for arsenic is non-linear (1,2). While populations exposed to very high levels of arsenic in drinking water (several hundred  $\mu\text{g/L}$ ) in Taiwan, Chile, Argentina, India, Bangladesh, and China have shown increased prevalence and mortality of skin, lung, and bladder cancers, epidemiological studies conducted in the U.S. populations exposed to lower levels of arsenic in drinking water have not shown a dose-response relationship between arsenic concentrations in drinking water and cancer mortality. The evidence for carcinogenic effects at very low concentration levels of arsenic is inconclusive. Current risk assessments are likely to overestimate arsenic toxicity and associated risks based on the use of default linearity assumptions and extrapolation from high dose data. The gap in scientific knowledge has to be filled by new epidemiological studies and a mechanistic understanding of arsenic health effects. However, numerous attempts to find an animal model for arsenic carcinogenesis in the last 30 years have mostly failed. This lack of an animal model has greatly hindered the understanding of the mechanism of arsenic carcinogenesis. Recently, an animal model was demonstrated to be successful when

arsenite (iAs(III)) acted as a co-carcinogen with solar ultraviolet (UV) radiation on mouse skin (3,4). The result substantiated the hypothesis that arsenic is not a carcinogen per se but acts as a co-carcinogen. Given the current state of knowledge, we hypothesized that arsenic can modulate the formation and repair of carcinogen-DNA adducts in human cells, which are the early events that lead to cancer.

This investigation of the effects of arsenic on the formation and repair of benzo(a)pyrene diol epoxide (BPDE)-DNA adducts has been divided into three interrelated phases: (1) developing a highly sensitive and specific analytical method for BPDE-DNA adduct measurement, capable of detecting the effects of arsenic on the levels of DNA damage (**Chapter 2**); (2) examining the effects of six arsenic species on the formation of BPDE-DNA adducts and investigating all relevant biochemical processes possibly involved (**Chapter 3**); (3) examining the inhibitory effects of six arsenic species on the repair of BPDE-DNA adducts and investigating possible mechanisms behind the apparent inhibition (**Chapter 4**). The key results from **Chapters 2-4** and a synthesis of the experimental findings, and finally comments on future research directions are summarized below.

## **5.2 Advancements in Knowledge**

### **5.2.1 Chapter 2: Developing and refining a tool for the measurement of BPDE-DNA adducts**

A highly sensitive and specific analytical method for BPDE-DNA adduct measurement was developed. This method was based on the affinity interaction between adducted DNA and a monoclonal antibody, capillary electrophoresis (CE) separation, and laser-induced fluorescence (LIF) detection. The parameters for affinity interaction and

CE separation were optimized and the method was successfully applied to detection of the BPDE-DNA adduct levels in human cells treated with BPDE or BaP. The method consumes a very low quantity of sample (1  $\mu\text{g}$ ) and does not require tedious sample handling, which are advantages over other methodologies for DNA damage measurement. Like other immunoassays, the CE-LIF method provides a fast approach to quantify relative concentrations of specific DNA adducts. The improved method enabled us to study the effects of six arsenic species on the formation (**Chapter 3**) and repair (**Chapter 4**) of BPDE-DNA adducts, with environmentally relevant arsenic concentrations.

### **5.2.2 Chapter 3: Examining and investigating the effects of arsenic on the formation of BPDE-DNA adducts**

Previous studies failed to demonstrate an effect of arsenic on the formation of DNA damage because the use of repair-proficient systems could not distinguish this effect from its effect on DNA repair. In our study, we used a repair-deficient SV40-transformed xeroderma pigmentosum complementation group A (XPA) cell line and therefore were able to distinguish the effects of arsenic on the formation of BPDE-DNA adducts from its effects on the repair of BPDE-DNA adducts. We treated the cells with various arsenic species for 24 h and then incubated them with BPDE for 30 min and found that arsenic pretreatment increased the levels of BPDE-DNA adducts over the controls in a dose-dependent manner. This dose-dependent increase by the various arsenic compounds followed a similar order as the arsenic cytotoxicities. Trivalent arsenic species were more potent than pentavalent arsenic species.  $\text{iAs(III)}$  enhanced the formation starting from 10  $\mu\text{M}$  and  $\text{MMA(III)}$  and dimethylarsinous acid ( $\text{DMA(III)}$ )

started the enhancement at 5  $\mu\text{M}$  while pentavalent arsenic compounds enhanced the formation only at millimolar concentrations. The enhancement of BPDE-DNA adducts increased with the increase of arsenic treatment time. After arsenic treatment, the cellular levels of GSH and the activity of GST were measured because as a major cellular defense system in response to various stresses, reduced glutathione (GSH) and glutathione-S-transferase (GST) are responsible for detoxifying both arsenic and BPDE. However, no inverse correlations between their levels and the BPDE-DNA adduct levels were observed, suggesting that the enhanced formation of BPDE-DNA adducts by arsenic was not due to a decrease in the GSH pool or GST activity. Chromatin accessibility was another factor that we considered in our study of DNA damage. Our results showed that arsenic treatment did not significantly change chromatin accessibility. However, arsenic pretreatment significantly increased the efficiency of BPDE uptake. The effect of arsenic on the cellular uptake of BPDE is probably the major factor leading to the enhanced BPDE-DNA adduct formation.

### **5.2.3 Chapter 4: Examining and investigating the effects of arsenic on the repair of BPDE-DNA adducts**

Having confirmed our findings of the effects of arsenic on the formation of BPDE-DNA adducts by use of a repair-deficient cell line (**Chapter 3**), we further examined the effects of six arsenic species on the repair of BPDE-DNA adducts in a repair-proficient cell culture system. We incubated normal human fibroblasts with BPDE for 30 min and then allowed the cells to repair for 24 h with or without the presence of arsenic compounds and found that the presence of arsenic led to elevated levels of BPDE-DNA adducts over the controls in a dose-dependent manner. Use of contact-inhibited,

confluent fibroblast cells prevented post-treatment replication. Therefore, both dilution of adducted DNA as a result of cell division and potential replication inhibition by arsenic could be dismissed. We concluded that all of the six arsenic compounds could inhibit the repair of BPDE-DNA adducts in a dose-dependent manner. The inhibition tended to increase against time-matched controls when the repair time was prolonged. The concentrations of arsenicals that caused observable inhibition were: iAs(III), 5  $\mu\text{M}$ ; MMA(III), 1  $\mu\text{M}$ ; DMA(III), 1  $\mu\text{M}$ ; arsenate (iAs(V)), 25  $\mu\text{M}$ ; monomethylarsonic acid (MMA(V)), 500  $\mu\text{M}$ ; and dimethylarsinic acid (DMA(V)), 100  $\mu\text{M}$ . These relative inhibitory potencies were consistent with the relative cytotoxicities of these arsenicals.

Western blot analysis of repair-related proteins revealed that MMA(III) did not alter the expression levels of XPA and p62, two key proteins involved in global genomic nucleotide excision repair (GG-NER). However, the presence of MMA(III) abrogated the accumulation of p53 and p21 induced by BPDE over time. Also, our results showed that the xeroderma pigmentosum complementation group C (XPC) protein was inducible in a p53-dependent manner in this cell line. Moreover, we observed a striking temporal correlation between DNA repair efficiency and p53 expression levels, which led to our hypothesis that MMA(III) inhibited the repair of BPDE-DNA adducts by downregulating the expression of p53. Although the exact role of p53 in GG-NER remains unclear, considerable evidence has implicated the involvement of p53 in GG-NER. Emerging evidence suggests that p53 has a potential role in recruiting repair proteins to participate in GG-NER. The most likely recruits are XPC and p48 (5-9). Therefore, for the first time, we have linked arsenic inhibition of DNA repair to p53. Our results on p53-dependent modulation of p21 suggested that p53 was still transcriptionally functional

because p21 is a downstream effector protein of p53. A better understanding of p53 function in GG-NER will eventually reveal the underlying mechanism of DNA repair inhibition by arsenic.

Cell cycle analysis of exponentially growing cells indicated that insufficient time for repair was not the reason for the apparent repair inhibition by arsenic because in our study MMA(III) did not override the G1/S arrest by BPDE. Taken together, we suggested that the effect of arsenic on p53 could result from destabilization of p53 via inhibition of poly(ADP-ribose) polymerase (PARP) activity by arsenicals. PARP activity has previously been shown to be inhibited by iAs(III).

### **5.3 Future Research**

By use of 1-chloro-2,4-dinitrobenzene (CDNB) as a generic substrate for GST, we did not observe an inverse correlation between total GST activity and BPDE-DNA adduct levels (**Chapter 3**). However, specific activity measurement using BPDE as the substrate needs to be done before we can draw a firm conclusion that suppression of GST activity is not relevant to the enhancement of BPDE-DNA adduct formation by arsenic. An HPLC method to determine the GST activity towards ( $\pm$ )-anti-BPDE was documented in the literature (10, 11). Subcellular distribution of [ $^3$ H]-BPDE, especially in the nucleus, also merits investigation. However, its structural integrity and DNA-binding activity cannot be examined by use of a radiolabelled compound only. If necessary, an HPLC based quantitative method needs to be established.

During the course of this thesis project, protein analysis was focused on only a few repair proteins, such as XPA, XPC, and p62-TFIIH. It is worthwhile to extend the protein analysis to other repair proteins involved in GG-NER, which will reveal the

impact of arsenic on the expression of other repair proteins and help define the role of p53 in NER. Although MMA(III), one of the arsenic metabolites from exposure to inorganic arsenic (iAs), has been intensively investigated in this study (**Chapter 4**), other arsenic metabolites warrant further attention. By comparing their effects on DNA damage formation and repair, we may understand how the various arsenic species modulate the repair protein expression differently and which is/are the key player(s) for DNA repair inhibition.

Because proliferation is necessary for mutation, a crucial step toward cancer development, exponentially growing cells need to be studied in order to provide data pertinent to carcinogenesis. Both Western blotting and cell cycle analysis need to be implemented in these additional studies to see how arsenic compounds alter cell cycle and repair protein expressions accordingly.

#### **5.4 Conclusions**

We demonstrated that arsenic compounds affected both the formation and the repair of BPDE-DNA adducts. By use of a repair-deficient cell line, we showed that each of the six target arsenic species (metabolites to iAs) enhanced the formation of BPDE-DNA adducts. These six arsenic species also inhibited the repair of BPDE-DNA adducts in confluent, contact-inhibited repair-proficient cells. Unaffected by DNA replication, confluent primary cells represent the condition close to skin cells *in vivo*. Also, repair inhibition by trivalent arsenic compounds was observed at concentrations as low as submicromolar levels. The arsenic concentrations we chose in our study are relevant to human populations chronically exposed to high concentrations (more than 100 µg/L) of arsenic in drinking water (12). DNA repair inhibition might be a contributing, if not the

predominant, factor leading to skin cancer caused by arsenic. Our findings may be relevant to the understanding of pathological effects observed in human epidemiological studies.

Based on an *in vitro* experimental model involving BPDE and MMA(III), we demonstrated a striking temporal correlation between DNA repair efficiency and p53 expression levels. Therefore, for the first time, we have linked arsenic exposure with DNA repair inhibition through p53. This provides a plausible mechanism of DNA repair inhibition by arsenic. Further efforts to study the exact role of p53 in NER will improve our understanding of arsenic co-carcinogenicity.

## 5.5 References

1. Schoen A, Beck B, Sharma R and Dube E. (2004) Arsenic toxicity at low doses: epidemiological and mode of action considerations. *Toxicol Appl Pharmacol*, 198, 253-267
2. Goering PL, Aposhian HV, Mass MJ, Cebrian M, Beck BD and Waalkes MP. (1999) The enigma of arsenic carcinogenesis: role of metabolism. *Toxicol Sci*, 49, 5-14
3. Rossman TG, Uddin AN, Burns FJ and Bosland MC. (2001) Arsenite is a cocarcinogen with solar ultraviolet radiation for mouse skin: an animal model for arsenic carcinogenesis. *Toxicol Appl Pharmacol*, 176, 64-71
4. Rossman TG, Uddin AN, Burns FJ and Bosland MC. (2002) Arsenic cocarcinogenesis: an animal model derived from genetic toxicology studies. *Environ Health Perspect*, 110 (Suppl 5), 749-752
5. Adimoolam S, Ford JM. (2003) p53 and regulation of DNA damage recognition during nucleotide excision repair. *DNA Repair*, 2, 947-954
6. Wang QE, Zhu Q, Wani A, Wani G, Chen J, Wani AA. (2003) Tumor suppressor p53 dependent recruitment of nucleotide excision repair factors XPC and TFIIH to DNA damage. *DNA Repair*, 2, 483-499
7. Wang QE, Zhu Q, Wani G, Chen J and Wani AA. (2004) UV radiation-induced XPC translocation within chromatin is mediated by damaged-DNA binding protein, DDB2. *Carcinogenesis*, 25, 1033-1043
8. Amundson SA, Patterson A, Do KT, Fornace AJ. (2002) A nucleotide excision repair master-switch: p53 regulated coordinate induction of global genomic repair genes. *Cancer Biol Ther*, 1, 145-149

9. Chu G. (2002) Global genomic repair and p53 in a dance after DNA damage. *Cancer Biol Ther.* 1, 150-151
10. Hu X, Srivastava SK, Xia H, Awasthi YC and Singh SV. (1996) An alpha class mouse glutathione S-transferase with exceptional catalytic efficiency in the conjugation of glutathione with 7 $\beta$ , 8 $\alpha$ -dihydroxy-9 $\alpha$ ,10 $\alpha$ -oxy-7,8,9,10-tetrahydrobenzo(a)pyrene. *J Biol Chem*, 271, 32684-32688
11. Hu X, Benson PJ, Srivastava SK, Mack LM, Xia H, Gupta V, Zaren HA and Singh SV. (1996) Glutathione S-transferases of female A/J mouse liver and forestomach and their differential induction by anti-carcinogenic organosulfides from garlic. *Arch Biochem Biophys*, 336, 199-214
12. NRC (National Research Council) (2001) Arsenic in drinking water (update). National Academy Press, Washington, DC. pp 117

## Appendix

### **Introduction to Capillary Zone Electrophoresis (CZE)**

As its name suggests, electrophoresis is performed in a capillary, with one end placed in a source vial and the other end in a destination vial. The source vial, the capillary, and the destination vial are filled with an electrolyte as running buffer. To start a run, the capillary inlet is placed into a sample vial and the sample is introduced electrokinetically or hydrodynamically. After sample introduction, the capillary inlet is placed back into the source vial and an electric field is applied between the source and destination vials. The solutes migrate through the capillary as zones and are detected by a detector. The output is displayed as an electropherogram, a plot of the detector response versus time.

The solutes are separated as they move through the capillary due to differences in their rates of migration, which are dependent on their electrophoretic mobilities. In a “normal” capillary electrophoresis, the buffer solution moves toward the cathode. This phenomenon is termed electro-osmotic flow (EOF). Since cations are attracted to the cathode in the same direction as the EOF, their rates of migration are faster than the EOF. Cations elute in order of their charge-to-size ratios, with small, highly-charged cations eluting first. Neutral molecules, which move through the capillary only under the influence of the EOF, elute after the cations. Neutral molecules are not separable in a normal capillary electrophoresis. Anions, which are attracted to the anode, tend to migrate in the direction opposite the EOF, and therefore elute after neutral molecules. Usually, the EOF is greater than the electrophoretic velocities of anions, especially for biomacromolecules such as DNA and proteins. Therefore, they are also carried toward

the cathode. Anions elute in reverse order of their charge-to-size ratios, with small, highly-charged anions eluting last.

The observed electrophoretic mobility ( $\mu_{OBS}$ ) of a solute can be represented as the sum of both its electrophoretic mobility ( $\mu_{EP}$ ) plus the electroosmotic mobility ( $\mu_{EOF}$ ):

$$\mu_{OBS} = \mu_{EOF} + \mu_{EP}$$

There are several factors that can change the EOF. For example, the EOF increases as the separation voltage or running buffer pH increases but decreases as the concentration or ionic strength of running buffer increases.

The migration time of a solute can be calculated using  $t_m = lL / (\mu_{EOF} + \mu_{EP})V$ , where  $l$  is the effective capillary length from inlet to detector,  $L$  is the total capillary length from inlet to outlet, and  $V$  is the applied voltage across the capillary.

As in high performance liquid chromatography (HPLC), the resolution reflects how narrow and how far apart adjacent peaks are. It can be calculated from an electropherogram using  $R = 2(t_2 - t_1) / (w_1 + w_2)$ , where  $t_1$  and  $t_2$  are migration times of adjacent peaks and  $w_1$  and  $w_2$  are peak widths of the same adjacent peaks.

The resolution can be increased by increasing the applied separation voltage, or capillary length, or by optimizing buffer pH and composition, or by optimizing EOF.

## References

1. Dale R. Baker ed. (1995) *Capillary Electrophoresis*. John-Wiley & Sons, New York, NY
2. Landers JP. ed. (1996) *Handbook of Capillary Electrophoresis* (2<sup>nd</sup> ed). CRC Press, Boca Raton, FL
3. Righetti PG. ed. (1996) *Capillary Electrophoresis in Analytical Biotechnology*. CRC Press, Boca Raton, FL